RESEARCH REPORT

HEALTH EFFECTS INSTITUTE

Number 135
October 2008

PRESS
VERSION
November 24, 2008

Mechanisms of Particulate Matter Toxicity in Neonatal and Young Adult Rat Lungs

Kent E. Pinkerton, Yamei Zhou, Caiyun Zhong, Kevin R. Smith, Stephen V. Teague, Ian M. Kennedy, and Margaret G. Ménache

Mechanisms of Particulate Matter Toxicity in Neonatal and Young Adult Rat Lungs

Report 135

Health Effects Institute

Boston, Massachusetts

Trusted Science • Cleaner Air • Better Health

Publishing history: The Web version of this document was posted at *www.healtheffects.org* in October 2008 and then finalized for print.

Citation for whole document:

Pinkerton KE, Zhou Y, Zhong C, Smith KR, Teague SV, Kennedy IM, Ménache MG. 2008. Mechanisms of Particulate Matter Toxicity in Neonatal and Young Adult Rat Lungs. HEI Research Report 135, Health Effects Institute, Boston, MA.

When specifying a section of this report, cite it as a chapter of the whole document.

CONTENTS

ABOUT HEI

The Health Effects Institute is a nonprofit corporation chartered in 1980 as an independent research organization to provide high-quality, impartial, and relevant science on the effects of air pollution on health. To accomplish its mission, the institute

- Identifies the highest-priority areas for health effects research;
- Competitively funds and oversees research projects;
- Provides intensive independent review of HEI-supported studies and related research;
- Integrates HEI's research results with those of other institutions into broader evaluations; and
- Communicates the results of HEI's research and analyses to public and private decision makers.

HEI receives half of its core funds from the U.S. Environmental Protection Agency and half from the worldwide motor vehicle industry. Frequently, other public and private organizations in the United States and around the world also support major projects or certain research programs. HEI has funded more than 280 research projects in North America, Europe, Asia, and Latin America, the results of which have informed decisions regarding carbon monoxide, air toxics, nitrogen oxides, diesel exhaust, ozone, particulate matter, and other pollutants. These results have appeared in the peer-reviewed literature and in more than 200 comprehensive reports published by HEI.

HEI's independent Board of Directors consists of leaders in science and policy who are committed to fostering the public–private partnership that is central to the organization. The Health Research Committee solicits input from HEI sponsors and other stakeholders and works with scientific staff to develop a Five-Year Strategic Plan, select research projects for funding, and oversee their conduct. The Health Review Committee, which has no role in selecting or overseeing studies, works with staff to evaluate and interpret the results of funded studies and related research.

All project results and accompanying comments by the Health Review Committee are widely disseminated through HEI's Web site (*www.healtheffects.org*), printed reports, newsletters, and other publications, annual conferences, and presentations to legislative bodies and public agencies.

ABOUT THIS REPORT

Research Report 135, *Mechanisms of Particulate Matter Toxicity in Neonatal and Young Adult Rat Lungs,* presents a research project funded by the Health Effects Institute and conducted by Kent E. Pinkerton of the University of California–Davis and his colleagues. This report contains three main sections.

The HEI Statement, prepared by staff at HEI, is a brief, nontechnical summary of the study and its findings; it also briefly describes the Health Review Committee's comments on the study.

The Investigators' Report, prepared by Pinkerton et al., describes the scientific background, aims, methods, results, and conclusions of the study.

The Critique is prepared by members of the Health Review Committee with the assistance of HEI staff; it places the study in a broader scientific context, points out its strengths and limitations, and discusses remaining uncertainties and implications of the study's findings for public health and future research.

This report has gone through HEI's rigorous review process. When an HEI-funded study is completed, the investigators submit a draft final report presenting the background and results of the study. This draft report is first examined by outside technical reviewers and a biostatistician. The report and the reviewers' comments are then evaluated by members of the Health Review Committee, an independent panel of distinguished scientists who have no involvement in selecting or overseeing HEI studies. During the review process, the investigators have an opportunity to exchange comments with the Review Committee and, as necessary, to revise their report. The Critique reflects the information provided in the final version of the report.

HEI STATEMENT

Synopsis of Research Report 135

Mechanisms of Particulate Matter Toxicity in Neonatal and Young Adult Rat Lungs

BACKGROUND

Ambient particulate matter (PM) is a complex mixture of solid and liquid particles suspended in air. Depending on the source of pollution, PM varies in size, chemical composition, and other physical and biologic properties. On the basis of epidemiologic findings and supporting results of toxicologic studies, many governmental agencies have set regulatory standards or guidelines for concentrations of ambient PM. Particles ≤ 10 μm in aerodynamic diameter (PM_{10}) are of most concern because these particles are considered to be respirable by humans. To protect the general population and groups considered most vulnerable to adverse effects from PM in the United States, the U.S. Environmental Protection Agency monitors PM_{10} levels and has promulgated National Ambient Air Quality Standards for particles ≤ 2.5 μm in aerodynamic diameter ($PM_{2.5}$ or fine particles). Some scientists believe that ultrafine particles (≤ 100 nm in diameter) may be particularly toxic.

Much work has focused on understanding the effects of particles derived from combustion sources: these particles are in the fine and ultrafine range and generally are composed of an elemental carbon core that binds metals (such as iron, vanadium, nickel, copper, and platinum), organic carbon compounds, and sulfates. Critical questions in PM research involve understanding the mechanisms by which particles may cause effects and the key characteristics of particles, both physical and chemical, that are associated with toxicity. To address these questions, HEI issued RFA 96-1, *Mechanisms of Particle Toxicity: Fate and Bioreactivity of Particle-Associated Compounds,* in 1996.

APPROACH

In response, Dr. Kent Pinkerton and colleagues from the University of California–Davis, conducted a study to evaluate the effects of short-term exposure on the airways of rats using laboratory-generated ultrafine metal particles, either alone or in combination with soot. The rationale for the study was that combinations of metal and soot should provide an understanding of the interaction between components of combustion source-derived particles found in ambient air.

The major objective of this study was to determine if the biologic response to inhaled ultrafine particles depended on particle composition. The investigators focused on oxidative stress and inflammatory responses in rat lungs and airways after exposure to three different particle compositions: iron, soot, or a combination of iron and soot.

To accomplish these objectives, the investigators constructed a flame combustion system connected to an animal exposure inhalation unit and generated particles of iron, soot, and combinations of iron and soot. The investigators characterized the particles physically and chemically. Young adult male rats were exposed for six hours per day on three consecutive days to: iron particles alone (57 or 90 $\mu g/m^3$/day); soot particles alone (250 $\mu g/m^3$/day); a combination of iron and soot particles (250 $\mu g/m^3$/day total, with an iron concentration of 45 $\mu g/m^3$); or a filtered air control. Male and female neonatal rats were exposed for six hours per day for three consecutive days at age 10–12 days and again at age 23–25 days, but only to the combination of iron and soot particles. In one experiment the concentration of iron was 30 $\mu g/m^3$ and in the other it was 100 $\mu g/m^3$; the total concentration of the combination of iron and soot particles was 250 $\mu g/m^3$/day.

Dr. Pinkerton and coworkers obtained bronchoalveolar lavage fluid 2 hours and lung tissue 24 hours after the end of the third day's exposure, respectively. They measured several oxidative stress, inflammatory response, and lung injury endpoints.

This Statement, prepared by the Health Effects Institute, summarizes a research project funded by HEI and conducted by Dr. Kent Pinkerton at the Center for Health and the Environment, University of California–Davis. Research Report 135 contains both the detailed Investigators' Report and a Critique on the study prepared by the Institute's Health Review Committee.

RESULTS

The iron particles generated were predominantly ultrafine ferric oxide. Ultrafine soot particles were found (20 nm), but formed chains or clusters larger than 100 nm (fine particles). Most combinations of iron and soot particles had a mean diameter of 70–80 nm (ultrafine particles), but some were in the fine particle range. In the exposures to particle combinations of iron and soot, most of the iron particles appeared separate from soot particles but in close proximity. On average, combinations of iron and soot particles contained 60% elemental carbon and 40% organic carbon, but the organic carbon species were not characterized further.

In adult rats exposure to the higher concentration of iron particles had effects that were not observed after exposure to the lower concentration of iron (changes in some measures of oxidative stress and increases in levels of ferritin and the proinflammatory cytokine IL-1β). In neonatal animals, exposure to either combination of iron and soot particles affected some markers of oxidative stress; only the combination containing the higher concentration of iron was also associated with increased ferritin and IL-1β levels, increased lactate dehydrogenase activity (a marker of cellular injury), and decreased cell viability. Exposure of neonatal rats to combinations of iron and soot particles also impaired cell proliferation in the alveolar region of the lung. Overt evidence of inflammation was not found, however, in either young adult or neonatal rats.

The investigators also found that a low concentration of iron particles (45 $\mu g/m^3$) in the presence of soot, which by itself induced no changes compared with controls, had more biologic effects than a similar concentration of iron particles alone (57 $\mu g/m^3$). The pattern of endpoints changed by exposure to the combination of iron and soot was similar to the pattern of endpoints affected by the higher concentration of iron particles alone (90 $\mu g/m^3$).

SUMMARY AND CONCLUSIONS

Using a flame generation system Pinkerton and colleagues successfully generated particles of iron, soot, and combinations of iron and soot and characterized the particles. Iron particles and soot particles were predominantly in the ultrafine range, but soot particles formed chains or clusters that were in the fine particle range. The combinations of iron and soot particles generated contained a high percentage of commingled particles, with a bimodal distribution similar to that of soot particles alone. Combinations of iron and soot particles contained elemental and organic carbon.

In both young adult and neonatal rats the biologic response in the airways and lung tissue to inhalation of ultrafine particles depended on particle composition, specifically on the iron content of the particles. In adult rats changes in some markers of oxidative stress, an increased release of the proinflammatory cytokine IL-1β, and increased levels of ferritin were detected at a higher but not at a lower iron concentration. In neonatal rats more effects were detected after exposure to particles containing a higher proportion of iron than to particles containing a lower proportion of iron (increased levels of ferritin and IL-1β, decreased cell viability, and increased cell injury). The finding that cell proliferation in the alveolar region of the lung was impaired after neonatal rats were exposed to combinations of iron and soot particles suggests that exposure to air pollutants during a period of rapid lung development may affect lung growth. Overt evidence of inflammation was not found, however, in either young adult or neonatal rats. Particle effects were measured in the airways and lung tissue at only one time point after exposure, so it is possible that different results might have been obtained at different time points.

The investigators also found that the presence of soot particles enhanced the effects seen with iron particles alone, suggesting that the effects of soot and iron were synergistic. If reproduced in other studies, this would suggest that the interaction between different particles may affect their toxicities.

The investigators suggest that their combinations of iron and soot particles bore a generic similarity to diesel exhaust particles; both contain carbon and iron and have a similar size distribution. However, the investigators also recognized that the particles differed in several other key physical and compositional characteristics; for example, the percentage of iron in diesel particles is much smaller than in the iron and soot mixtures evaluated in this study. Thus, although both iron and carbon particles are abundant in the atmosphere, the relevance of the particles generated in this study to the emissions of a particular source such as diesel is uncertain. Extrapolating the study findings to humans is difficult because of likely differences in oxidative stress responses between rats and humans and because the levels of particles were high compared with human ambient air exposures.

INVESTIGATORS' REPORT

Mechanisms of Particulate Matter Toxicity in Neonatal and Young Adult Rat Lungs

Kent E. Pinkerton, Yamei Zhou, Caiyun Zhong, Kevin R. Smith, Stephen V. Teague, Ian M. Kennedy, and Margaret G. Ménache

Center for Health and the Environment (K.E.P., Y.Z., C.Z., K.R.S., S.V.T.,), Department of Anatomy, Physiology, and Cell Biology, School of Veterinary Medicine (K.E.P.), Graduate Group in Comparative Pathology (Y.Z., C.Z.), and Department of Mechanical and Aeronautical Engineering, College of Engineering (I.M.K.), University of California–Davis; New Mexico Center for Environmental Health Sciences and Department of Pediatrics, School of Medicine, University of New Mexico Health Sciences Center, Albuquerque (M.G.M.)

ABSTRACT

Particulate matter (PM*) has been associated with a variety of adverse health effects, primarily involving the cardiovascular and respiratory systems. Researchers continue to investigate biologic mechanisms that may explain how exposure to PM exacerbates or directly causes adverse effects. Particle composition may play a critical role in these effects. In this study we used a diffusion flame system to generate ultrafine iron, soot, and iron combined with soot particles and exposed young adult and neonatal rats to different compositions of these particles.

Young adult rats inhaled all three PM compositions on three consecutive days for 6 hours per day. Exposure to soot PM at 250 μg/m^3 or to iron PM at 57 μg/m^3 demonstrated no adverse respiratory effects. However, we observed mild pulmonary stress when the iron concentration was increased to 90 μg/m^3. The most striking effects resulted when the rats inhaled PM composed of iron (45 μg/m^3) combined with soot particles (total mass 250 μg/m^3). This type of exposure produced significant indicators of oxidative stress, signs of inflammation, and increases in the levels of cytochrome P450 isozymes in the lungs.

Repeated three-day exposure of neonatal rats to soot and iron particles in the second and the fourth weeks of life produced significant oxidative stress (elevations in oxidized and reduced glutathione) and ferritin induction. Neonatal rats exposed to PM in the second week of life also had a subtle but significant cell proliferation reduction in the centriacinar regions of the lungs. These findings suggest that iron combined with soot PM can lead to changes in the respiratory tract not found with exposure to iron or soot PM alone at similar concentrations. Unique effects in the neonate suggest that age may play an important role in susceptibility to inhaled particles.

INTRODUCTION

OVERVIEW OF HEALTH EFFECTS

The scientific literature leaves little doubt that exposure to PM poses a potentially significant human health risk, and growing evidence supports the basic concept that the fine and ultrafine PM components of ambient air have adverse effects. Acute as well as long-term exposure to increased amounts of ambient PM have been associated with asthma exacerbation, lung function decline, increases in chronic respiratory disease, increased frequency of emergency hospitalizations for respiratory and cardiovascular diseases, and increases in cardiovascular and respiratory mortality in susceptible subpopulations (Pope et al. 1995; Schwartz 1995; Schwartz and Morris 1995; Gamble and Lewis 1996). The mechanisms by which adverse health effects are linked causally with PM exposure are not entirely clear. Healthy humans and laboratory animals do not suddenly die when exposed to PM, even when

* A list of abbreviations and other terms appears at the end of the Investigators' Report.

This Investigators' Report is one part of Health Effects Institute Research Report 135, which also includes a Commentary by the Health Review Committee and an HEI Statement about the research project. Correspondence concerning the Investigators' Report may be addressed to Dr. Kent E. Pinkerton, Center for Health and the Environment, One Shields Avenue, University of California, Davis, CA 95616-8615.

Although this document was produced with partial funding by the United States Environmental Protection Agency under Assistance Award R82811201 to the Health Effects Institute, it has not been subjected to the Agency's peer and administrative review and therefore may not necessarily reflect the views of the Agency, and no official endorsement by it should be inferred. The contents of this document also have not been reviewed by private party institutions, including those that support the Health Effects Institute; therefore, it may not reflect the views or policies of these parties, and no endorsement by them should be inferred.

experimental exposures are much higher than ambient levels. Therefore, it is assumed that unique factors in ambient PM exert a much greater adverse effect in susceptible populations, resulting in increased morbidity and mortality. However, a number of major scientific uncertainties about the health effects caused by inhaling PM exist. For example, the relation between the nature and severity of these health effects and particle composition has not been fully characterized.

Many fine and ultrafine particles present in the environment have a complex composition. Exposure to particles with a mixed composition may be associated with different health effects than exposure to particles of unmixed composition.

TRANSITION METAL TOXICOLOGY

One plausible toxicologic hypothesis suggests that fine and ultrafine PM are sources of bioavailable transition metals that induce acute biochemical effects in the form of oxidative stress. It is well known that transition metals — such as vanadium, copper, iron, and platinum — are capable of redox cycling, resulting in the production of reactive oxygen species (ROS). Oxidative stress occurs when ROS formation overwhelms the cell's antioxidant capacity. Iron, the most abundant transition metal in ambient PM, is the key element in the formation of extremely reactive hydroxyl radicals via the Fenton reaction in the presence of the precursors superoxide and hydrogen peroxide. Hydroxyl radicals can attack critical macromolecules and cause cellular injury, by lipid peroxidation, protein modification, and DNA damage. Oxidative stress may lead to the depletion or alteration of intracellular antioxidants, antioxidant enzymatic activity, or both. Oxidative stress may also initiate inflammation and activation of the nuclear factor-kappa B (NF-κB) signaling pathway. NF-κB is a redox-sensitive transcription factor.

Coal fly ash (CFA) and residual oil fly ash (ROFA) are examples of combustion particles rich in transition metals. Studies using CFA and ROFA have documented the role of their transition metals in causing oxidative stress, inflammation, and in activating the NF-κB signaling pathway. CFA has been shown to provide bioavailable iron (Smith et al. 1998) that induces inflammatory cytokines in human lung epithelial cells (Smith et al. 2000). ROFA has been shown to induce inflammatory cytokines in human bronchial epithelial cells (Carter et al. 1997) and it is associated with lung inflammation (Kadiiska et al. 1997) and cardiac arrhythmias in animals (Watkinson et al. 1998).

Intratracheal instillation of iron, copper, manganese, nickel, and vanadium in rats and humans has been shown to induce acute pulmonary inflammation (Lay et al. 1999; Rice et al. 2001). Solublized transition metals from combustion and ambient PM have been associated with acute lung inflammation in animals (Costa and Dreher 1997). Water-soluble transition metals (Dreher et al. 1997; Ghio et al. 1999; Soukup et al. 2000), metals associated with organic material (Ghio et al. 1996), and metals mobilized by an intracellular chelator at physiologic conditions (Smith and Aust 1997) have been studied.

Dye and colleagues (1999) reported that rat tracheal epithelial cells exposed to vanadium, which is found in ROFA, exhibited depleted glutathione levels and increased activity of proinflammatory cytokines interleukin-6 (IL-6) and macrophage inflammatory protein-2, inducible nitric oxide synthase, and lactate dehydrogenase (LDH) (Dye et al. 1999). Kennedy and colleagues (1998) found that BEAS-2B cells exposed to copper present in particulates from the air of Provo, Utah, showed induction of IL-8 and activation of NF-κB. Jimenez and coworkers (2000) reported that activation of NF-κB in A549 cells occurred via an iron-mediated mechanism after exposure to fine PM.

A number of investigations suggest that the release of iron from fine particles inside cells can lead to intracellular iron overload, causing changes indicative of oxidative stress (Chao et al. 1994; Aust et al. 1995; Smith and Aust 1997; Smith et al. 1998; Smirnov et al. 1999).

However, few studies have tested the effects of inhaling transition metals — the actual route by which humans are exposed to airborne pollutants. In the few studies of inhaled PM-containing transition metals, the average particle masses generated have been unusually high (milligram versus microgram quantities) (Campen et al. 2001; Vincent et al. 2001; Fernandez et al. 2002).

DIESEL PM

Studies with diesel- and gasoline-powered vehicles show that their tailpipe emissions should also be considered a source of ambient particulate iron, because investigators found a release of 10 to 50 mg iron/mile (Schauer et al. 1999). Diesel exhaust particles have also been reported to generate ROS and cytokines in human bronchial cells (Vogl and Elstner 1989).

SOOT PM

Soot is primarily composed of elemental carbon (EC) but also contains oxygen, nitrogen, hydrogen, and polyaromatic hydrocarbons (PAHs). PAHs and other organic compounds are major contributors to the ultrafine fraction of soot (Hughes et al. 1998). Soot may be considered an inert particle that has little effect when inhaled alone. For example, in several animal inhalation studies, no changes

were observed in the respiratory system of mice exposed (4 hours/day for 4 days) to carbon black (10 mg/m^3), a surrogate for soot) (Jakab 1992, 1993; Jakab and Hemenway 1994). However, due to the large surface area of soot particles, copollutants, such as gases and transition metals, could form a coating on the soot surface and be transported into the respiratory tract. Binding to soot may alter the deposition and clearance of particles, and perhaps change their biologic potential (Sun et al. 1989; Lindenschmidt and Witschi 1990; Schlesinger 1995; Oberdörster 2001).

GENERATING METALLIC PM

Metallic PM can be produced by a variety of means, including evaporation-condensation processes. Karg and colleagues (1998) used an electric-spark system to generate a pure silver PM for animal exposure studies. However, the generation of iron combined with soot PM of the type that might be emitted from a diesel engine with iron as a fuel additive is best accomplished through the use of a combustion system. We found that the passage of iron through a flame has a major impact on the morphology of the resulting particles. Hence, it is important that the experimental combustion system reproduce, to the greatest extent possible, the temperature and other conditions that are typical of PM sources such as engines.

We generated ultrafine particles of iron, soot, and iron combined with soot for our study. We then used these particles with two animal models under well-characterized and controlled exposure conditions to investigate the effects of various particle compositions on the epithelial cells lining the respiratory tract.

PARTICLE DEPOSITION IN THE LUNGS

The epithelium of the respiratory tract begins at the nares and extends to the alveoli. The cellular composition of the epithelium varies by function and anatomical site along the respiratory tract. Airborne substances carried into the respiratory tract first pass over epithelial cells in the nares. These cells represent a natural barrier and aid in the removal of inhaled foreign substances. They are likely to be the primary cells to exhibit the adverse consequences of exposure to inhaled particles and thereby could serve as a sensitive and direct measure of particle toxicity. Epithelial cells lining the tracheobronchial tree, central acini, and alveoli of the lungs may also serve as sensitive indicators of the pattern of induced injury due to particle deposition and subsequent particle-mediated events in these regions. Ozone-induced changes of epithelial cells in each of these regions have been well documented (Plopper et al. 1994; Cho et al. 1999).

Two important sites for particle deposition in the lungs are the respiratory bronchioles and central acini. These structures form the transitional zone between the airways (air conduction) and alveoli (gas exchange). In the rat, the transition from the terminal bronchiole to the alveolar duct is abrupt. In contrast, monkeys and humans possess a more complex transitional zone, with one to three generations of airways. For both species, this zone — with its interdigitation of bronchiolar and alveolar epithelial cells — represents a unique microcosm for cellular and tissue responses to particles and gases.

Because the respiratory bronchioles and central acini are primary sites for lung injury after exposure to airborne pollutants (Pinkerton et al. 2000), it is critical to understand the effects of particle deposition on structural and functional changes in this region. The lungs of young children are particularly susceptible to the adverse effects of inhaled pollutants. Neonatal processes of cellular differentiation, proliferation, physiological function, and xenobiotic metabolizing enzymes within the respiratory system are rapidly changing during this time (Fanucci and Plopper 1997). The respiratory bronchioles and central acini undergo dramatic growth during perinatal development, with continued cell proliferation and expansion. However, little information is available about the deposition or clearance of particles from these regions or their influence on development in young children. Specifically, does exposure to environmental air pollutants such as particles and gases during perinatal and postnatal development represent an increased toxicity risk compared with that of children who breathe unpolluted air?

Because exposure to environmental toxicants during early life may significantly affect the maturation, growth, and function of the respiratory tract, the effects of exposing children to environmental insults are likely to differ substantially from those of adults. Our study used two animal models: young adult male rats exposed to particles of iron, soot, and iron combined with soot and neonatal rats exposed to particles of iron combined with soot. We examined the biochemical and cellular responses of their respiratory systems, with a focus on the particles' effect on producing oxidative stress.

RELEVANCE OF INHALATION STUDIES WITH FINE AND ULTRAFINE PARTICLES CONTAINING IRON COMBINED WITH SOOT

Humans are often exposed to particles of iron combined with soot. Hughes and colleagues (1998) reported that iron is the predominant metal in all particle size ranges in the ambient PM of Los Angeles. Other constituents of ambient PM included organic compounds, soot, sulfates, nitrates, and trace elements. Potential sources of iron in the atmosphere

are multifarious. Relatively large particles (> 1 μm) may be derived from crustal dusts, whereas ultrafine particles probably originate from high-temperature sources. Ultrafine iron can be emitted from coal-burning power plants where iron is present as part of the mineral matter of the fuel. In Europe, iron is sometimes added to diesel fuel as a soot suppressant. In this case, the iron is emitted into the atmosphere in the form of an ultrafine aerosol in association with residual amounts of soot. Iron is a well-known soot and flame suppressant — it has been used and studied in both contexts (Reinelt and Linteris 1996; Zhang and Megaridis 1996; Rumminger et al. 1999).

We designed our study to find out what effects the composition of inhaled particles may have on respiratory health. Studies using particles of known composition and concentration are clearly needed to help elucidate the mechanisms by which PM exerts adverse health effects.

STUDY DESIGN

In our study, a flame combustion system was used to simulate typical combustion processes and to generate ultrafine particles of iron, soot, and iron combined with soot. Healthy young male adult rats were exposed to these particles by inhalation over a period of 3 days. Neonatal rats of both genders were exposed in a similar manner. To document potential adverse effects, we measured oxidative stress, cytotoxicity, production of proinflammatory cytokines, and activation of the redox-sensitive transcription factor NF-κB.

SPECIFIC AIMS

This project was designed to improve our understanding of the health effects of inhaled PM in young adult and neonatal rats. It had four specific aims:

1. Design, construct, and characterize a combustion system that will generate ultrafine iron, soot, and soot containing various amounts of iron. This combustion system will interface with a small animal exposure unit for inhalation studies.
2. Determine the characteristics of the iron combined with soot particle matrix formed during the fuel combustion process.
3. Determine the lung toxicity in healthy young adult and neonatal rats after exposing them to iron, soot, or variable combinations of iron combined with soot particles for short (6-hour), repeated (3-day) intervals.
4. Identify endpoints that best correlate with acute respiratory toxicity caused by iron, soot, or variable combinations of iron combined with soot particles.

METHODS AND MATERIALS

CHEMICALS

Iron pentacarbonyl, reduced glutathione, glutathione disulfide (GSSG), glutathione reductase, 5,5′-dithio-bis (2-nitrobenzoic) acid, 1-chloro-2, 4-dinitrobenzene, NADPH, 2-vinylpyridine, ferrous sulfate, ferric chloride, and tripyridytriazine were purchased from Sigma-Aldrich Chemical Co. (St. Louis, MO).

ANIMALS AND HOUSING

Timed pregnant dams and young adult male Sprague-Dawley rats 10 to 12 weeks of age were purchased from Harlan Laboratories (Indianapolis, IN). All rats were housed at the Center for Health and the Environment Inhalation Facility at the University of California, Davis, in 20 × 43 × 18 cm polycarbonate boxes with a wire-top system containing food and water provided ad libitum. All animals were maintained on a 12-hour-light/12-hour-dark cycle.

Young adult male rats were housed 3 to a box and allowed to acclimate for one week prior to the experiments. For neonatal studies, timed pregnant dams were received on gestation day 3 and housed singly in standard polycarbonate rat cages with Tech Pellet bedding. Each dam was allowed to give birth spontaneously (typically 21.5 days gestation). Litters were reduced to 10 and kept with the natural mother until weaning at 21 days of age.

Animals were handled in accordance with standards established by the U.S. Animal Welfare Acts as set forth in the National Institutes of Health Guidelines and by the University of California, Davis, Animal Care and Use Committee.

PARTICLE GENERATION AND EXPOSURE SYSTEMS

Overview

The generation of ultrafine iron particles as a PM aerosol was accomplished by premixing vapors of ethylene with iron pentacarbonyl prior to introduction to the burner nozzle (Figure 1). In the presence of ethylene gas and iron pentacarbonyl vapors, combustion results in the nearly complete oxidation of ethylene, leaving predominantly iron oxide particles in the post-flame plume. These particles pass through a primary dilution chamber (Figure 2) and are subjected to Venturi turbulent airflow to minimize particle entrainment or coagulation. From the primary dilution chamber, particles are passed to a secondary dilution chamber (Figure 2) and mixed with filtered air to

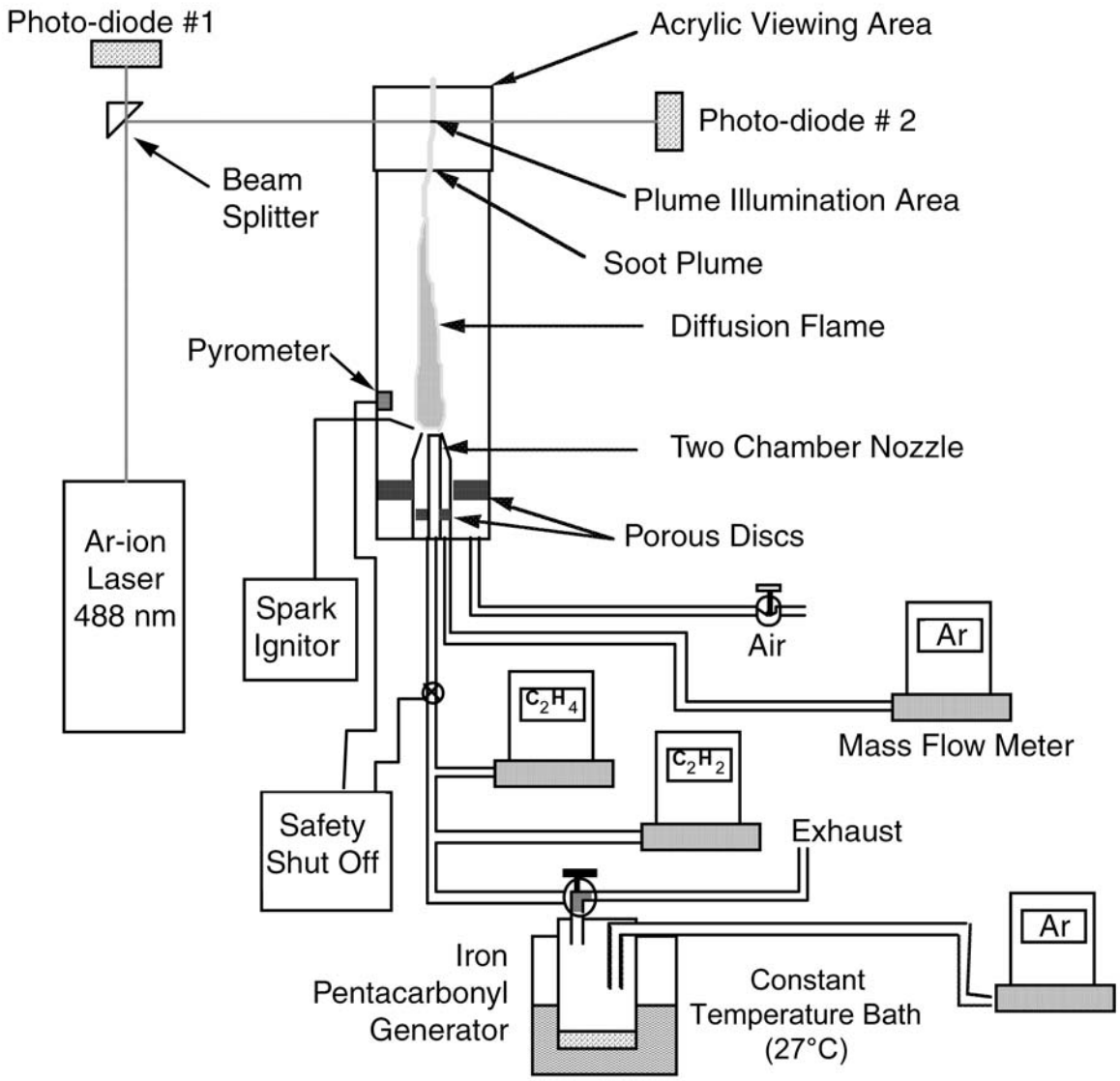

Figure 1. Diffusion flame apparatus.

reduce the overall concentration and temperature of the freshly generated iron PM. A series of tubes connects the secondary dilution chamber to each of four exposure units. The air in each exposure unit is in equilibrium with the air in the secondary dilution chamber. Airflow exits each exposure unit through two perforated exhaust tubes running the length of each unit (Figure 3). This airflow configuration allows particles to enter from the top and exit from the bottom of each exposure unit. Net airflow through each exposure unit equals the combined airflow required for fuel combustion in the diffusion flame system, air added to particles passing from the primary to the secondary dilution

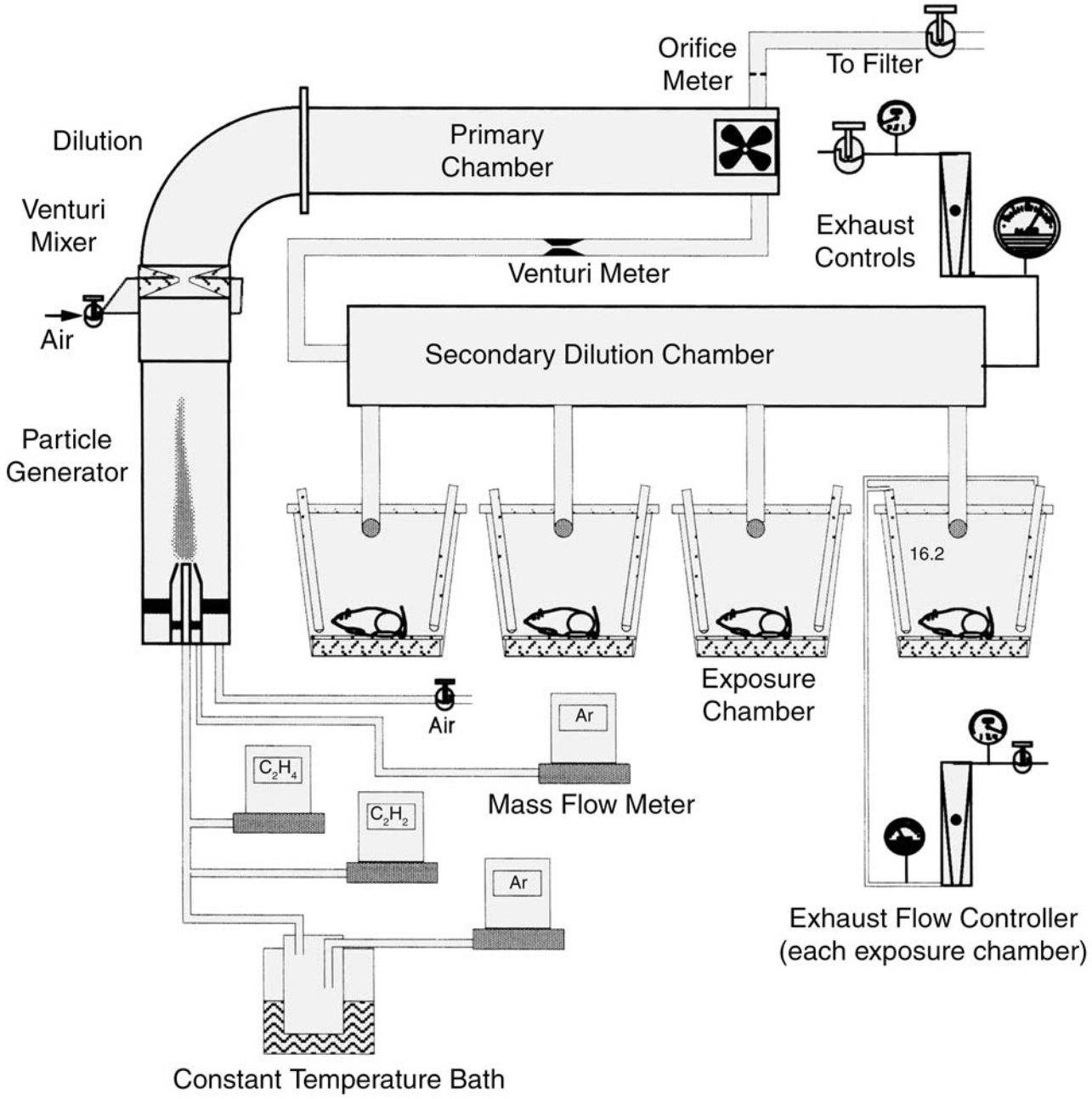

Figure 2. Particle generation and exposure systems.

chamber, and air "pulled" by a vacuum pump positioned beyond each exposure unit.

The diffusion flame system is designed to produce soot at a constant rate. Iron loading can be varied from 0 to 100 μg/m^3 in the diluted post-flame gases. To maintain the constant soot production rate, acetylene is added to the fuel to counteract the soot-retardant effects of iron.

We collected particle samples from within the flame and downstream of the flame to better understand the generation and formation of the iron particles. Particles collected on carbon-coated copper grids were examined by

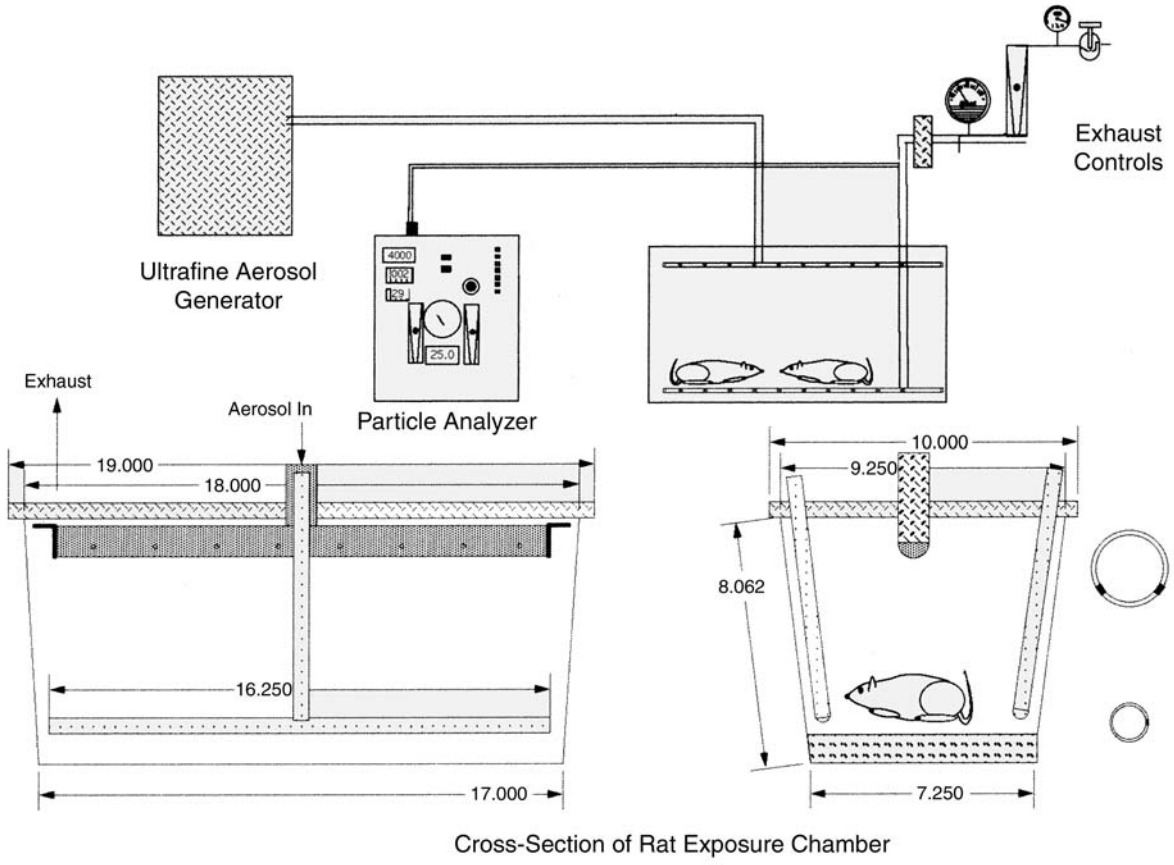

Figure 3. Detailed schematic of exposure system.

transmission electron microscopy (TEM). A differential mobility analyzer was used to measure the size distribution of the PM. The iron particles, typically 40 nm in diameter, were often separated from the soot particles, suggesting either that they were not formed concurrently with the soot or that they remained after oxidation of the surrounding soot.

We found that iron could not be detected in the combustion flame at mid level or immediately post-flame in the soot plume. At both of these levels, the soot and iron were detected only as amorphous masses. Only beyond the post-flame plume were we able to observe particles of iron. TEM confirmed that iron was present as small particles commingled with soot. The iron particles likely melted and coalesced with the soot as they passed through the flame tip and then crystallized as the post-flame gases cooled.

The diffusion flame system produced steady concentrations of soot, iron, and iron combined with soot PM for delivery to the inhalation system. Gaseous species, including carbon monoxide (CO) and nitrogen oxides (NO_x), were also routinely measured. Concentrations of these substances were highest in the primary dilution chamber and reduced by approximately 10-fold in the secondary dilution chamber. These concentrations were so low that they were unlikely to have any significant effect on the animals.

Particle Generation System

A small, square diffusion flame burner system was constructed as shown in Figure 1. The configuration is a standard arrangement consisting of a burner nozzle surrounded by a coflowing stream of air. Initial trials using iron pentacarbonyl resulted in iron deposits forming at the lip of the fuel nozzle. The deposits built up to such an extent that they disturbed the flow. We modified the burner nozzle by adding a concentric outer tube to the first

tube. The two tubes were separated by an annular porous metal disk that maintained an even flow of inert argon carrier gas around the fuel nozzle. This arrangement prevented the diffusion of oxygen to the fuel nozzle exit, where the oxidation of iron pentacarbonyl vapor could take place, and thus prevented iron buildup. The burner assembly was mated at the top to a round acrylic section with access for laser extinction measurements of soot volume fractions.

Two mass flow controllers were used to regulate the flow of fuels. A third mass flow controller regulated the flow of argon through a constant-temperature bath. A fourth mass flow controller maintained the flow of argon to the annular region of the burner. A small electrode was used at the nozzle exit to ignite the flame; it was withdrawn after a steady flame was established. A pyrometer (ultraviolet flame detector, Honeywell, Morristown, NJ) was connected to a solenoid as a safety feature designed to shut off the gas flow if the flame was extinguished.

The apparatus must deliver a constant soot emission while various amounts of iron enter the flow. Ethylene is the primary fuel, but because iron effectively suppresses soot, an additional fuel is required to compensate for the addition of iron. Acetylene, chosen for its strong propensity to form soot, was mixed with the ethylene to maintain a constant soot volume fraction in the exhaust stream.

The iron was added to the fuel mixture as a vapor in the argon carrier gas. Iron pentacarbonyl was used as the source of iron; it is a viscous yellow liquid (mol wt = 195.9; specific gravity = 1.457; melting point = −21°C; boiling point = 102.8°C). Pentacarbonyl vapor was generated in a 250 mL stainless-steel vessel with a shut-off valve at the entrance and a 3-way valve at the exit. The valves were used to isolate the pentacarbonyl source from back-diffusion of O_2 or other contaminants between experiments. The vessel was immersed in a water bath kept at 27°C to maintain a saturated vapor.

Soot volume fractions were measured above the flame using an air-cooled argon ion laser. The beam of the laser was directed through the soot-laden plume and onto a photodiode. An interference filter was used to remove extraneous radiation. A neutral-density filter ensured that the detector operated in its linear range. Soot volume fractions were calculated by measuring light extinction through the plume 27 to 29 cm downstream from the nozzle exit. Analysis of the extinction data assumed the Rayleigh approximation, ignoring scattering from the particles and ascribing light extinction entirely to absorption. It is known that this approximation may not be altogether valid for agglomerated soot particles (Dobbins and Megaridis 1991; Dobbins et al. 1994; Köylü and Faeth 1994a,b). Nevertheless, the approximation is adequate for the purposes of this study.

The soot volume fraction, F_v, is calculated from the equation:

$$F_v = \{(\lambda/L)*\ln(I_0/I_t)\}/6\pi \text{ Im } (m),$$

where λ is the laser wavelength (488 nm), L is the beam path length (across the plume), I_0 is the beam intensity, I_t is the beam intensity after passing through the plume, and Im (m) is the imaginary part of $\{(m^2 - 1)/(m^2 + 2)\}$.

The complex refractive index was taken to be $m = 1.57 - 0.56i$ (i is the square root of −1). This is the manner in which absorption is represented for a refractive index. It should be noted that this value of the complex refractive index may be appropriate for soot particles, but it is less valid for heterogeneous mixtures of iron combined with soot. Charalampopoulos and colleagues (1992) carried out full Mie[†] scattering calculations for composite particles of iron combined with soot and found that the soot volume fraction inferred from an extinction measurement was affected by the choice of refractive index. The volume fraction of particles above the flame was determined with the refractive index shown above and with a calculated variable refractive index. The inferred volume fractions derived with the composite refractive index were found to be up to twice the values obtained with the refractive index we used. Although the iron loading in the experiments of Charalampopoulos and colleagues (1992) was much higher than in our case, their analysis indicates that our soot volume fractions with iron loading may slightly underestimate the true concentration.

The iron combined with soot emitted by the flame was diluted with a metered flow of air about 300 mm above the nozzle exit. The air was injected through opposing annular holes in a constriction that promoted turbulent mixing of the air and PM. The mixing helped to prevent additional agglomeration. Two dilution chambers brought the ultimate concentration of PM into the range targeted for delivery to the animal exposure chambers. Samples of the diluted PM were withdrawn from the second dilution chamber for analysis with a differential mobility analyzer (model 3080, TSI, Shoreview, MN) and condensation nuclei counter (CNC, model 3010, TSI). Stabilization of the PM concentration was obtained via a feedback system using a second CNC to monitor particle concentration in

[†] Mie scattering theory provides a general description of the elastic scattering of light with small spherical particles. The theory includes the effect of scattering angle, refractive index, and particle size on the intensity of light that is scattered at the same wavelength as the incident radiation. Mie theory is useful in interpreting scattering data in terms of particle size and volume fraction.

samples from the secondary chamber. The output of this CNC was used as an input to the feedback system to control the flow of dilution air. The ultimate soot loading after dilution and delivery to an animal exposure chamber was monitored by direct measurements of soot deposited on a filter. The iron loading was measured by x-ray fluorescence of the filter samples drawn from the exposure chambers.

During the course of our experiments, we decided to discontinue the laser-based measurement of the soot plume. We found it as efficient to monitor particle concentrations using CNC readings at the interface between the primary and secondary chambers, where airflow to the secondary chamber could be adjusted. The CNC provided a rapid measure of particle number and number fluctuations during operation. These readings were used to adjust airflow.

To collect samples from within the flame, beyond the flame, and in the secondary dilution chamber, a stainless-steel probe was constructed from concentric tubes with an innermost diameter of 4 mm. The outer tube is closed at the end so that samples were first drawn into the inner tube. Holes drilled 6 mm from the entrance of the inner tube allowed dilution air to enter from the outer tube. Samples were drawn at 0.8 L/min; with a dilution flow rate of 0.7 L/min. Both flow rates were set by mass flow controllers. The residence time in the probe from the entrance to deposition on a filter was about 0.29 seconds. Samples from the flame were taken during a radial traverse across the middle of the flame toward the edge. Downstream samples were taken from the end of the primary dilution chamber. Samples were also drawn from the secondary dilution chamber at a flow rate of 0.25 L/min.

Ethylene and acetylene are used as the combustion fuels in the diffusion flame system, so trace amounts of soot could be generated along with the iron PM. When only iron particles were desired, conditions were set to minimize soot formation. Iron concentrations were measured using x-ray fluorescence. The chemical composition and stoichiometric form of the iron particles was further determined using electron energy loss spectroscopy (EELS) and x-ray diffraction. EELS allows for the determination of elemental composition, while both EELS and x-ray diffraction provide information on the stoichiometry of individual particles.

PM was collected on grids for TEM and EELS. Samples for TEM were collected on 3-mm carbon-coated copper grids using a point-to-plane electrostatic precipitator and a 5 μA current. Samples for EELS were collected on 3-mm carbon-coated grids with perforations in the carbon film (holey grids), using the same precipitator and current. The TEM examination ensured that particles collected were representative of the actual particle size distribution in the PM.

An EELS–transmission electron microscope (model JEM-200CX, JEOL-USA, Peabody, MA) at the National Center for Electron Microscopy at Lawrence Berkeley National Laboratory (Berkeley, CA) was used to study particles deposited on the edges of the grid holes. Particles with a diameter of 1 to 2 μm were examined with EELS. Although this system could resolve the L2 and L3 peaks, it did not have sufficient resolution (< 1 eV) to resolve the +2 and +3 features with enough accuracy to determine the oxidation state.

The total amount of iron in the mixture was determined via calibrated x-ray fluorescence. This analysis showed that the flame system consistently generated iron concentrations close to the target (50 $\mu g/m^3$). The soot mass concentration was found by weighing 25 mm Teflon-coated filters (Teflo, Pall, East Hills, NY) on a microbalance before and after sample collection. The system consistently yielded soot concentrations close to the target (200 $\mu g/m^3$). Gravimetric analysis of the filter samples showed that the total PM mass concentration was 259 ± 13 $\mu g/m^3$ over a 3-day period. The iron concentration in the samples was measured by x-ray fluorescence to be 46 ± 0.9 $\mu g/m^3$ over the same period.

Because the system was designed to provide PM for animal exposure studies, it was important to ensure that other toxic materials produced in the combustion process were not delivered to the animals. CO concentrations were measured with a nondispersive infrared (NDIR) gas analyzer system (model 880, Beckman Coulter, Fullerton, CA) with a minimum detection limit of 0.1 ppm. In the primary chamber the CO concentration was 5.8 ± 0.6 ppm; in the secondary chamber it was 0.8 ppm to nondetectable. NO_x was measured with a chemiluminescent oxides-of-nitrogen analyzer (model 2108, Dasibi Environmental Corp., Glendale, CA) with a minimum detection limit of 2 ppb. NO_x concentrations in the primary chamber were 4.7 ± 0.1 ppm; in the secondary chamber they were 0.4 ppm to nondetectable. Analyses for PAHs were carried out with filters and a polyurethane cartridge. Samples were extracted from both chambers at a flow rate of 4.0 L/min for 30 minutes. The filters and cartridges were Soxhlet-extracted for 16 hours. The extracts were reduced to 1-mL volumes and analyzed on a gas chromatograph (Model CP-3800, Varian, Palo Alto, CA), using a 30 m × 0.32 μm column (model DB-5MS, Varian). Deuterated phenanthrene and terphenyl were used as internal standards at a concentration of 100 μg/mL in a methyl chloride solution. Only the internal standards could be detected — combustion-produced PAHs were not observed. Hence, CO, NO_x, and PAHs were not expected to affect the toxicity of the aerosol delivered to the animals.

Concentrations of the iron pentacarbonyl vapors generated in the diffusion flame system were difficult to estimate. The vapor pressure of iron pentacarbonyl at 30°C was 40 mm Hg. Since the partial pressure in the argon flow was 40 mm Hg, we assumed the flow in our system was saturated with iron pentacarbonyl vapor. Iron carbonyl decomposes at low temperatures. Because the flame temperature in our system was about 2000°C any pentacarbonyl would have decomposed to CO and Fe. Although we could not analyze for pentacarbonyl in the post-flame gas, it is unlikely that any survived the flame. Therefore, it is unlikely that iron-containing gases were present in the exposure system.

Exposure System

The system used to expose rats to iron PM alone, soot PM alone, or iron combined with soot PM is illustrated in Figures 2 and 3. The particle generation system was directly attached to the exposure system.

During exposure periods the wire-top lid was replaced with a sealed top and high-efficiency airflow system to deliver PM by unidirectional flow. It also included the dilution valve, secondary dilution chamber, and equipment for monitoring particle number and size. The concentration of iron in the boxes was monitored by collecting air samples on Teflon filters analyzed by x-ray fluorescence.

Rats were exposed to PM by whole-body exposure for 6 hours per day for 3 consecutive days. The mean temperature during each exposure period was 21°C (± 1°), with a relative humidity ranging from 20% to 50%. During exposures, animals were provided with food pellets but no water. The boxes contained a special low-dust bedding (pelleted paper bedding 7084, Harlan Techlad, Madison, WI) to minimize and reduce wetness and ammonia waste. A total of 172 animals were used in this study, including 96 young adult male rats, 160 neonatal rats from 16 pregnant dams. Table 1 shows how these rats were allocated to the biologic endpoint studies. Within each age group, assignment to the studies was random.

Exposure Protocol

Our studies aimed to define the injury to the rat lung resulting from whole-body exposure to iron combined with soot PM, iron PM, and soot PM. Animals from each exposure scenario were divided into two groups, one to contribute bronchoalveolar lavage (BAL) fluid samples and one for lung homogenate samples. The BAL and lung homogenate samples were examined for a variety of endpoints.

Four exposure scenarios were tested in healthy young adult rats: (1) iron combined with soot PM, (2) iron PM, (3) soot PM, and (4) filtered air (control). Total target particle concentrations were designed to not exceed an average of 250 $\mu g/m^3$/day for 3 days. Exposures to iron PM alone were designed to not exceed 100 $\mu g/m^3$/day for 3 days. Pulmonary response to exposure was evaluated after each exposure protocol was completed. BAL evaluations were performed within two hours; lung tissue biochemistry and histopathology evaluations were performed within 24 hours.

Neonatal rats were exposed at ages 10 to 12 days and again at 23 to 25 days in three exposure scenarios: (1) iron combined with soot PM at 30 ± 7 $\mu g/m^3$/day for 3 days (low-dose); (2) iron combined with soot PM at 100 ± 28 $\mu g/m^3$/day for 3 days (high-dose); and (3) filtered air control. The various endpoints examined allowed us to determine the effects of iron combined with soot PM exposure after critical stages of lung development. The lungs of rats 4 to 14 days of age undergo dramatic growth; lung size doubles every 4 to 6 days because of intense cellular proliferation (Dietert et al. 2000). By 21 to 28 days of age, cell proliferation in the lungs has slowed, but the lungs continue to grow as the animal grows (Dietert et al. 2000). Exposure to iron combined with soot PM during these critical stages of lung development may have immediate and lasting adverse effects on the respiratory system (Pinkerton et al. 2000).

BRONCHOALVEOLAR LAVAGE

Preparation

The BAL procedure followed the Harrod protocol (Harrod et al. 1998). Within 2 hours of completing the 3-day exposure protocol, rats were anesthetized with sodium pentobarbital (Nembutal, Cardinal Health, Sacramento, CA). The trachea was exposed, cannulated, and secured with a suture. The lungs were lavaged four times with a single volume of phosphate-buffered saline (Dulbecco PBS, Mg^{2+} and Ca^{2+}-free, pH 7.4, GibcoBRL, Grand Island, NY), 35 mL/kg body weight.

Cell Number, Viability, and Differentials

A hemocytometer was used to count the total number of cells in BAL fluid samples from each rat. Cell viability was determined by trypan blue exclusion while doing total cell counts with the hemocytometer. Samples containing at least 5×10^4 cells were divided and centrifuged at 1500 rpm (~200*g*) for five minutes in duplicate vials using a cytospin (model 3, Shandon Instruments, Pittsburgh, PA). The cell layer from each vial was smeared onto a glass slide and stained with Hema 3 (Fisher Scientific Co., Swedesboro, NJ). A minimum of 500 cells were counted from each slide

Table 1. Animal Allocation by Age Group and PM Exposure Group for Each Biologic Endpoint in BALF and Lung Tissue[a,b]

	Young Adult Male Rats (*n*)				26 Day Neonatal Rats (*n*)	
	Iron 57 PM ($\mu g/m^3$)	Iron 90 PM ($\mu g/m^3$)	Iron 45 Combined with Soot Total PM = 250 ($\mu g/m^3$)	Soot 250 PM ($\mu g/m^3$)	Iron 30 Combined with Soot Total PM = 250 ($\mu g/m^3$)	Iron 100 Combined with Soot Total PM = 250 ($\mu g/m^3$)
BALF						
Viability	8	8	8	8	8	8
Protein	8	8	8	8	8	8
LDH	8	8	8	8	8	8
GST	8	8	8	8	8	8
FRAP	8	8	8	8	8	8
GSSG	7	8	8	8	8	8
GRR	8	8	8	8	8	8
NO	8	8	8	8	—	—
Lung tissue						
Ferritin	—	—	4	4	4	4
FRAP	—	—	4	4	8	8
GST	8	8	8	8	8	8
GSSG	8	8	8	8	8	8
GSH	8	8	8	8	8	8
GRR	8	8	8	8	8	8
NO	8	8	—	—	—	—
NF-κB	4	4	4	4	4	4
IL-1β	6	6	—	—	6	6
TNF-α	6	6	—	—	6	6

[a] For each PM exposure group, an equal number of control animals were analyzed at the same time.

[b] Definition: — indicates biologic endpoint not determined.

to determine the proportion of macrophages, lymphocytes, and neutrophils (differentials).

Total Protein and Lactate Dehydrogenase Assays

Measurement of total protein in the supernatant of BAL fluid samples was performed by a modified Bradford (1976) assay according to the manufacturer's instructions (BioRad, Hercules, CA) with bovine serum albumin as the standard. The amount of LDH was measured using a colorimetric assay kit (Sigma-Aldrich, St. Louis, MO) based on the activity of LDH released from the cytoplasm of damaged cells into the BAL fluid supernatant.

BIOCHEMICAL ASSAYS IN LUNG TISSUE

Preparation

Lungs were immediately removed from the thorax and frozen in liquid nitrogen. Twenty-four hours later, a portion of the lung tissue was homogenized in 0°C Tris-hydrochloride (HCl) buffer (25 mM Tris, 1 mM EDTA, 10% glycerol, 1 mM dithiothreitol, pH 7.4) with a glass homogenizer. The homogenate was centrifuged at 10,000*g* for 20 minutes at 4°C. The supernatant and sediment fractions were separated. The supernatant was divided into aliquots, stored at −70°C, and used for biochemical analyses.

The sediment was collected and washed three times with Tris-HCl buffer containing Triton X-100 and then washed once in just the buffer. Nuclear protein was extracted with buffer C (20 mM HEPES, 25% glycerol, 0.42 M NaCl, and 1 mM EDTA) by centrifuging at 50,000*g* for 30 minutes and collecting the supernatant.

To obtain supernatant for the glutathione (GSH) assay, a portion of the frozen lung tissue was homogenized in 0°C Tris-HCl buffer and 6% metaphosphoric acid with a glass homogenizer. The homogenate was centrifuged at 10,000*g* for 20 minutes at 4°C. The supernatant and sediment fractions were separated. The supernatant was divided into aliquots, and stored at −70°C, the sediment fraction was discarded.

Glutathione Assay

Glutathione content of lung tissue supernatant was measured by an enzymatic method (Tietz 1969; Anderson 1985), using the 5,5′-dithio-bis (2-nitrobenzoic) acid-oxidized glutathione reductase recycling assay. The reduced GSH contained in the supernatant described above was oxidized by 5,5′-dithio-bis(2-nitrobenzoic) acid to yield GSSG (oxidized GSH) with stoichiometric formation of 5-thio-2-nitrobenzoic acid. The rate of 5-thio-2-nitrobenzoic acid formation was measured at 412 nm and was proportional to the sum of GSH and GSSG present. GSSG was reduced to GSH by the action of glutathione reductase and NADPH. GSSG content was determined after treatment for derivatization with 2-vinylpyridine.

Glutathione-S-Transferases Assay

Glutathione-S-Transferases (GST) enzyme activity of lung tissue supernatant was measured spectrophotometrically using the standard substrate 1-chloro-2,4-dinitrobenzene, as described by Habig and colleagues (1974). The activity was reported as micromoles of 1-chloro-2,4-dinitrobenzene conjugated with GSH per minute per milligram protein, as monitored by the rate change in absorbance at 340 nm at 25°C. The reaction rate was determined by subtracting the background rate of conjugation in the absence of the enzyme from the rate in the presence of the enzyme.

Nitric Oxide Assay

The free radical nitric oxide (NO) is rapidly oxidized to stable metabolites, nitrite and nitrate. This sum concentration was determined with nitrate reductase followed by the Greiss reagent, which reacts with nitrite, but not nitrate, to yield a diazo chromophore. NO was quantified using the absorbance at 540 nm of identically processed nitrate standards. The enzymatic recovery of nitrate standards was evaluated by comparing the absorbance of nitrate standards with those of nitrite.

Malondialdehyde Assay for Lipid Peroxidation

Malondialdehyde (MDA) is one of the end products derived from the peroxidation of polyunsaturated fatty acids and related esters. MDA in the lung tissue supernatant was measured using a lipid peroxidation kit (Calbiochem, San Diego, CA). MDA measurement is based on the reaction of a chromogenic reagent (N-methyl-2-phenylindole) with MDA at 45°C. Condensation of one molecule of MDA reacts with two molecules of N-methyl-2-phenylindole and yields a stable chromophore with a maximal absorbance at 586 nm.

Ferric Reducing Antioxidant Power Assay

Total antioxidant power in lung tissue supernatant was determined by the ferric reducing antioxidant power (FRAP) assay (Benzie and Strain 1999). At low pH, ferric tripyridyltriazine complex is reduced to the ferrous form and monitored by measuring the change in absorption at 593 nm. The change in absorbance is directly related to the total reducing power of the electron-donating antioxidants present in the reaction mixture.

Cytokine Assays

The amounts of the proinflammatory cytokines IL-1β and tumor necrosis factor-α (TNF-α) were assessed in lung tissue supernatant by rat enzyme-linked immunosorbent assay kits according to the manufacturer's instructions (R&D System, Minneapolis, MN). A 1:2 dilution of samples into the calibrator diluent provided in the kit was used for cytokine determination. Quantitation of cytokines was normalized to total protein in the sample.

Ferritin Assays

Western blotting was used to measure ferritin protein levels in the lungs. Samples of the lung homogenate supernatant were loaded and separated on 12% SDS-PAGE followed by transblotting to a polyvinylidenedifluoride membrane (ImmunBlot PVDF, Bio-Rad, Hercules, CA). The membrane was then probed with primary antibody against human ferritin (rabbit anti-human ferritin polyclonal antibody, Dako, Carpinteria, CA) at a dilution of 1:1000. Secondary antibody (horseradish peroxidase–linked goat anti-rabbit immunoglobulin G, Santa Cruz Biotech, Santa Cruz, CA) was added at 1:3000 dilution. The blots were subsequently developed using an enhanced chemiluminescence detection kit (Amersham Pharmacia Biotech, Piscataway, NJ). After exposure on autoradiography film, immunoreactive protein bands were quantified by densitometry.

NF-κB DNA BINDING ACTIVITY

Electrophoretic mobility shift assay (EMSA) was performed to determine NF-κB DNA binding activity in the supernatant containing the nuclear protein. The oligonucleotide used as a probe (Promega, Madison, WI) for EMSA

is double-stranded DNA containing NF-κB consensus sequence (5′-CCTGTGCTCCGGGAATTTCCCTGGCC-3′) labeled with [α-^{32}P] 2′-deoxyadenosine 5′-triphosphate using T4 polynucleotide kinase. The binding reaction of nuclear proteins to the probe was assessed by incubation of mixtures containing 5 μg nuclear protein, 0.5 μg polydeoxyinosinic-polydeoxycytidylic acid) and a 40,000 cpm ^{32}P-labeled probe in the binding buffer (7.5 mM HEPES, 35 mM NaCl, 1.5 mM magnesium chloride, 0.05 mM EDTA, 1 mM dithiothreitol, 7.5% glycerol) for 30 minutes at 25°C. For the competitive assay, excess unlabeled oligonucleotides were incubated with proteins before using the radiolabeled probe. Protein-DNA binding complex was separated by 5% polyacrylamide gel electrophoresis and autoradiographed overnight.

CYTOCHROME P450 ISOFORMS ASSAY

The presence of 3 major isoforms of cytochrome P450: CYP1A1, CYP2B1, and CYP2E1, were determined by immunoblotting analyses (Laemmli 1970; Towbin et al. 1979). Briefly, the supernatant was heated for 5 minutes at 95°C to denature the microsomal proteins. The tissue supernatant was then centrifuged at 105,000*g* for 75 minutes. The microsomal protein fraction was separated in 10% SDS-PAGE and electroblotted onto nitrocellulose membranes. Membranes were blocked for 1 hour at 25°C in Tris-buffered saline containing 0.1% Tween 20 and 5% nonfat dry milk, and then incubated with primary polyclonal goat anti-rat CYP1A1, CYP2B1, and CYP2E1 antibodies in blocking buffer. After washing with Tris/NaCl/Tween 20, the membranes are incubated with a horseradish peroxidase–conjugated secondary antibody. After further washing in Tris/NaCl/Tween 20, the blots were developed by the in situ enhanced chemiluminescence reagent (Super Signal West Pico Chemiluminescent Substrate, Pierce, Rockford, IL) according to the manufacturer's instructions and quantitated by image densitometry.

BROMODEOXYURIDINE AND MORPHOMETRIC ANALYSES

Bromodeoxyuridine Labeling to Assess Cell Proliferation

5-bromo-2-deoxyuridine (BrdU), a thymidine analog, is incorporated into DNA by cells undergoing DNA synthesis. Its presence indicates cell proliferation and is a marker for cell repair. In young adult rats, miniosmotic pumps containing BrdU (Sigma-Aldrich Chemical Co., St. Louis, MO) at 30 mg/mL in physiologic buffered saline were implanted subcutaneously one day before the start of each exposure.

One day after the end of the exposure, animals were anesthetized with an overdose of sodium pentobarbitol. The abdomen was opened by midline incision and exsanguinated via the systemic aorta. Lungs were fixed by inflating through the trachea with 4% paraformaldehyde (Z-Fix, Anatech Ltd, Battle Creek, MI), at a constant pressure of 30 cm H_2O and transferred into 70% ethanol, dehydrated in 95% and 100% ethanol. Tissues were embedded in paraffin (Paraplast-20, Fisher Scientific, Pittsburgh, PA) and prepared as 5-μm-thick sections using a microtome (Microm Laborgeräte GmbH, Waldorf, Germany).

For BrdU assays in neonatal rats, rats exposed to either filtered air or iron (100 μg/m^3) combined with soot PM from days 10–12 after birth received an intraperitoneal injection of 20 mg/mL BrdU two hours prior to being killed on day 13. The lungs were fixed as described for young adult rats, but with 1% paraformaldehyde and 0.1% glutaraldehyde. After fixation, the left lobe was cut into three pieces, embedded in paraffin, and prepared as 5-μm-thick sections.

Bromodeoxyuridine Assay

Incorporated BrdU was detected using a monoclonal antibody and immunocytochemical techniques using the avidin-biotin peroxidase method. Endogenous peroxidase activity was blocked with 3% hydrogen peroxide in water, followed by an incubation with pronase (5.4 units/mg; 0.1 mg/mL for 30 minutes at 37°C) until the activity was stopped with undiluted calf serum. Sections were incubated overnight at 4°C with a primary antibody (mouse monoclonal anti-BrdU, Dakopatts, Kyoto, Japan), washed in PBS, incubated for 30 minutes at 20°C with a secondary antibody (biotinylated rabbit anti-mouse immunoglobulin that was absorbed with rat cells), washed in PBS, incubated for 30 minutes at 20°C according to the manufacturer's directions using a Vectastain ABC kit (Vector Labs, Burlingame, CA), washed in PBS, and incubated 3 to 5 minutes with diaminobenzidine as the chromogen substrate with hydrogen peroxide. Standard controls were included to ensure no artifactual immunohistochemical staining of tissue sections. The primary antibody was replaced with: (1) PBS, biotinylated equine anti-rabbit immunoglobulin G or antibody-conjugated horseradish peroxidase; or (2) normal serum. Counterstaining was done with methylene blue and basic fuchsin.

Evaluation of BrdU Cell Labeling

These studies were designed to examine cell proliferation as a marker of injury and repair after short-term exposure to particles in neonatal and young adult Sprague Dawley rats. Regions of lung parenchyma were selected at random. Lung tissue sections were coded so that the morphometric analysis was done without knowledge of the

experimental treatments. The labeling index was calculated as the percentage of BrdU-positive stained epithelial cells of the total number of epithelial cells counted. Duodenum samples were used as controls for the lung samples.

Sections were examined by light microscopy to determine the labeling index of BrdU in terminal bronchioles, proximal alveolar regions, and lung parenchyma. Labeling indices were determined for the following regions of the respiratory tract — the alveolar zone, terminal bronchioles, respiratory bronchioles, intrapulmonary large airways, and trachea. In the alveolar zone, 500 to 1000 cells per lung were counted in randomly selected fields. Cells were differentiated into type II epithelial cells (identified by their cuboidal shape and by being located mostly in the corners of the alveoli), type I epithelial cells (long, elongated flat nuclei), and cells in the alveolar wall (endothelial and interstitial cells) according to established criteria (Witschi and Morse 1983). As in our previous studies (Rajini et al. 1993), all epithelial cells in randomly selected conducting airways were counted. In young adult rats, terminal bronchioles were identified by their opening into alveolar ducts and intrapulmonary large airways by their diameter (0.5–1.5 mm). In neonatal rats, terminal bronchioles were defined as the last conducting airway opening onto an alveolar duct (Figure 4). Proximal alveolar regions were defined as all alveoli within 300 µm of the bronchiole-alveolar duct junction (Figure 5).

Microdissection and Morphometry of the Central Acinus

En bloc tissue microdissection of the pulmonary acinus was used to examine tissue changes after PM exposure. The method is highly sensitive and can characterize histologic changes in the ventilatory unit of the lung (the centriacinar region composed of the terminal bronchiole and proximal alveolar ducts and alveoli) (Figures 4–5).

Animals were anesthetized with an overdose of sodium pentobarbitol. The abdomen was opened by midline incision and exsanguinated via the systemic aorta. To obtain the lungs, the trachea was exposed with a midline incision in the neck and cannulated at the larynx. The thorax was collapsed via incision through the diaphragm, and the rib cage was opened anteriorally. Lungs were fixed as described for BrdU.

Slabs of fixed lung tissue were embedded in deep wells, serially cut into 1-mm slices, and examined under a dissecting microscope (Pinkerton et al. 1992). Briefly, terminal bronchiole–alveolar duct junctions oriented longitudinally in the sections were identified, isolated, and mounted on blank beam stubs for additional sectioning. Sections were cut until the long axes of at least two alveolar ducts were identified in the sections. Morphometric analysis consisted of superimposing concentric arcs at 100-µm intervals from the center point of the junction between the most proximal alveolus and the bronchiolar epithelium. At the intersection of each arc with the epithelium, the thickness and cellular characteristics of the epithelium were quantified. We successfully applied this morphometric analysis to a number of ozone-exposure regimens and identified a close relation between calculated ozone dose at site and degree of injury (Pinkerton et al. 1992).

IRON MOBILIZATION

The amount of iron mobilized in 24 hours from iron combined with soot PM was determined as previously described by Lund and Aust (1990), Aust and Lund (1991), Smith and Aust (1997), and Smith and colleagues (1998) with the following modifications. Particles, on filters, were suspended in 50 mM NaCl (1 mg/mL) at a pH of 7.5. The

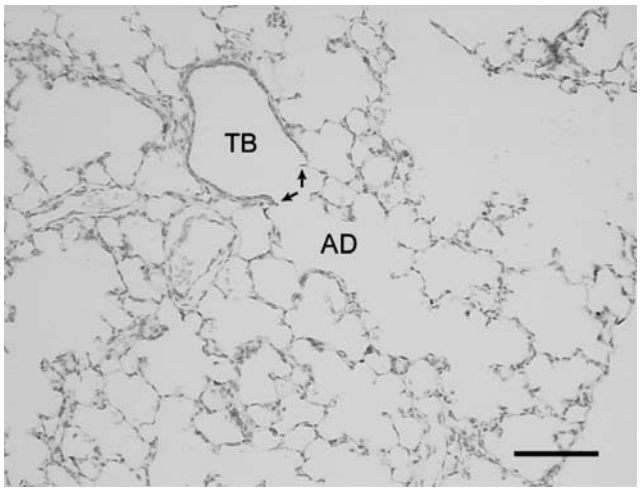

Figure 4. Light micrograph of the terminal bronchiole–alveolar duct (TB-AD) junction in a 13-day old neonatal rat lung. The scale bar is 100 µm.

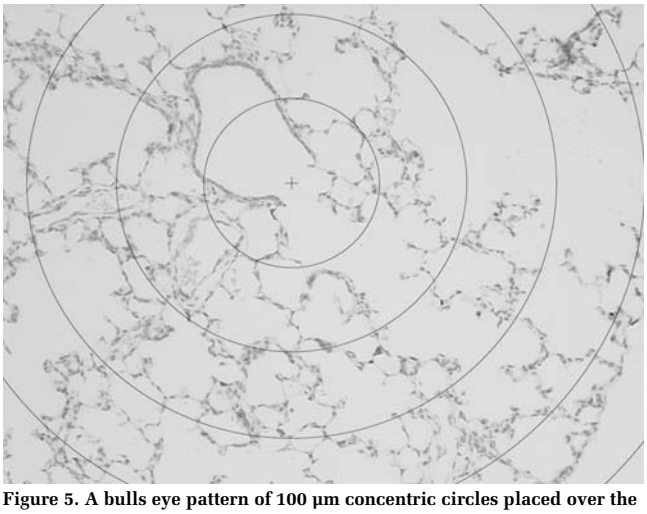

Figure 5. A bulls eye pattern of 100 µm concentric circles placed over the TB-AD junction shown previously. These concentric circles serve as a guide for the relative distance parenchymal tissues are found from the TB-AD junction.

samples were mixed by vortexing for 30 seconds, citrate was added to obtain a final concentration of 1 mM, and all samples were placed on an orbital shaker for 24 hours. After 24 hours, a 1.0 mL sample was withdrawn and centrifuged at 13,300*g* for 8 minutes to remove the particles. The amount of iron mobilized as the citrate–Fe complex in the supernatant was determined as originally described by Brumby and Massey (1967) for nonheme iron determination, except that ferrozine (0.4%, w/vol) was used instead of 1,10-phenanthroline. The pH was readjusted at regular intervals throughout the incubation period to prevent changes in the rates of iron mobilization. The concentration of iron mobilized by citrate is reported as nmol of Fe per milligram of particles.

STATISTICAL ANALYSIS

Data from the three experiments were analyzed independently. In all cases, the data were analyzed using analysis of variance (ANOVA). Before ANOVA, data were tested for homogeneity of variance using the Bartlett test. The results of this test were examined over the Tukey ladder of powers ranging from −3 to +2. The data were transformed as needed. The posthoc Levene test was run with the ANOVA. Any Bartlett transformations still not normalized by the Levene test were changed until an appropriate statistical transformation was found.

The endpoints were classified as a cytotoxic, oxidative-stress, or proinflammatory response. Within each classification, one or two endpoints considered most likely to reflect the toxic insult were treated as the primary variable or variables. The other end points were treated as secondary to the primary variables. This strategy was used to aid interpretation of the statistical results of a large number of tests.

RESULTS

EXPOSURE TO IRON PM IN YOUNG ADULT RATS

Particle Characterization

For experiments with exposure to iron PM, two concentrations of iron PM were generated, 57 μg/m^3 and 90 μg/m^3. The majority of iron particles generated were ultrafine (< 0.1 μm in aerodynamic diameter) (Figure 6, panel A), and stoichiometric composition was determined by EELS (Figure 6, panels B & C). Many particles were polyhedrons (Figure 6, panel A). In general, isolated iron particles were complexed with oxygen (Figure 6, panel B);

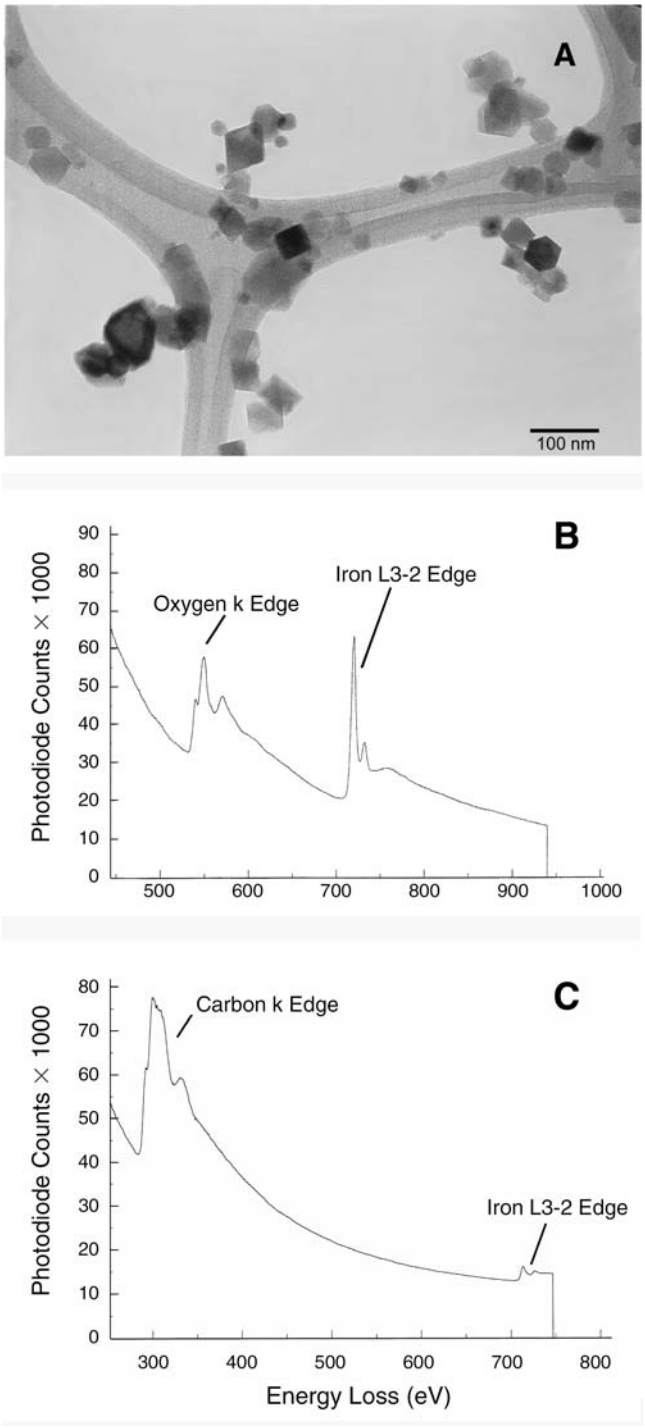

Figure 6. Ultrafine iron particles generated under diffusion flame conditions. (A) Transmission electron micrograph of a holey carbon-coated grid containing particles collected from the exposure unit. Many of these particles were hexagonal or rhomboidal. **(B)** EELS spectrum obtained from a single particle showing both oxygen and iron peaks. The ratio of the areas under the curve of these peaks is 0.66, which suggests a stoichiometric formula of Fe_2O_3. **(C)** EELS spectrum for a single particle showing peaks for iron and carbon but not oxygen. This type of particle was relatively rare.

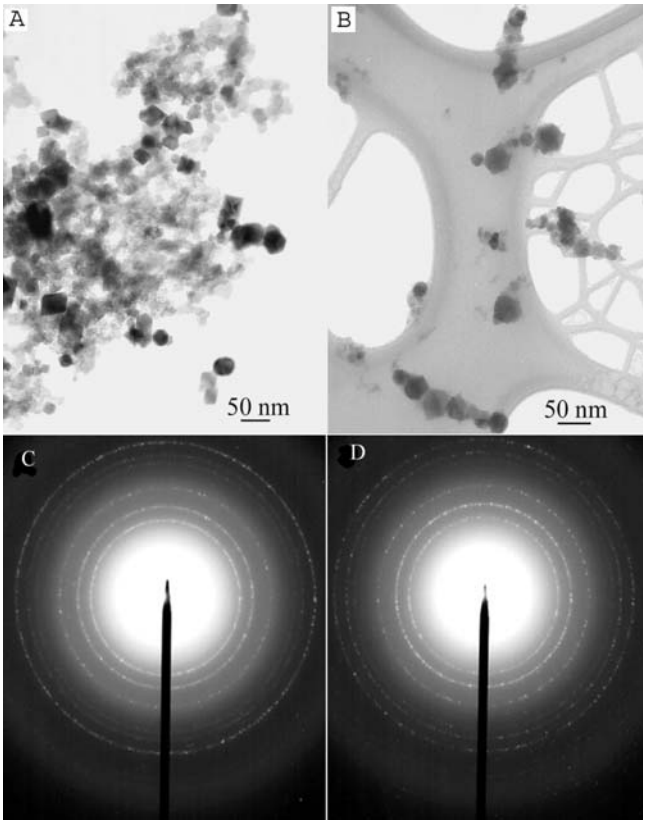

Figure 7. Bright-field transmission electron micrographs of (A) Iron combined with soot sample and (B) Iron sample. Iron oxide crystals are 10 to 50 nm in diameter. Note the presence of more soot and larger iron oxide/soot agglomerates in the iron combined with soot sample. **(C)** Selected area diffraction patterns for the iron combined with soot sample and **(D)** Selected area diffraction patterns for the iron sample. In both C and D the diffraction patterns match the γ-Fe_2O_3 (maghemite) phase.

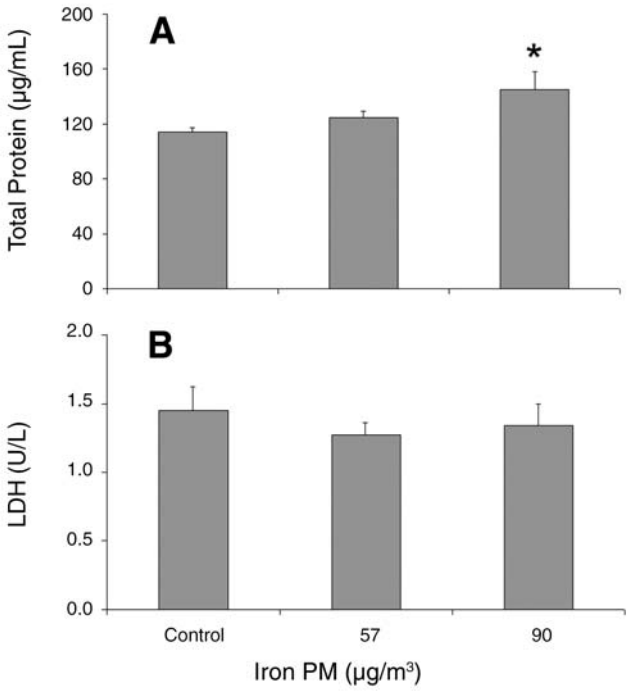

Figure 8. (A) Total protein and **(B) LDH in BALF from young adult rats exposed to iron PM.** Values are means ± SE; n = 8/group. *Significant difference ($P < 0.05$) from filtered air control.

occasional particles were complexed with carbon (Figure 6, panel C). Although a limited number of particles could be analyzed by TEM and EELS, we found the iron-to-oxygen ratio for these particles was consistent with the stoichiometry of Fe_2O_3. Since the completion of this study, further analysis by x-ray diffraction and EELS has shown that the majority of iron oxide particles formed are gamma maghemite (Figure 7).

Further analysis of iron combined with soot PM from the diffusion flame system, after completion of all exposure studies, allowed for additional characterization of the soot. Samples collected on filters from the secondary dilution chamber were analyzed for EC and OC. The soot was found to be 60% EC and 40% OC. However, the specific chemical composition of the OC is not known.

Cytotoxicity Assessments

Inhalation of 90 µg/m^3 iron (compared with 57 µg/m^3 iron or filtered air) was associated with a significant increase in total protein in the lavage fluid (Figure 8, panel A). However, no significant increase in LDH activity was noted in either group exposed to iron (Figure 8, panel B). No significant changes were observed in total cell number, cell viability, or cell differentials in BAL fluid after exposure of animals to either iron PM concentration compared with the control (filtered air) group (Table 2).

Table 2. Cell Number, Viability, and Differentials in BALF of Young Adult Male Rats After Exposure to Iron Particles[a]

Control or PM Exposure Group	Total Cell Number ($\times 10^6$)	Viability (%)	Macrophage (%)	Lymphocyte (%)	Neutrophil (%)
Control (filtered air)	2.24 ± 0.28	82 ± 1	98.8 ± 0.2	0.9 ± 0.2	0.3 ± 0.1
Iron					
57 μg/m^3	2.51 ± 0.11	79 ± 2	98.7 ± 0.2	0.6 ± 0.2	0.32 ± 0.1
90 μg/m^3	2.70 ± 0.23	80 ± 2	99.1 ± 0.2	0.6 ± 0.1	0.4 ± 0.1

[a] Values are mean ± SEM (n = 8 per group).

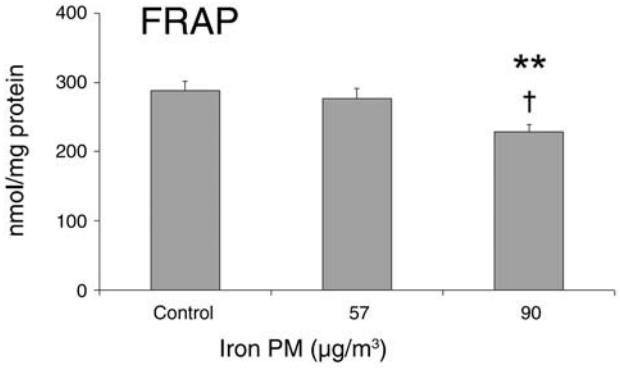

Figure 9. Total antioxidant power (FRAP value) in lung tissue supernatant from young adult rats exposed to iron PM. Values are means ± SE; n = 8/group. **Significant difference ($P < 0.01$) from control. †Significant difference ($P < 0.05$) from exposure to 57 μg/m^3 iron.

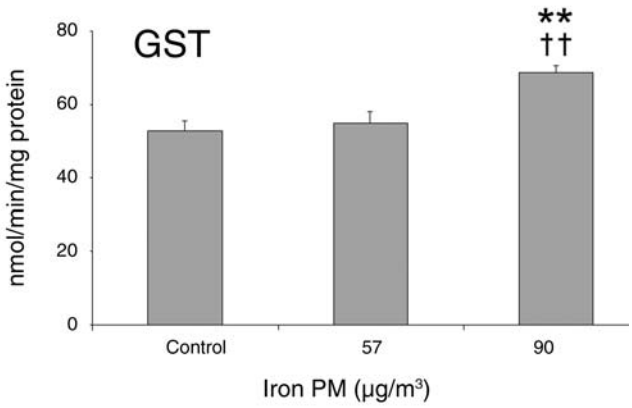

Figure 10. GST activity in lung tissue supernatant from young adult rats exposed to iron PM. Values are means ± SE; n = 8/group. **Significant difference ($P < 0.01$) from control. ††Significant difference ($P < 0.01$) from animals exposed to 57 μg/m^3 iron.

Oxidative Stress

Three endpoints that indicate oxidative stress, total antioxidant power, GST activity, and intracellular GSH concentrations were analyzed in the supernatants of lung tissue homogenates. FRAP assay values show a statistically significant decrease in total antioxidant power after exposure to 90 μg/m^3 iron compared with exposure to 57 μg/m^3 iron or to filtered air (Figure 9). Rats exposed to 90 μg/m^3 iron had a significant induction of GST activity compared with rats exposed to 57 μg/m^3 iron or to filtered air (Figure 10). Although a trend of increasing GSH and GSSG was noted in rats after 90 μg/m^3 iron exposure, no statistically significant changes in the amounts of GSH or GSSG were observed compared with rats exposed to 57 μg/m^3 iron or to filtered air (Figure 11).

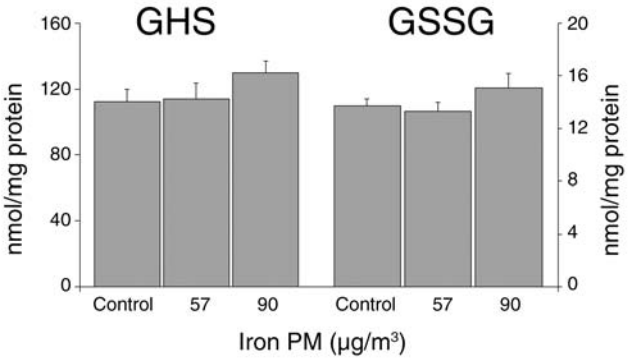

Figure 11. Intracellular GSH and GSSG in lung tissue supernatant from young adult rats exposed to iron PM. Values are means ± SE; n = 8/group.

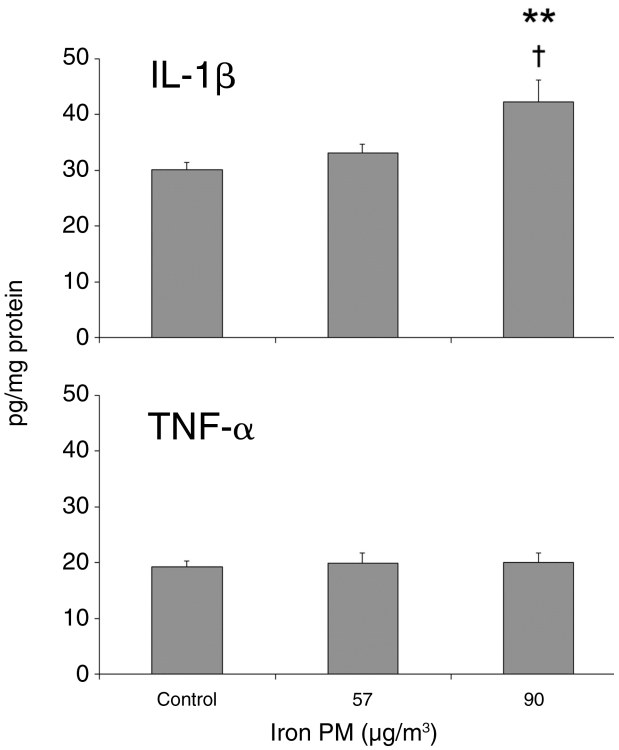

Figure 12. Protein concentrations of IL-1β and of TNF-α in lung tissue supernatant from young adult rats exposed to iron PM. Values are means ± SE; $n = 6$/group. **Significant difference ($P < 0.01$) from control. †Significant difference ($P < 0.05$) from animals exposed to 57 μg/m^3 iron.

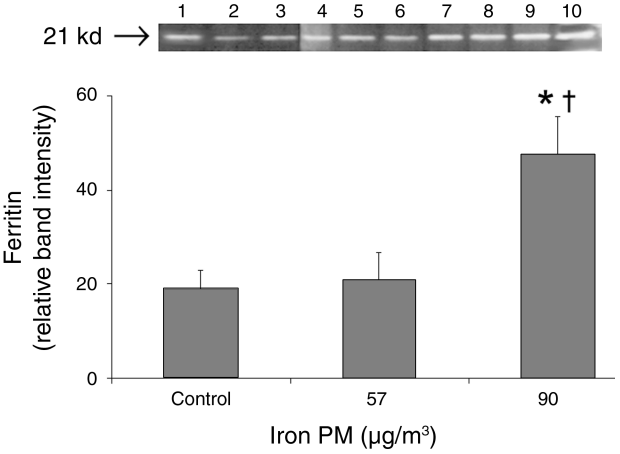

Figure 13. Intracellular ferritin protein concentrations in lung tissue supernatant from young adult rats exposed to iron PM. (A) Lanes 1–3: Western blot of 25 μg protein samples from control rats. **Lanes 4–6:** Western blot of 25 μg protein samples from rats exposed to 57 μg/m^3 iron PM. **Lanes 7–9:** Western blot of protein samples from rats exposed to 90 μg/m^3 iron PM. **Lane 10:** Positive control. Samples were loaded into lanes and separated by SDS-PAGE through a 12% gel. Bands represent the sample at the position for about 21 kd molecular weight. **(B)** Quantification of ferritin was analyzed by image densitometry. Ferritin content in rats exposed to 90 μg/m^3 iron PM was increased 2.5-fold and 2.3-fold compared with control and with rats exposed to 57 μg/m^3 iron PM, respectively ($n = 3$). *Significant difference ($P < 0.05$) from control. † Significant difference ($P < 0.05$) from rats exposed to 57 μg/m^3 iron PM.

Proinflammatory Cytokines

Proinflammatory cytokines IL-1β and TNF-α are markers of inflammatory response in lung tissue. IL-1β was significantly increased in lung tissue supernatants of rats exposed to 90 μg/m^3 iron compared with those of rats exposed to 57 μg/m^3 iron or to filtered air (Figure 12). No difference in TNF-α was found between groups (Figure 12).

Ferritin

We determined ferritin content by Western blot (Figure 13) to obtain a quantitative comparison of the amount of ferritin in the supernatant of lung tissue homogenate from rats exposed to iron particles. Exposure to 90 μg/m^3 iron resulted in a significant increase in intracellular ferritin content compared with exposure to 57 μg/m^3 iron (2.3-fold) or to filtered air (2.5-fold). No significant difference

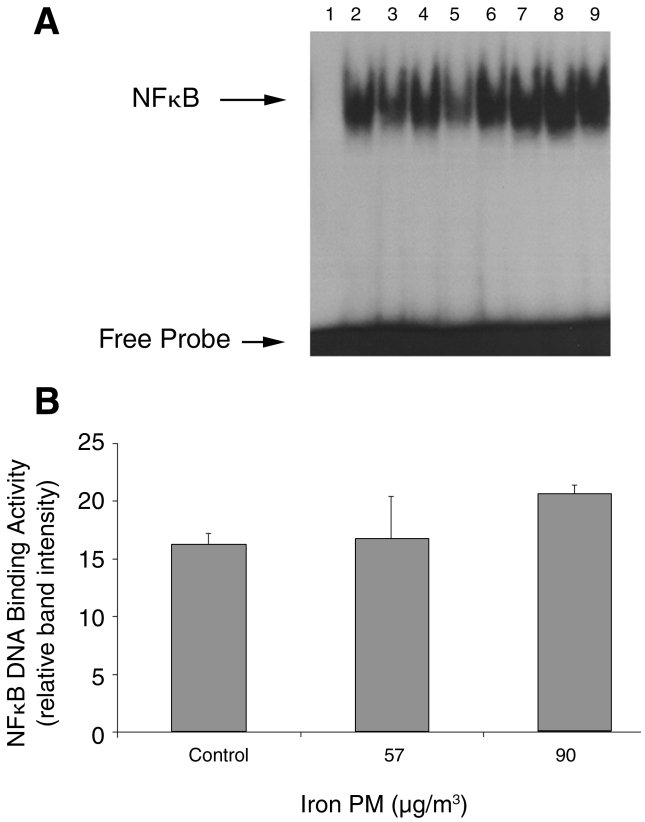

Figure 14. NF-κB DNA binding activity in nuclear extracts from lung tissue of young adult rats exposed to iron PM. (A) Nuclear extracts prepared from lung tissue and subjected to EMSA for ^{32}P-labeled NF-κB oligonucleotide binding. The specificity of NF-κB binding activity was tested by adding to the nuclear extract a 100-fold molar excess of unlabeled competing NF-κB DNA probe and incubating for 20 min before adding radiolabeled NF-κB DNA probe. **Lane 1:** unlabeled probe; **Lanes 2–4:** control; **Lanes 5–6:** 57 μg/m^3 iron PM; **Lanes 7–9:** 90 μg/m^3 iron PM. Bands were analyzed by densitometry. **(B)** A 1.3-fold increase in NF-κB DNA binding activity was noted after exposure to 90 μg/m^3 iron PM ($P = 0.10$).

in ferritin content was noted between rats exposed to 57 μg/m^3 iron or filtered air.

NF-κB DNA Binding Activity

EMSA was performed to measure NF-κB DNA binding activity in the nuclear fraction of lung tissue homogenate. A 1.3-fold increase in NF-κB DNA binding activity was observed in samples from rats exposed to 90 μg/m^3 iron compared with controls (Figure 14). This increase was not statistically significant ($P = 0.10$).

Statistical Summary

The results of the statistical analyses are shown in Table 3. Before ANOVA, data were tested for homogeneity

Table 3. Statistical Test Results for Young Adult Male Rats Exposed to Iron Particles[a]

		Statistical Tests					
					F Test		Trend Test
Sample / Effect Biologic Endpoint	Required Transformations	Bartlett	Levene	MSE	Single Factor	*P* Value	*P* Value
BALF / cytotoxicity							
LDH	None	0.27	0.5	1.67×10^{-1}	0.43	0.6566	0.58
Lymphocytes (%)	None	0.12	0.21	2.20×10^{-1}	1.34	0.2827	0.16
Macrophages (%)	None	0.66	0.69	3.04×10^{-1}	1.59	0.2273	0.19
Neutrophils (%)	None	0.88	0.9	2.11×10^{-2}	1.07	0.3613	0.18
Protein	−Recip		0.07	5.95×10^{-10}	1.45	0.2579	0.14
Viability (%)	None	0.2	0.44	24	0.81	0.4573	0.37
Total cell number ($\times 10^6$)	None	0.07	0.09	3.84×10^{-1}	1.11	0.3466	0.15
BALF / oxidative stress							
FRAP	−Recip		0.22	2.22×10^{-4}	0.10	0.9040	0.72
GSH	None	0.19	0.37	7.97×10^{-2}	0.70	0.5058	0.81
GSSG	None	0.12	0.35	1.12×10^{-3}	0.82	0.4540	0.51
GST	None	0.08	0.07	214	0.42	0.6595	0.43
GRR	None	0.13	0.1	2.60×10^{-3}	1.06	0.3632	0.44
BALF / proinflammatory							
NO	None	0.28	0.25	1.41×10^{-1}	1.22	0.3150	0.19
Lung tissue / proinflammatory							
IL-1β	−Recip	0.62	0.19	1.60×10^{-5}	7.83	0.0047[b]	0.00[b]
TNF-α	None	0.46	0.49	14	0.06	0.9416	0.74
NO	−Recip		0.1	27,310,377	1.29	0.2969	0.69
Lung tissue / oxidative stress							
FRAP	None	0.64	0.36	1443	5.38	0.0130[b]	0.01[b]
GSH	None	0.8	0.82	579	0.92	0.4159	0.23
GSSG	None	0.18	0.09	5.18	1.37	0.2768	0.24
GST	None	0.58	0.39	50	11.63	0.0004[b]	0.00[b]
GRR	None	0.78	0.67	7.84×10^{-4}	0.05	0.9469	0.74
MDA	None	0.99	0.99	2.77×10^{-3}	1.74	0.2005	0.08

[a] Definitions: MSE indicates mean squares due to error; −Recip indicates a negative reciprocal transformation.

[b] Statistically significant.

Table 4. Means and Standard Errors for Young Adult Male Rats Exposed to Iron Particles[a]

Sample / Effect Biologic Endpoint	Control			Iron Exposure					
				57 μg/m^3			90 μg/m^3		
	Mean	SE	*N*	Mean	SE	*N*	Mean	SE	*N*
BALF / cytotoxicity									
LDH	1.454	0.173	8	1.266	0.092	8	1.338	0.156	8
Viability (%)	82.213	1.029	8	79.225	1.887	8	79.975	2.074	8
Protein	114.500	2.904	8	124.525	4.555	8	145.100	13.224	8
Total cell number ($\times 10^6$)	2.238	0.282	8	2.511	0.108	8	2.698	0.230	8
Macrophages (%)	98.750	0.224	8	98.663	0.198	8	99.125	0.157	8
Lymphocytes (%)	0.940	0.222	8	0.613	0.156	8	0.603	0.095	8
Neutrophils (%)	0.301	0.046	8	0.320	0.056	8	0.401	0.052	8
BALF / oxidative stress									
GSH	0.553	0.118	8	0.712	0.112	8	0.587	0.059	8
GSSG	0.035	0.008	8	0.057	0.009	7	0.046	0.016	8
GST	22.463	4.709	8	22.400	7.066	8	16.600	2.826	8
FRAP	4.441	0.171	8	4.744	0.327	8	4.541	0.153	8
NO	1.169	0.167	8	1.165	0.132	8	0.913	0.088	8
BALF / proinflammatory									
GRR	0.071	0.018	8	0.088	0.023	8	0.051	0.010	8
Lung tissue / proinflammatory									
IL-1β	30.103	1.237	6	33.130	1.601	6	42.363	3.858	6
TNF-α	19.325	1.021	6	19.872	1.852	6	20.041	1.576	6
NO	4.944	0.367	8	4.489	0.136	8	4.915	0.099	8
Lung tissue / oxidative stress									
GSH	112.350	7.709	8	113.713	9.756	8	127.075	7.901	8
GSSG	13.738	0.553	8	13.313	0.665	8	15.113	1.094	8
GST	52.925	2.552	8	55.038	2.934	8	68.700	1.947	8
FRAP	287.525	14.362	8	276.063	14.967	8	228.750	10.531	8
MDA	0.448	0.019	8	0.471	0.019	8	0.497	0.018	8
GRR	0.112	0.008	8	0.109	0.010	8	0.107	0.011	8

[a] In a second statistical analysis, endpoints measured in both the lung tissue and BALF (GRR, NO, FRAP, GSH, GSSG, and GST) were compared with each other using analysis of covariance and Pearson correlation coefficients. Both analyses (results not shown) indicated low correlation between lung tissue and BALF for all endpoints except FRAP. As FRAP in BALF increased, FRAP in lung tissue decreased (Pearson $\rho = -0.35$, $P = 0.10$; analysis of covariance slope = -25.5, $P = 0.04$).

of variance using the Bartlett test. The post hoc Levene homogeneity of variance test on the residuals was also performed as part of the ANOVA. Test results and the required transformations are indicated in the table. Also shown are the F test for the single factor and its *P* value. A trend test was also performed.

Means and standard errors for all the endpoints are given in Table 4. FRAP decreased with increasing iron concentrations, whereas GST and IL-1β increased with increased iron concentration. The linear trend tests were also statistically significant for these variables. Examined by uncorrected *t* tests, the values after exposure to 90 μg/m^3 iron were significantly different than those from exposure to either 57 μg/m^3 iron or to filtered air. Results for rats exposed to 57 μg/m^3 iron and for controls were not statistically significantly different from each other.

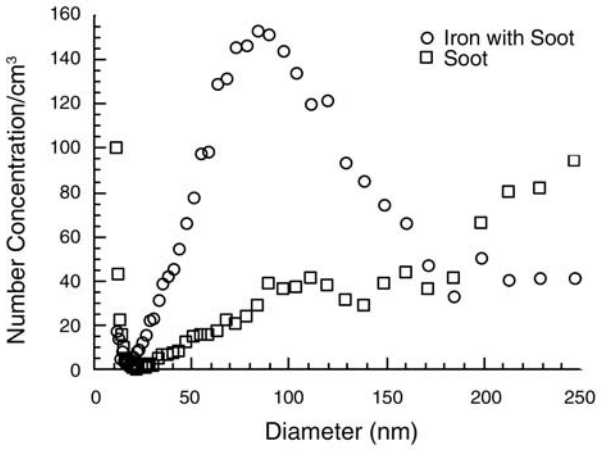

Figure 15. Size distribution of iron combined with soot PM from the exposure chamber.

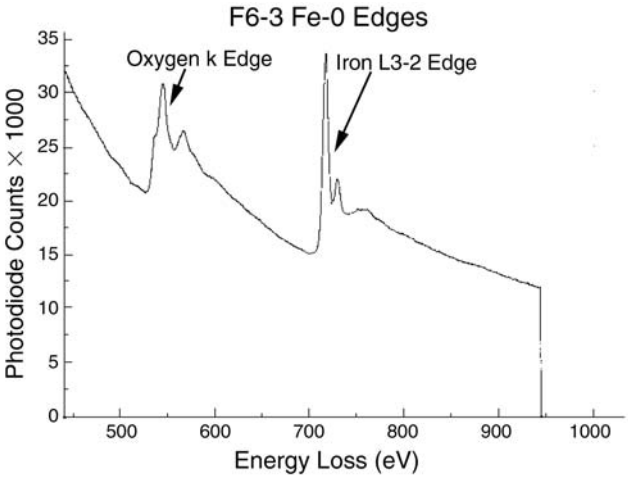

Figure 17. EELS spectrum of iron combined with soot PM collected from the exposure chamber after dilution of postflame gases. The oxygen k edge and iron L3-2 edge identify the presence and speciation of oxygen and iron respectively in iron particles generated under combustion conditions.

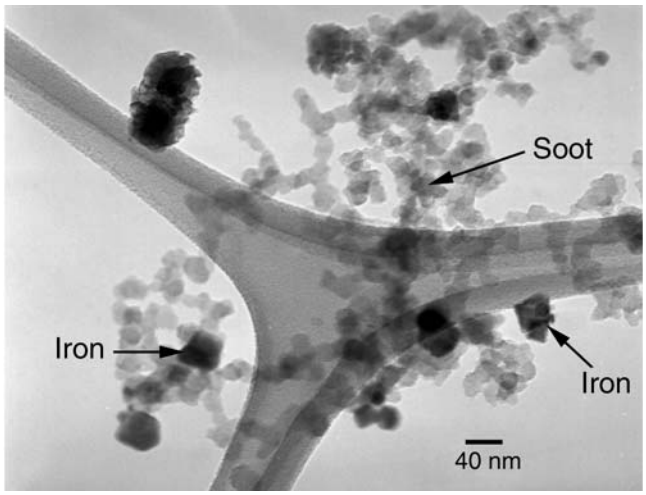

Figure 16. Electron micrograph of iron combined with soot PM on holey grid.

EXPOSURES TO IRON COMBINED WITH SOOT PM AND SOOT PM IN YOUNG ADULT RATS

Another series of experiments examined the effects of exposure to iron combined with soot PM in young adult rats.

Characterization of Soot PM and Iron Combined with Soot PM

Particle number concentration and particle diameter range for iron combined with soot PM and soot PM are shown in Figure 15. There is a bimodal size distribution of particles formed in our diffusion flame system. Typical primary particles of soot in laminar diffusion flames are 20 to 40 nm in diameter (Köylü et al. 1997). In our samples, soot formed clusters larger than 100 to 200 nm. It should be noted that a differential mobility particle sizer measures an aerodynamic diameter equivalent to a sphere of unit density. The drag on a large, loose soot aggregate may reduce its mobility and lead to an overestimate of physical size. Oxidation of the soot, promoted by the presence of iron, removes the carbon and also breaks up aggregates. In the case of iron combined with soot PM, oxidation by iron can remove the larger diameter particles (> 200 nm) found in the soot distribution (Figure 15).

For this series of experiments, the average total mass concentration of iron generated was 57 $\mu g/m^3$. For exposures to soot PM only, the total mass concentration was 250 $\mu g/m^3$. For exposures to iron combined with soot PM, the total mass concentration was also 250 $\mu g/m^3$. The concentration of iron was 45 $\mu g/m^3$ of the 250 $\mu g/m^3$. Average particle diameter ranged from 70 to 80 nm, with a complete distribution range of 10 to 250 nm (Figure 15).

Electron microscopy demonstrated that soot consisted of carbon in somewhat crystalline particles approximately 20 nm in diameter. Typically they formed chains of soot particles. In contrast, iron particles formed hexagonal and rhomboidal crystals that were entirely separate and distinct from the carbon particles (Figure 16). However, it was noted that many of these iron crystals were found in close association with soot particles. EELS demonstrated that the iron particles were iron oxide, and further analysis of the particle spectra demonstrated a ratio of iron to oxygen of approximately 0.5 to 0.7, indicating that the particles were Fe_2O_3 (Figure 17).

Iron Mobilization

Our iron mobilization studies examined the amount of free (bioavailable) iron present in iron combined with soot PM. The physiologically relevant chelator citrate was selected because previous studies have shown that the amount of iron mobilized from crocidolite asbestos by citrate in vitro was indicative of the amount of iron mobilized from crocidolite in A549 cells (Chao et al. 1994). Incubation of iron combined with soot PM in the absence of a metal chelator did not result in mobilization of iron (data not shown). The amount of iron mobilized by citrate from iron combined with soot PM was found to be 37.7 ± 0.9 nM iron/mg particle (mean ± SD). The amount of iron mobilized from various iron-containing particles in previous studies (Smith and Aust 1997; Smith et al. 1998; Aust et al. 2002) is shown in Table 5. These findings demonstrate that the amount of iron mobilized from the iron combined with soot PM generated in our system is similar to that from a variety of coals after combustion.

Cytotoxicity Measurements

Inhalation of soot PM (250 μg/m^3), iron PM (57 μg/m^3), or iron combined with soot PM (45 μg/m^3 Fe, 250 μg/m^3 total particulate) demonstrated no significant differences from control in protein concentration or LDH activity measured in BAL fluid (Figure 18). In addition, no significant

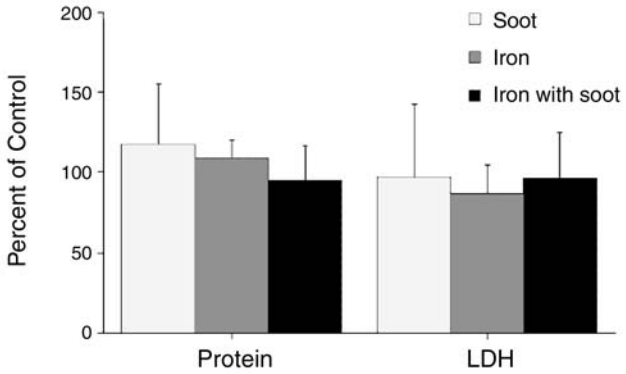

Figure 18. Protein concentration and LDH activity in BALF after exposure to soot PM, iron PM, or iron combined with soot PM. No significant changes were observed among groups.

Table 5. Mobilization of Iron from Particles by 1 mM Citrate

Particle[a] (1 mg/mL, unless otherwise noted)	Iron Content[b] (% by Mass)	Iron Mobilized[c] (nmol/mg Particle)	Reference
Utah coal fly ash (< 2.5 μm)	5.1	56.7 ± 1.8	Smith et al 1998
SRM 1649	3.0	52.9 ± 2.4	Smith and Aust 1997
North Dakota coal fly ash (< 2.5 μm)	3.1	44.1 ± 2.4	Smith et al 1998
Illinois (< 2.5 μm)	15.0	43.3 ± 1.8	Smith et al 1998
Utah coal fly ash (2.5–10 μm)	4.4	40.2 ± 1.9	Smith et al 1998
Iron combined with soot PM	10	37.7 ± 0.9	Current study
Crocidolite	27	36.9 ± 1.5	Smith and Aust 1997
Illinois coal fly ash (2.5–10 μm)	11.0	27.9 ± 1.5	Smith et al 1998
SRM 1648	3.9	24.9 ± 0.8	Smith and Aust 1997
North Dakota coal fly ash (2.5–10 μm)	5.9	24.6 ± 1.6	Smith et al 1998
Illinois coal fly ash (> 10 μm))	11.0	24.0 ± 2.4	Smith et al 1998
Utah coal fly ash (> 10 μm)	4.9	22.0 ± 0.7	Smith et al 1998
North Dakota coal fly ash (> 10 μm)	7.1	22.3 ± 0.8	Smith et al 1998
Metallurgic tailings	3.1	20	Aust et al 2002
Diesel exhaust particulate	ND	17.1	Aust et al 2002
Mancos clay dust	2.9	4	Aust et al 2002
Desert dust	3.0	2	Aust et al 2002
Magnetite, Fe_3O_4 (10 mg/mL)	72	7.8 ± 1.2	Unpublished, Smith and Aust
Hematite, Fe_2O_3 (10 mg/mL)	70	0	Unpublished, Smith and Aust

[a] Particle size measured in aerodynamic diameter.

[b] ND = not determined.

[c] All results with standard deviations (±) have $n = 3$. Otherwise $n = 1$.

differences were observed in total cell number, cell viability, or cell differentials in the fluid in any of the exposure groups (data not shown).

Oxidative Stress

Amounts of nitric oxide measured in BAL fluid (Table 6) or supernatant from lung tissue homogenate (Table 7), and expressed as a percent difference from control (Figure 19), demonstrated no significant difference in any of the exposure groups. MDA measured in the BAL fluid (Table 6) or supernatant from lung tissue homogenate (Table 7) and expressed as a percent difference from control (Figure 20) also demonstrated no significant difference in any of the exposure groups. In contrast, there was a significant reduction in total antioxidant power, measured using the FRAP assay, in both BAL fluid (Table 6) and supernatant from lung tissue homogenate (Table 7) in animals exposed to iron combined with soot PM. When FRAP values for animals exposed to iron combined with soot PM were expressed as a percent difference from control, there was a

Table 6. Changes Related to Oxidative Stress in BALF of Young Adult Male Rats[a]

Control or PM Exposure Group[b,c]	GST (nmol/min/ mg protein)	MDA (nmol/mL)	NO (nmol/mL)	FRAP (nmol/mL)	GSH (nmol/mL)	GSSG (nmol/mL)	GRR
FA1	40.3 ± 21.7	ND	1.04 ± 0.33	4.95 ± 1.17	0.429 ± 0.216	0.082 ± 0.041	0.166 ± 0.063
Soot	41.7 ± 18.5	ND	1.01 ± 0.32	5.88 ± 2.17	0.441 ± 0.299	0.098 ± 0.073	0.181 ± 0.083
FA2	22.5 ± 13.3	ND	1.17 ± 0.47	4.44 ± 0.48	0.553 ± 0.334	0.035 ± 0.023	0.071 ± 0.051
Iron	22.4 ± 20.0	ND	1.16 ± 0.37	4.74 ± 0.93	0.878 ± 0.319	0.057 ± 0.024	0.088 ± 0.066
FA3	68.8 ± 9.5	ND	1.49 ± 0.58	9.09 ± 0.34	0.344 ± 0.333	0.029 ± 0.014	0.105 ± 0.046
Iron with soot	86.1 ± 12.6	ND	1.47 ± 0.39	8.64 ± 0.30*	0.5333 ± 0.506	0.086 ± 0.044**	0.177 ± 0.076

[a] Values are mean ± SD (n = 8 per group). * $P < 0.05$, ** $P < 0.01$, significantly different from filtered air (FA3) group after exposure to iron combined with soot PM. No changes were observed after exposure to soot PM or iron PM.

[b] FA: filtered air. FA1, FA2 and FA3 were the controls of soot PM, iron PM, and iron combined with soot PM, respectively.

[c] Soot = soot PM 254 μg/m^3. Iron = iron PM 57 μg/m^3. Iron with soot = iron combined with soot PM with 250 μg/m^3 total suspended particles and 45 μg/m^3 iron.

Table 7. Changes Related to Oxidative Stress in Lungs of Young Adult Male Rats[a]

Control or PM Exposure Group[b,c]	GST (nmol/min/ mg protein)	MDA (nmol/mg/ protein)	NO (nmol/mg/ protein)	FRAP (nmol/mg/ protein)	GSH (nmol/mg/ protein)	GSSG (nmol/mg/ protein)	GRR
FA1	83.7 ± 14.5	0.22 ± 0.04	5.63 ± 0.48	578 ± 97	94 ± 14	16.2 ± 2.6	0.149 ± 0.033
Soot	89.7 ± 17.2	0.25 ± 0.05	5.46 ± 0.77	566 ± 88	91 ± 32	21.0 ± 7.8	0.194 ± 0.065
FA2	52.9 ± 7.2	0.45 ± 0.05	4.94 ± 1.04	287 ± 41	112 ± 22	13.7 ± 1.6	0.112 ± 0.024
Iron	55.0 ± 8.3	0.47 ± 0.05	4.49 ± 0.39	276 ± 42	114 ± 28	13.3 ± 1.9	0.109 ± 0.029
FA3	81.3 ± 5.9	0.21 ± −.07	6.68 ± 1.06	540 ± 62	118 ± 51	5.7 ± 4.0	0.051 ± 0.029
Iron with soot	88.4 ± 12.9	0.25 ± 0.10	6.75 ± 0.77	422 ± 89**	112 ± 36	11.3 ± 6.9	0.096 ± 0.049*

[a] Values are mean ± SD (n = 8 per group). * $P < 0.05$, ** $P < 0.01$, significantly different from filtered air (FA3) group after exposure to iron combined with soot PM. No changes were observed after exposure to soot PM or iron PM.

[b] FA: filtered air. FA1, FA2 and FA3 were the controls of soot PM, iron PM, and iron combined with soot PM, respectively.

[c] Soot = soot PM 254 μg/m^3. Iron = iron PM 57 μg/m^3. Iron with soot = iron combined with soot PM with 250 μg/m^3 total suspended particles and 45 μg/m^3 iron.

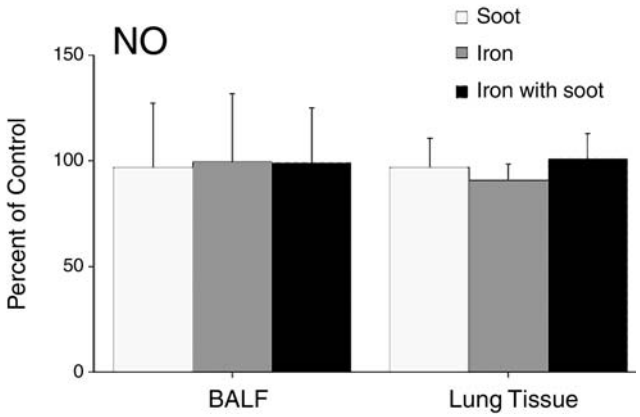

Figure 19. NO in BALF and lung tissue supernatant of adult rats after exposure to soot PM, iron PM, or iron combined with soot PM. NO is expressed as percent difference from control. No significant changes were observed among groups.

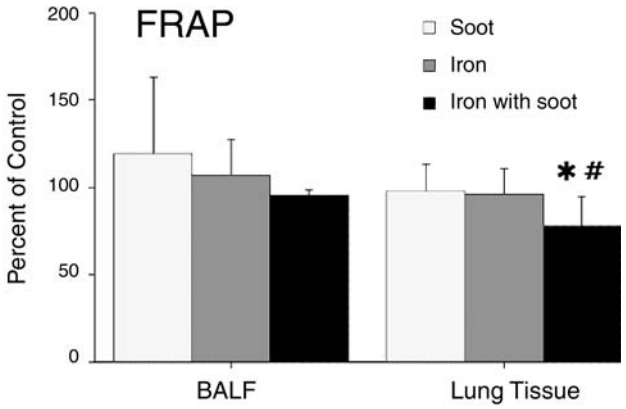

Figure 21. Total antioxidant power (FRAP) in BALF and lung tissue and lung tissue supernatant of adult rats after exposure to soot PM, iron PM, or iron combined with soot PM. FRAP is expressed as percent difference from control. Iron combined with soot PM versus soot PM: $^{*}P < 0.05$. Iron combined with soot PM versus iron PM: $^{\#}P < 0.05$.

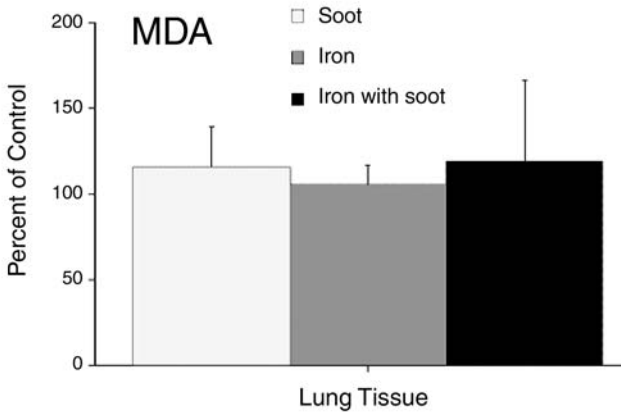

Figure 20. MDA in lung tissue supernatant of adult rats after exposure to soot PM, iron PM, or iron combined with soot PM. MDA is expressed as percent difference from control. No significant changes were found among groups.

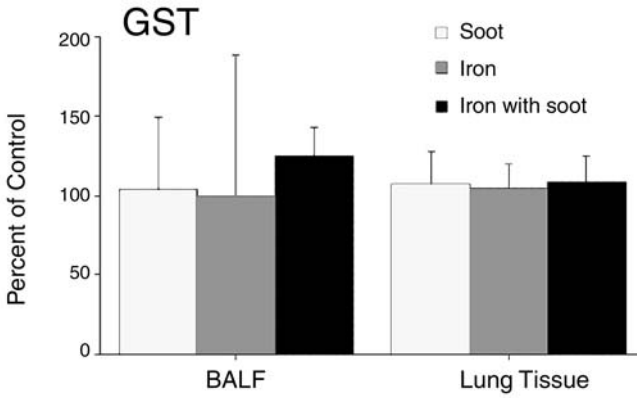

Figure 22. GST activity in BALF and lung tissue supernatant of adult rats after exposure to soot PM, iron PM, or iron combined with soot PM. GST activity is expressed as percent difference from control. No significant changes were observed among groups.

significant difference for the supernatant from lung tissue homogenate but not for BAL fluid (Figure 21). In contrast, animals exposed only to iron PM or soot PM showed no differences in the absolute values of FRAP or the percent difference from control. GST measured in BAL fluid (Table 6) or lung homogenate (Table 7) and expressed as percent difference from control (Figure 22) did not show any significant differences in any of the exposure groups. Glutathione amounts were measured in BAL fluid (Table 6) and the supernatant from lung tissue homogenate (Table 7) and were then expressed as percent differences from control (Figure 23). Glutathione was measured both as the reduced (GSH) and the oxidized (GSSG) forms. The glutathione redox ratio (GRR; the ratio of oxidized to total glutathione) was also computed (GRR = GSSG/[GSSG + GSH]). No significant differences were noted in GSH in any of the exposure groups. In contrast, GSSG showed a statistically significant increase for animals exposed to iron combined with soot PM. No differences were noted for animals exposed to iron PM or soot PM. In animals exposed to iron combined with soot PM, GRR showed a significant difference in lung homogenate but not in BAL fluid (Figure 23).

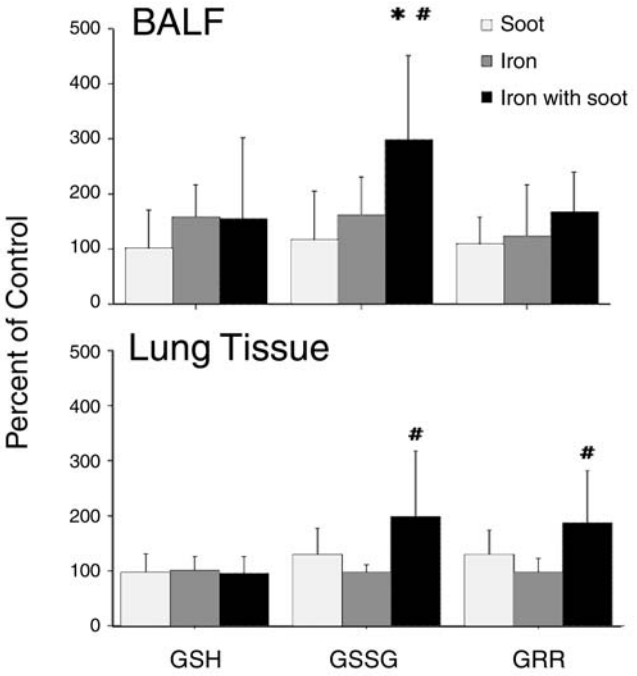

Figure 23. Glutathione redox status of adult rats after exposure to soot PM, iron PM, or iron combined with soot PM in BALF and in lung tissue supernatant. Values are expressed as percent difference from control. Iron combined with soot PM versus soot PM: $^{*}P < 0.01$. Iron combined with soot PM versus iron PM: $^{\#}P < 0.05$.

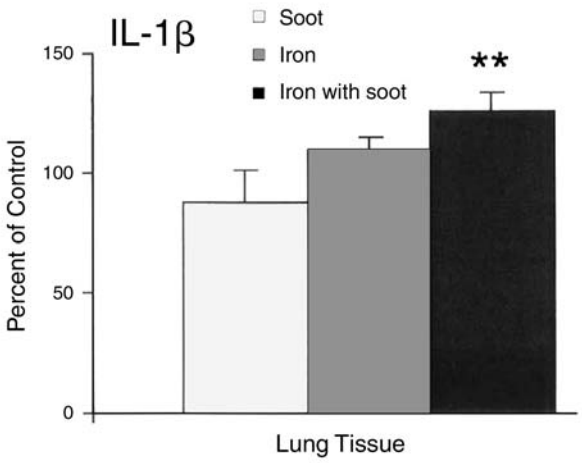

Figure 24. IL-1β concentrations in lung tissue supernatant of adult rats after exposure to soot PM, iron PM, or iron combined with soot PM. IL-1β activity is expressed as percent difference from control. Statistically significant difference between soot PM compared with iron combined with soot PM ($^{**}P < 0.01$).

Proinflammatory Cytokines

The amount of proinflammatory cytokines IL-1β and TNF-α in lung tissue of animals exposed to particles was compared with that of control animals. IL-1β was significantly increased after exposure to iron combined with soot PM but not after exposure to iron PM or soot PM (Figure 24). No statistically significant differences were noted in values of TNF-α in any of the exposure groups compared with control (Figure 25).

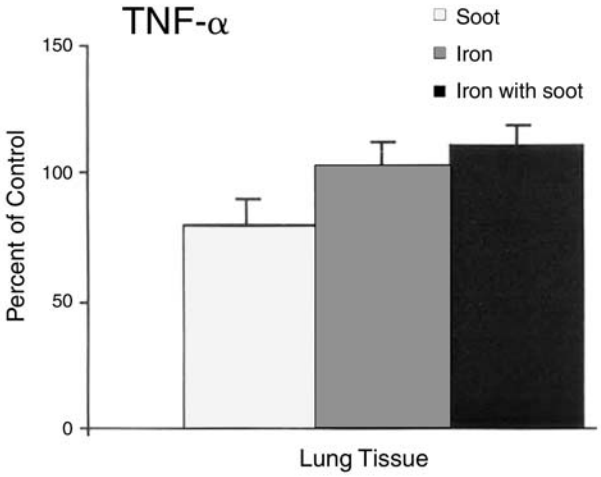

Figure 25. TNF-α concentrations in lung tissue supernatant of adult rats after exposure to soot PM, iron PM, or iron combined with soot PM. TNF-α activity is expressed as percent difference from control. No statistical significance observed among exposure groups.

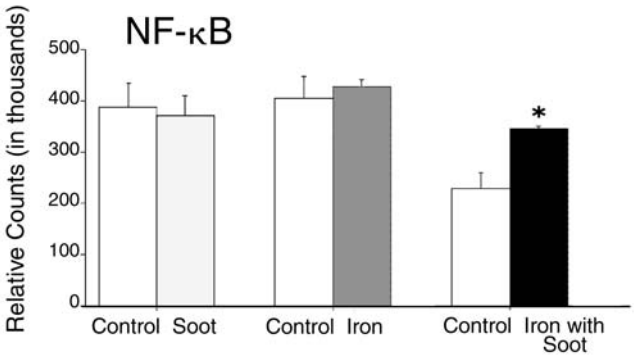

Figure 26. NF-κB DNA binding activity in lung tissue supernatant of adult rats after exposure to soot PM, iron PM, or iron combined with soot PM. NF-κB DNA binding activity was significantly increased after exposure to iron combined with soot PM ($^{*}P < 0.01$).

NF-κB DNA Binding Activity

NF-κB DNA binding activity increased significantly in the nuclear fraction of lung homogenate from animals exposed to iron combined with soot PM but not in that of animals exposed to iron PM or soot PM (Figure 26).

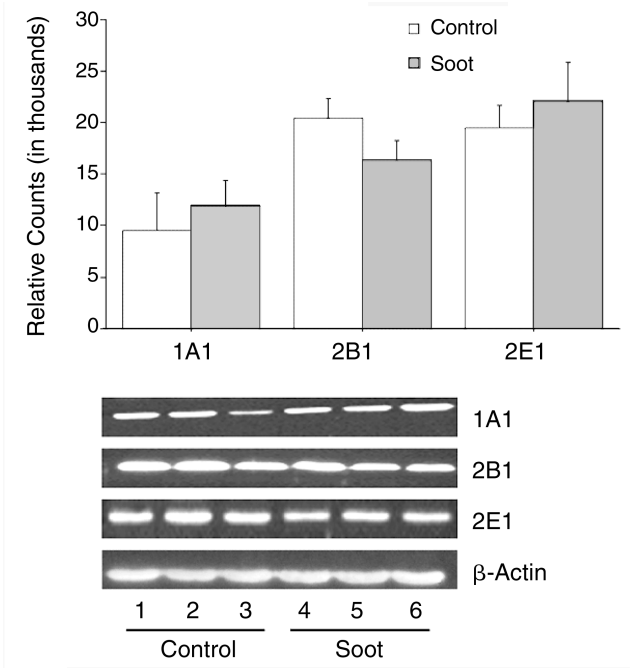

Figure 27. CYP1A1, 2B1, and 2E1 expression in lung tissue supernatant of adult rats after exposure to soot PM. β-Actin serves as the loading control for each lane.

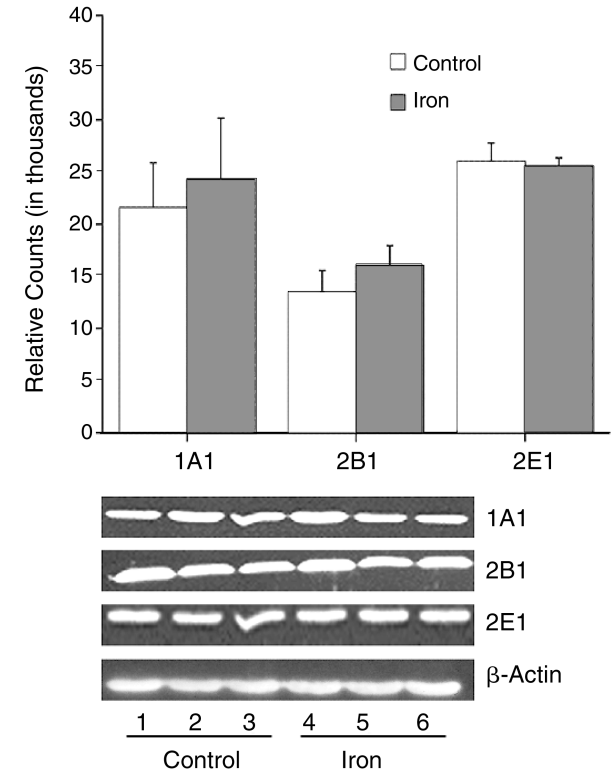

Figure 28. CYP1A1, 2B1, and 2E1 expression in lung tissue supernatant of adult rats after exposure to iron PM. β-Actin serves as the loading control for each lane.

Cytochrome P450 Isoforms

Amounts of the cytochrome P450 isoforms CYP1A1, CYP2E1, and CYP2B1 showed no significant change in animals exposed to iron PM or soot PM compared with controls (Figures 27 and 28). In contrast, amounts of CYP1A1 and CYP2E1 showed significant increases in animals exposed to iron combined with soot PM (Figure 29). Although the amount of CYP2B1 also increased, the increase was not statistically significant. When the amounts of each isoform were expressed as a percent of control value, the data showed that there were significant differences for all three isoforms in animals exposed to iron combined with soot PM but not those exposed to iron PM or soot PM (Figure 30).

Lung Histopathology and Bromodeoxyuridine Immunolabeling

Sites in the respiratory tract of all animals were extensively examined. Figure 31 illustrates the appearance of terminal bronchioles and lung parenchyma immediately beyond the bronchioles in the lungs of animals exposed to

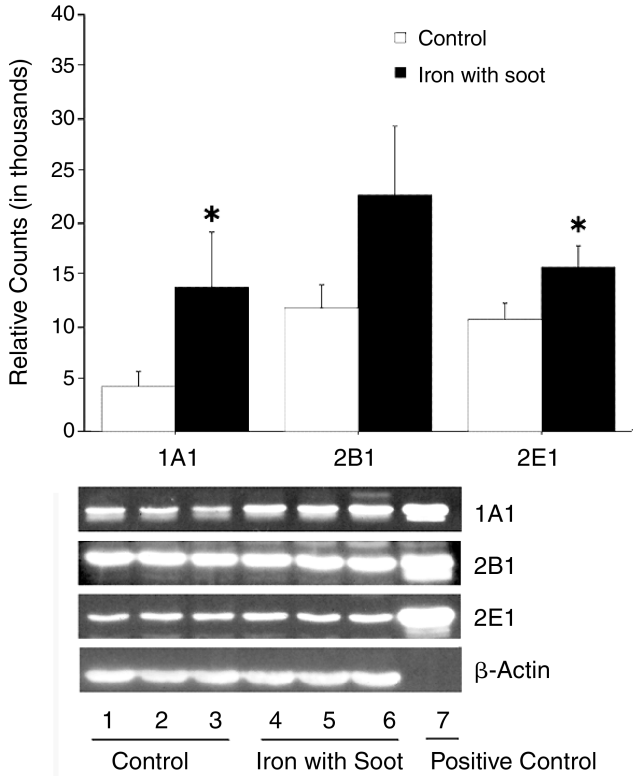

Figure 29. CYP1A1, 2B1, and 2E1 expression in lung tissue supernatant of adult rats after exposure to iron combined with soot PM. β-Actin serves as the loading control for each lane. *$P < 0.05$.

soot PM, iron combined with soot PM, or filtered air (control). We did not observe any significant changes in the terminal bronchioles of any exposure group. We did not detect differences in the septal wall structure of the parenchyma, but there appeared to be patchy areas of slight septal-wall thickening in the lungs of animals exposed to iron combined with soot PM. These changes were subtle and not considered to be significant.

Uptake of BrdU was measured in the main axial airway epithelium, the epithelial lining over airway bifurcations, and the underlying interstitium at airway bifurcations and proximal alveolar regions. We did not find significant differences in the labeling index for the uptake of BrdU into any cells from animals in any exposure group compared with control animals (Table 8).

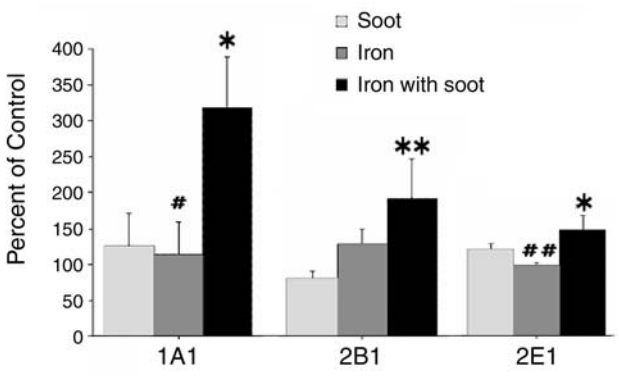

Figure 30. CYP1A1, 2B1, and 2E1 expression in lung tissue supernatant of adult rats after exposure to soot PM, iron PM, or iron combined with soot PM. Values expressed as percent difference from control. Iron combined with soot PM versus soot PM: $^{*}P < 0.05$; $^{**}P < 0.01$. Iron combined with soot PM versus soot PM: $^{\#}P < 0.05$; $^{\#\#}P < 0.01$.

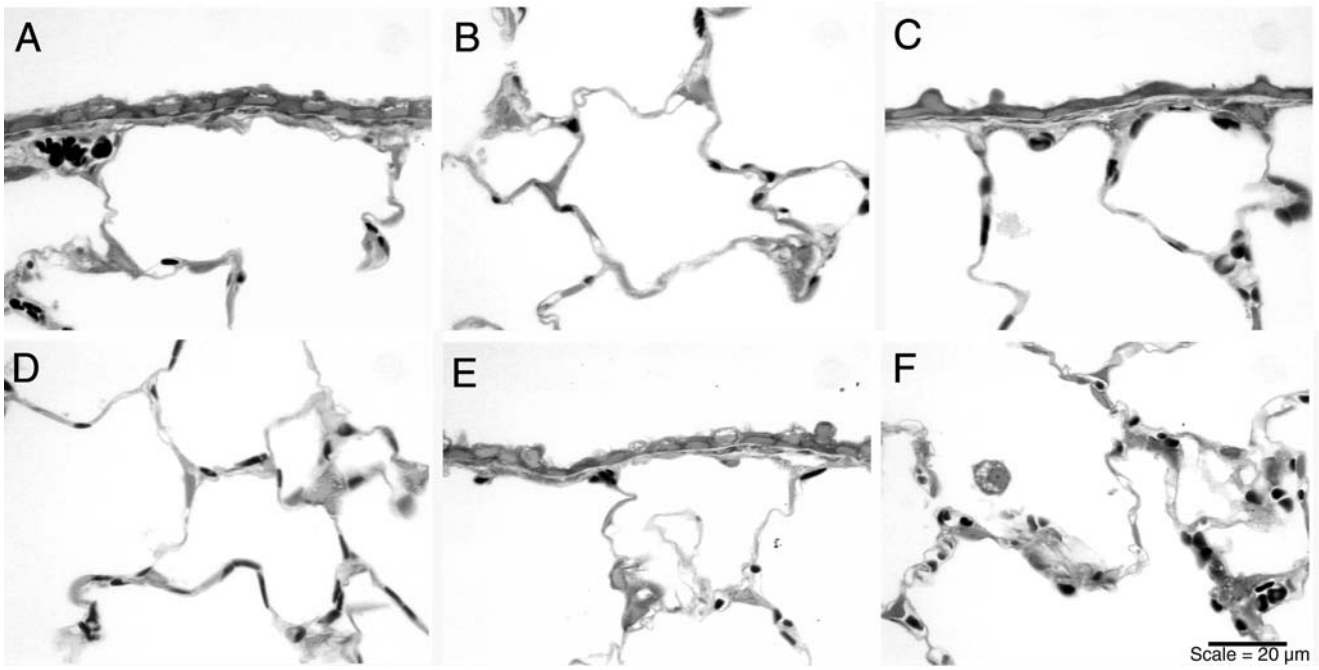

Figure 31. Light micrographs of terminal bronchioles (A, C, E) and alveolar parenchyma (B, D, F) from adult rat lungs after exposure to filtered air (A, B), soot PM (C, D), or iron combined with soot PM (E, F).

Table 8. BrdU Labeling Index (% of Total Cells) in the Young Adult Male Rat Lung[a]

Control or PM Exposure Group	Main Axial Airway (Epithelium)	Airway Bifurcation (Epithelium)	Airway Bifurcation (Interstitium)	Proximal Alveolar Region
Control (filtered air)	2.02 ± 0.25	2.67 ± 0.55	6.71 ± 1.0	13.90 ± 1.43
Iron with soot[b] (iron = 47 µg/m^3)	2.34 ± 0.21	2.99 ± 0.94	6.68 ± 1.55	13.50 ± 1.14

[a] Values are mean ± SEM. (n = 6 per group).

[b] Definition: iron with soot indicates iron combined with soot PM.

EXPOSURES TO IRON COMBINED WITH SOOT PM IN NEONATAL RATS

The final series of experiments examined the effects of exposure to iron combined with soot PM in neonatal rats. The PM contained either 30 μg/m^3 or 100 μg/m^3 of iron combined with soot.

Particle Characterization

As described earlier, the total mass concentrations of iron particles generated under low-dose and high-dose conditions were 30 ± 7 μg/m^3 and 100 ± 28 μg/m^3, respectively. The total mass concentration of iron combined with soot PM for both conditions was 250 μg/m^3. The majority of iron particles generated were again polyhedral crystals of iron oxide (Fe_2O_3), as determined by TEM and EELS.

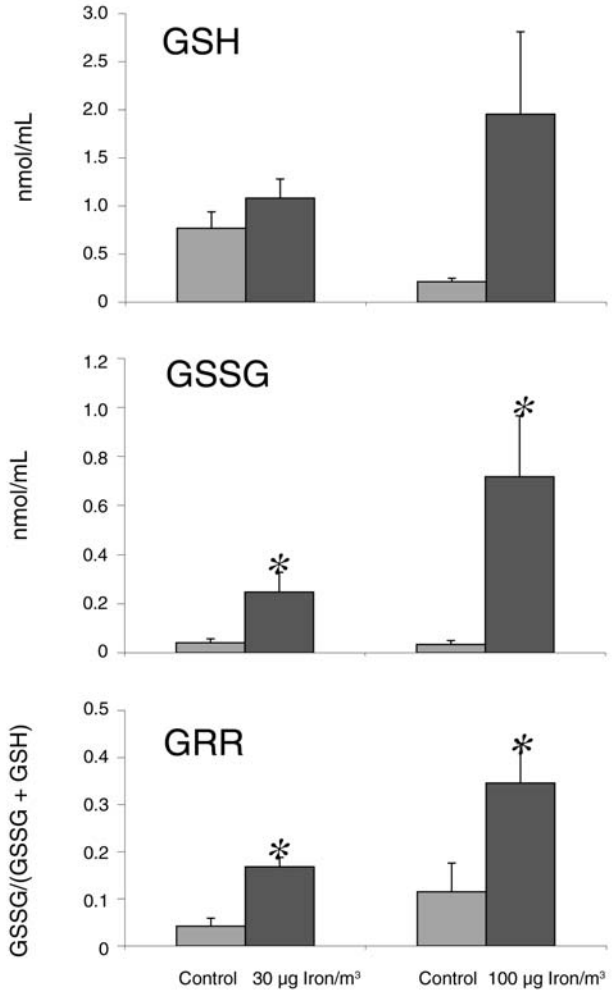

Figure 32. Glutathione redox status in BALF of neonatal rats. Data are presented as means ± SE (n = 8 per group). GSSG and GRR were significantly increased after exposure to iron combined with soot PM for both iron concentrations. *P < 0.05, significant difference from control.

Cytotoxicity

To assess the cytotoxicity of iron combined with soot PM, total cell number, cell viability, and LDH activity in BAL fluid were determined at 26 days of age (Table 9). No significant differences in cell number or differential were noted between the low-dose or high-dose groups of iron combined with soot PM compared with controls (data not shown). However, cell viability was significantly reduced by 18.7% in high-dose animals (P < 0.05). LDH activity increases were also significantly increased in high-dose animals (P < 0.05).

Oxidative Stress

Markers of oxidative stress were: reduced GSH, GSSG, GRR (Figure 32), GST (Figure 33), and total antioxidant

Table 9. Changes in Cell Viability and LDH in BALF of Neonatal Rats[a]

Control or PM Exposure Group	Cell Number (× 10^5)	Viability (%)	LDH (U/L)
Control	8.23 ± 2.72	93.8 ± 2.2	4.18 ± 1.47
Low dose exposure (iron = 30 μg/m^3)	7.38 ± 2.73	91.6 ± 2.6	5.09 ± 0.92
Control	16.93 ± 10.16	80.9 ± 6.1	4.09 ± 1.83
High dose exposure (iron = 100 μg/m^3)	12.74 ± 7.76	65.8 ± 17.0[b]	6.96 ± 2.60[b]

[a] Values are mean ± SD (n = 8 per group).

[b] P < 0.05 compared with control group.

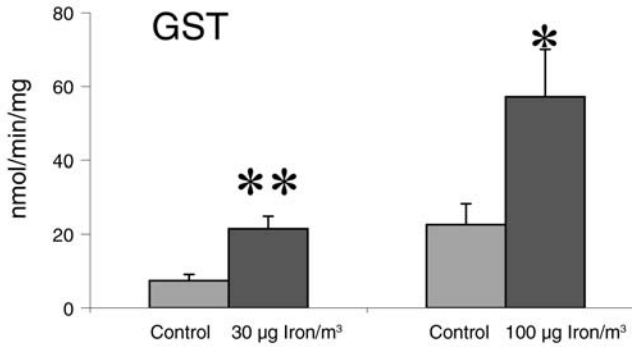

Figure 33. GST activity in BALF of neonatal rats. Data are presented as means ± SE (n = 8 per group). Exposure to iron combined with soot PM for both iron concentrations resulted in significant elevation of GST activity. *P < 0.05, significant difference from control. **P < 0.01, significant difference from control.

power measured by FRAP (Figure 34). There were no significant differences in GSH level between exposure groups and controls. However, there were significant differences between both exposure groups and their respective controls in BAL fluid for GSSG and GRR (Figure 32), GST activity (Figure 33), and FRAP (Figure 34).

Significant changes in GSSG, GRR, and GST activity were also noted in lung tissue after exposure to either concentration of iron combined with soot PM; FRAP was significantly different in the lung tissue after exposure to 100 μg/m^3 iron combined with soot PM. These data are not shown, but are summarized in Table 10.

Proinflammatory Cytokines

High-dose exposure was associated with a significant increase in IL-1β (Figure 35) compared with control. Neither high-dose nor low-dose exposure was associated with a significant difference in TNF-α (Figure 35) compared with control.

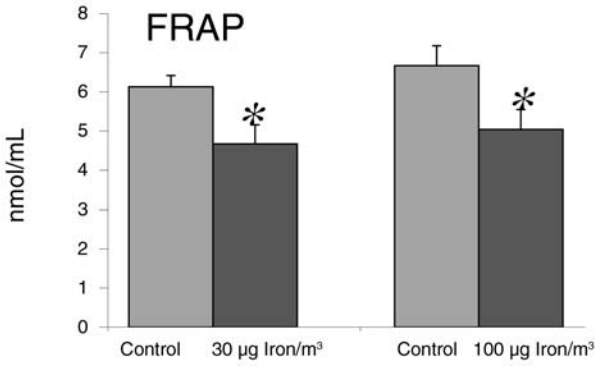

Figure 34. Change of total antioxidant power (FRAP assay) in BALF of neonatal rats. Data are presented as means ± SE (n = 8 per group). Exposure to iron combined with soot PM for both iron concentrations resulted in significant reduction of total antioxidant power. *P < 0.05, significant difference from control.

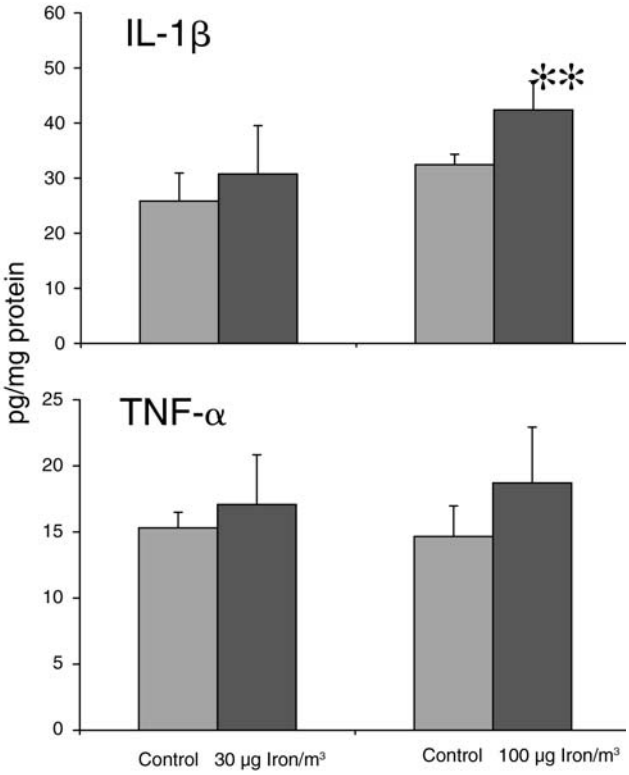

Figure 35. Effect of iron combined with soot PM exposure on the protein levels of IL-1β and of TNF-α in neonatal rat lung tissue supernatant. Values are means ± SE (n = 6 per group). **P < 0.01, significant difference from control.

Table 10. Exposure Effects of Iron Combined with Soot PM on Young Adult Male and Neonatal Rats[a]

Age / PM Exposure Group	Iron / Total PM (μg/m^3)	BALF						Lung Tissue					
		Viability	LDH	GST	FRAP	GSSG	GRR	Ferritin	FRAP	GST	GSSG	GRR	NF-κB
Young Adult Male													
Iron	57	−	−	−	−	−	−	−	−	−	−	−	−
Iron	90	−	−	+	+	−	−	+	+	+	−	−	−
Iron with soot	45 / 250	−	−	+	+	+	+	+	+	+	−	−	+
Soot	250	−	−	−	−	−	−	−	−	−	−	−	−
Neonatal													
Iron with soot	30 / 250	−	−	+	+	+	+	−	−	+	+	+	NM
Iron with soot	100 / 250	+	+	+	+	+	+	+	+	+	+	+	NM

[a] Definitions: − indicates no change compared with filtered air controls; + indicates statistically significant change from control (P < 0.05); NM indicates not measured; iron with soot indicates iron combined with soot PM.

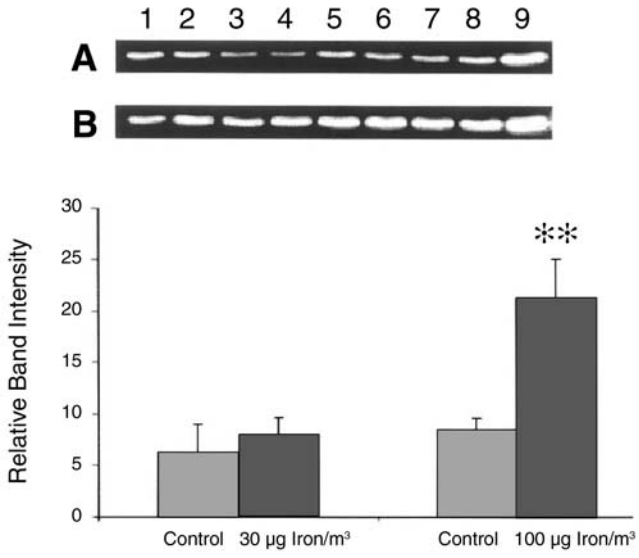

Figure 36. Western blot analysis of ferritin expression in neonatal rat lung tissue supernatant after exposure to iron combined with soot PM. (*A*) 30 µg/m³ iron (*B*) 100 µg/m³ iron. $^{**}P < 0.01$ when compared with control.

Table 11. BrdU Labeling Index in the Neonatal Rat Lung[a]

Anatomic Site	Control (Filtered Air)	Iron with Soot Exposure[b]
Terminal bronchioles	1.84 ± 0.86	2.19 ± 0.44
Proximal alveolar region	2.26 ± 0.30	1.70 ± 0.14[c]
Random alveolar regions	1.94 ± 0.35	1.82 ± 0.68

[a] Values are mean ± SD ($n = 4$ per group).

[b] Definition: iron with soot indicates iron combined with soot PM.

[c] $P < 0.05$ compared with control group.

Ferritin

A significant increase of intracellular ferritin was noted (2.5-fold) after high-dose exposure (Figure 36) compared with control. No significant difference was noted after low-dose exposure.

Bromodeoxyuridine Immunolabeling

In 13-day-old neonatal rats, no significant differences were noted in the cell labeling index of terminal bronchioles or random alveolar regions of animals exposed to high or low doses of iron combined with soot PM compared with controls. In contrast, statistically significant reductions were noted in the cell labeling index of proximal alveolar regions (Table 11).

DISCUSSION

A major finding in these studies is that exposure to particles of iron combined with soot induces a pulmonary response not observed with exposure to particles containing equivalent amounts of iron alone or soot alone. A prevailing concept for health effects observed after PM exposure suggests transition metals present in PM may induce oxidative stress. PM contains transition metals such as iron, copper, nickel and vanadium, which can catalyze the one-electron reduction of molecular oxygen to generate ROS, including the formation of highly reactive hydroxyl radicals through the Fenton reaction. Halliwell and Gutteridge (1999) postulated that ROS have the potential to damage biological molecules. Therefore, it would be highly plausible that oxidative injury could be one of the major mechanisms of PM toxicity.

The diffusion flame system in our laboratory produced steady concentrations of iron PM, soot PM, and iron combined with soot PM. Gaseous species, including CO and NO_x, were routinely measured and found to be at concentrations not considered likely to have a significant effect on the exposed animals. We tested for sixteen PAHs, but did not detect any of them. The biologic implications of the EC and OC composition observed in our iron combined with soot PM (60% EC, 40% OC) are unknown, because we do not have comparable measurements for EC or OC composition of soot PM produced in the absence of iron. The soot PM generated in our laboratory bears a generic similarity to diesel PM in terms of particle size. However, our soot PM is emitted from an ambient-pressure flame fueled with simple, low-molecular-weight hydrocarbons, conditions quite different from those of a diesel engine. This may be why the relative amounts of EC and OC are quite different from diesel PM. On average, the composition of the soot in the iron combined with soot PM was 60% EC and 40% OC, which may be comparable to some diesel exhaust PM. The composition of the OC is unknown. Similar measurements were not made for soot PM. These particles are relevant because now we are able to introduce metals while the soot plume is formed during combustion. This allows evaluation of biologic responses to such exposures.

The target concentrations of ultrafine PM in these studies were higher than those of the National Ambient Air Quality Standard. The concentration of iron in the ultrafine PM was also higher than that found in the environment, in which concentrations of iron typically represent no more than 2% to 5% of the total mass present. However, iron is one of the most common transition metals in the 50 to 300 nm size range of ambient PM.

Ambient PM is complex. It is critical to identify and characterize the biologic activities of the many elements of PM to elucidate their role in its health effects. Exposure of rat tracheal epithelial cells to residual oil fly ash containing soluble metals has been shown to produce oxidative stress, cytotoxicity, and inflammation (Dye et al. 1997, 1999). In vitro studies have further demonstrated both iron- and copper-dependent inflammation and activation of NF-κB resulting from PM exposure (Kennedy et al. 1998; Jimenez et al. 2000). Intratrachael instillation of PM in animals has been shown to cause lung injury by solubilized transition metals, including iron and nickel (Li et al. 1996; Kodavanti et al. 1998). Our goal was to describe the effects of the transition metal iron, using an inhalation model, the natural route by which exposure to ambient airborne pollutants occurs. Because iron is one of the major transition metals found in ambient PM, the purpose of the present study was to explore the respiratory effects of inhaling iron PM. Our study demonstrates that inhalation of iron PM induces mild adverse effects, including oxidative stress, and lung inflammation in healthy rats.

Induction of intracellular ferritin indicates the presence of bioavailable iron. Increased expression of ferritin has been observed in respiratory epithelial cells treated with PM containing iron (Fang and Aust 1997; Smith and Aust 1997). Ferritin synthesis is known to be regulated by a posttranscriptional mechanism. Available iron reacts with the iron-regulatory protein to remove the inhibitory protein from ferritin messenger RNA, allowing the translation of ferritin to proceed (Klausner et al. 1993; Theil 1994; Harrison and Arosio 1996). Our study demonstrated that inhalation of iron particles at a concentration of 90 μg/m^3 significantly increases ferritin expression in lung tissue. This suggests that at least part of the iron from particles deposited in the lungs becomes bioavailable. The major form of iron particles generated in our experiment was the iron oxide Fe_2O_3, which is considered to be an iron of low bioavailability (Stokinger 1984). A recent study (Lay et al. 1999) reported that intrapulmonary instillation of 2.6-μm-diameter iron oxide particles induced cellular and biochemical responses in both humans and rats. This was thought to result from the small portion of soluble iron and intermediate species generated during Fe_2O_3 formation. We do not believe that the bioavailable iron in our study was due to the Fe_2O_3 present in the aerosol, but that it could be due to other forms of iron that account for some of the total iron particles present after combustion (Figure 6). However, the actual composition or concentration of these iron PM and iron combined with soot PM is unknown. It is also important to emphasize that the size of iron particles generated in our study is in the ultrafine range, with an average diameter of 72 nm. Ultrafine particles (especially those less than 100 nm in diameter) contribute very little to the overall particle mass but dominate in number concentration and surface area. Ultrafine particles can be deposited in the most distal parts of the lungs. This results in ultrafine particles coming in direct contact with the surface lining of airways and alveoli (Stokinger 1984), enhances particle transfer to cell surfaces, and subsequent movement across membranes (Brown et al. 2000) and incorporation into cells. These particles have greater retention time in the lungs, which may be associated with intimate contact of particles with potential target cells (Oberdörster 2001). Prolonged presence of these particles in the lungs may significantly facilitate biologic responses.

In our study, the relatively short 3-day exposures to iron combined with soot PM were associated with distinct oxidative stress in the lungs of young adult rats. Similar findings were noted in neonatal animals after two 3-day exposures to iron combined with soot PM during the second and fourth weeks of life. In contrast, there was no evidence of oxidative stress or lung injury in young adult rats exposed to soot PM at the same concentration used for iron combined with soot PM. Exposure to 57 μg/m^3 iron PM, a concentration equivalent to or slightly higher than that used in the iron combined with soot PM exposure, also showed no evidence of oxidative stress. However, when the concentration of iron PM was sufficiently high, signs of oxidative stress could be found.

These findings provide interesting insights into possible mechanisms of injury resulting from exposure to complex PM in the environment. We are not exposed to a single pollutant, but rather to a complex mixture. Interactions among various pollutant components may lead to effects that would not be seen with single-pollutant exposures. Our findings emphasize the importance of studying the health effects of complex PM. They also point to the critical need for understanding minor components in PM. Alone, these may have no effect on the lungs, but in combination with other particles they may have strong, adverse effects on the respiratory and other organ systems of the body. The fact that no changes in protein or LDH levels were found in BAL fluid in adult animals corresponds to the lack of any obvious anatomical or histopathologic changes.

The amounts of NO and GST were not affected by any experimental PM exposure in adult animals. However, significant differences were noted in GSSG, GRR, and FRAP in animals exposed to iron combined with soot PM. Similar changes were noted in neonatal animals. There was also a significant increase in NF-κB DNA binding activity after exposure to iron combined with soot PM.

These findings provide further evidence of the adverse effects of complex particle mixtures on respiratory cell signaling pathways.

Increases in BAL fluid total protein and LDH activity serve as indicators of lung injury and cytotoxicity, reflecting an increase in cell permeability, cell lysis, or both. A significant increase in BAL fluid total protein content was noted after exposure to 90 μg/m^3 iron PM, but no change was observed in LDH activity. We speculate that the toxic effect may not have been severe enough to cause significant cell lysis, only increases in epithelial or alveolar capillary membrane permeability. The absence of changes in total cell number or cell differentials in BAL fluid (Table 4) is compatible with these results in total protein and LDH protein values in BAL fluid.

In recent years, many studies have demonstrated that oxidative stress plays an important role in the inflammatory response and activation of transcription factor NF-κB. Excessive release of ROS and depletion of antioxidants could trigger signal transduction pathways leading to the activation of NF-κB (Rahman 2000; Rahman and MacNee 2000). The genes regulating the proinflammatory cytokines, such as IL-1β and TNF-α, and antioxidant enzymes, such as GST-Pi — one of the isozymes in the GST superfamily, are among the most prominent regulated by NF-κB (Hayes and Pulfor 1995; Barnes and Karin 1997). We found in our study that exposure to 90 μg/m^3 iron PM was associated with a significant decrease in total antioxidant power, the induction of GST activity, and an increase in IL-1β in the lungs. These changes were accompanied by a 1.3-fold increase in NF-κB DNA binding activity (Figure 14), a level that did not reach statistical significance (P = 0.10), perhaps due in part to limited sample sizes (n = 2–3 animals/group). Our study also demonstrated that the amounts of oxidative stress and inflammatory mediator release were dependent on the iron concentration present during exposure. As a critical antioxidant in the lung, GSH accounts for 90% of intracellular nonprotein thiols. It protects cells by scavenging reactive electrophilic intermediates, forming hydrogen peroxide, and reducing disulfide bonds in proteins and DNA precursors (Kelly 1999; Rahman and MacNee 1999). Although statistically significant changes were not observed in GSH and GSSG, the trend of an increase in both after exposure to the higher concentration of iron may suggest that GSH acts as a buffer to minimize oxidative stress. A change in GSH redox status that decreases GSH and increases GSSG could trigger the synthesis of GSH and may recruit more GSH to target sites from the circulatory and other organ systems. It is well established that GSH is maintained at relatively abundant concentrations in cells (1–10 mM) under most physiologic conditions (Kelly 1999; Rahman and MacNee 2000).

Significant increases in the levels of three major isoforms of cytochrome P450 in the lungs of adult animals were found only after exposure to iron combined with soot PM. Exposure to soot PM at an identical mass concentration in the absence of iron failed to elicit the same changes as iron combined with soot PM. Exposure to 50 μg/m^3 iron PM also failed to induce changes in the cytochrome P450 isoforms but was not studied at the higher iron concentration (90 μg/m^3).

We conclude that oxidative stress and pulmonary cytochrome P450 1A1 and 2E1 isoforms are significantly induced in the lungs of healthy young adult rats after exposure to iron combined with soot PM.

Extensive testing was done to determine whether the soot fraction generated by our combustion system produced OC, including PAHs. We found OC to be present, but the 16 most common PAHs formed through fuel combustion were not detected.

Although we demonstrated the presence of bioavailable iron, we could not identify its form. Previous studies using urban ambient PM demonstrated that the amount of iron mobilized from PM or CFA was not dependent on the amount of iron present (Smith and Aust 1997; Veranth et al. 2000). It was more likely dependent on the form of iron or the PM surface area. Fang (1999) demonstrated that iron present as mixed oxides is not bioavailable. Hardy and Aust (1995) demonstrated that in silicates only the iron ionically associated with particles is bioavailable. The bioavailable iron in urban PM (Smith and Aust 1997), crocidolite (Lund and Aust 1992), and silicates (Hardy and Aust 1995) has been demonstrated to be responsible for catalyzing the formation of ROS.

Exposure of neonatal animals to iron combined with soot PM also demonstrated significant oxidative stress and other markers of pulmonary toxicity. Our studies of the impact of iron combined with soot PM on cell proliferation during early postnatal development demonstrate a significant retardation of DNA synthesis in the proximal alveolar region, a site of important alveolar growth and proliferation during the postnatal period. Impaired lung growth and lung function associated with PM exposure have also been observed in children (Gauderman et al. 2000, 2002; Horak et al. 2002).

Our study provides the first in vivo evidence that ultrafine iron PM generated through a combustion process can provoke mild adverse effects in the respiratory system of healthy young adult rats. A dose-dependent response to iron PM was also observed. However, these observations may also suggest merely a threshold effect (Figures 8–10,

12–13). However, when iron PM is combined with soot, even lower concentrations of iron PM are associated with observed effects (Figures 32–36). A fraction of their iron becomes bioavailable, both of which suggest mechanisms of PM-mediated toxicity via oxidative stress. These data further implicate iron in PM-related health effects. Because the data in this study are based on healthy animals, further studies should determine whether responses would be more striking in compromised animals. Additional studies should also examine the potential effects of iron in a readily accessible bioavailable state, in combination with other atmospheric pollutants, such as particles of other compositions and sizes, as well as ozone, and nitrogen dioxide to further elucidate the role of transition metals in ambient-PM-induced health effects.

Although our studies of iron combined with soot PM demonstrate significant respiratory changes as measured through changes in BAL fluid and lung tissue, these changes were minimal after a relatively short 3-day exposure period. They failed to demonstrate histopathologic changes in the airways or lung parenchyma. The absence of histopathologic changes emphasizes the importance of changes in demonstrating oxidative stress and mild cytotoxicity. Such subtle but significant changes may have a lasting impact and be exacerbated by longer-term exposures. The studies also emphasize the importance of better understanding the effects of particle size and composition. Under some conditions, such as exposure to iron PM or soot PM alone, no effects were observed. In contrast, exposure to iron combined with soot PM was associated with significant effects. These observations suggest potential interactions between soot- or organic carbon-based materials and trace elements or transition metals that may play a key role in particle-induced lung toxicity.

The selection of a time point for examination after exposure was based on our best estimate of the optimal time for detecting biologic changes in BAL fluid and lung tissue. Based on this estimate, all studies of BAL cells and fluids were done within 2 hours after the end of the exposure period. Studies of lung tissue were done 24 hours after exposure. It is possible we missed the optimal time for observing changes due to the time selected. It is also possible that the timing and duration (3 days in a row, 6 hours at a time) of exposures were not optimal.

Particle studies with exposures of longer duration would be of tremendous benefit to determine how or if our short-term (3-day) effects would be changed. In a similar manner, studies with longer post-exposure times could help determine whether residual effects associated with exposure persist. Such knowledge would be of great interest because little or no pathological change was noted in the lungs of animals examined in our study.

It would also be of interest to observe the kinetic fate and biologic effects of combustion-generated PM. Interactions between iron combined with soot particles may influence the surface characteristics of iron particles as well as the speciation of OC in the soot fraction. Longer particle exposures, along with the measurement of biologic effects during the course of particle exposure, could facilitate the exploration of early biomarkers leading to inflammation, cell injury, and necrosis. In studies with longer exposure times, we may be able to observe alterations in epithelial cell populations, the thickness of the interstitium, collagen, and elastin, as well as systemic effects measured via hematologic parameters and cardiovascular changes in order to better assess the long-term effects of exposure to particulate matter.

Table 10 summarizes the major directional changes among the BAL fluid and lung tissue variables measured in young adult and neonatal rats exposed to either ultrafine particles of iron alone, soot alone, or iron combined with soot. The table facilitates a simple determination of those same variables measured in young adult rats and neonatal rats, although exposure conditions were not identical for these two groups. Young adult rats were exposed for a single 3-day period, while neonatal rats were exposed sequentially for 3 days in both the second and fourth weeks of life.

CONCLUSIONS

From this study, we conclude the following:

1. In young adult and neonatal rats, exposure to ultrafine iron combined with soot PM is associated with significant evidence of oxidative stress in the absence of obvious lung injury or inflammation.
2. Oxidative stress assays (i.e., GSH, GSSG, GST, and FRAP) are sensitive measures of adverse health effects in the lungs.
3. The degree of oxidative stress and elevation of the proinflammatory cytokine IL-1β observed in neonatal rats exposed to iron combined with soot PM are dependent on the concentration of iron combined with the soot.
4. In neonatal rats, exposure to iron combined with soot PM during critical periods of growth is associated with a significant reduction in uptake of BrdU in cells of the proximal alveolar region of the lungs, suggesting impairment of lung development and function.

ACKNOWLEDGMENTS

The authors appreciate Dr. GoSu Yang of the University of California, Davis for helping to design the diffusion flame system, and Dale Uyeminami for technical expertise in generating iron and soot aerosols during the course of these experiments. Assistance in histologic preparations and analyses was provided by Janice Peake, Imelda Espiritu, and Rebecca Walther. The analyses of iron content were performed by Chester Labnet in Tigard, Oregon. Iron analysis was performed by Drs. Valerie J. Leppert and J. Jasinski at the University of California, Merced. EC and OC analyses were completed by Dr. Kochi Fung of ATM AA Inc. in Calabasas, California.

REFERENCES

Anderson ME. 1985. Determination of glutathione and glutathione disulfide in biological samples. Methods Enzymol 113:548–555.

Aust AE, Lund LG. 1991. Iron mobilization from crocidolite results in enhanced iron-catalyzed oxygen consumption and hydroxyl radical generation in the presence of cysteine. In: Mechanisms in Fibre Carcinogenesis. Brown RC, Hoskins JA, Johnson NF, eds. Plenum Press, New York, NY.

Aust AE, Smith KR, Ball JC. 1995. Iron in airborne particulates may be important in lung damage. In: Particulate Matter: Health and Regulatory Issues VIP-49. Air and Waste Management Associates, Pittsburgh, PA.

Aust AE, Ball JC, Hu AA, Lighty JS, Smith KR, Straccia AM, Veranth JM, Young WC. 2002. Particle Characteristics Responsible for Effects on Human Lung Epithelial Cells. Research Report 110. Health Effects Institute, Boston, MA.

Barnes PJ, Karin M. 1997. Nuclear factor-KappaB: a pivotal transcription factor in chronic inflammatory diseases. N Engl J Med 336:1066–1071.

Benzie IFF, Strain JJ. 1999. Ferric reducing/antioxidant power assay: Direct measure of total antioxidant activity of biological fluids and modified version for simultaneous measurement of total antioxidant power and ascorbic acid concentration. Methods Enzymol 299:15–27.

Bradford MM. 1976. A rapid and sensitive method for the quantitation of microgram quantities of protein utilizing the principal of protein-dye binding. Anal Biochem 72:248–254.

Brown JS, Kim CS, Reist PC, Zeman KL, Bennett WD. 2000. Generation of radiolabeled "soot-like" ultrafine aerosols suitable for use in human inhalation studies. Aerosol Sci Technol 32:325–337.

Brumby PE, Massey V. 1967. Determination of nonheme iron, total iron, and copper. In: Methods in Enzymology. Estabrook RW, Pullman ME, eds. Academic Press, New York, NY.

Campen MJ, Nolan JP, Schladweiler MCJ, Kodavanti UP, Evansky PA, Costa DL, Watkinson WP. 2001. Cardiovascular and thermoregulatory effects of inhaled PM-associated transition metals: A potential interaction between nickel and vanadium sulfate. Toxicol Sci 64:243–252.

Carter JD, Ghio AJ, Samet JM and Delvin RB. 1997. Cytokine production by human airway epithelial cells after exposure to an air pollution particle is metal-dependent. Toxicol Appl Pharmacol 146:180–188.

Chao CC, Lund LF, Zinn KR, Aust AE. 1994. Iron mobilization from crocidolite asbestos by human lung carcinoma cells. Arch Biochem Biophys 314:384–391.

Charalampopoulos TT, Hahn DW and Chang H. 1992. Role of metal additives in light scattering from flame particulates. Appl Opt 31:6519–6528.

Cho HY, Hotchkiss JA, Harkema JR. 1999. Inflammatory and epithelial responses during the development of ozone-induced mucous metaplasia in the nasal epithelium of rats. Toxicol Sci 51:135-145.

Costa DL, Dreher KL. 1997. Bioavailable transition metals in particulate matter mediate cardiopulmonary injury in healthy and compromised animal models. Environ Health Perspect 105(Suppl):1053–1060.

Dietert RR, Etzel RA, Chen D, Halonen M, Holladay SD, Jarabek AM, Landreth K, Peden DB, Pinkerton KE, Smialowicz RJ, Zoetis T. 2000. Workshop to identify critical windows of exposure for children's health: Immune and respiratory systems work group summary. Environ Health Perspect 108(Suppl 3):483–490.

Dobbins RA, Megaridis CM. 1991. Absorption and scattering of light by polydisperse aggregates. Appl Opt 30:4747–4754.

Dobbins RA, Mulholland GW, Bryner NP. 1994. Comparison of a fractal smoke optics model with light extinction measurements. Atmos Environ 28:889–897.

Dreher KL, Jaskot RH, Lehmann JR, Richards JH, McGee JK, Ghio AJ, Costa DL. 1997. Soluble transition metals

mediate residual oil fly ash induced acute lung injury. J Toxicol Environ Health 50:285–305.

Dye JA, Adler KB, Richards JH, Dreher KL. 1997. Epithelial injury induced by exposure to residual oil fly-ash particles: Role of Reactive Oxygen Species. Am J Respir Cell Mol Biol 17:625–633.

Dye JA, Adler KB, Richards JH, Dreher KL. 1999. Role of soluble metals in oil fly ash-induced airway epithelial injury and cytokine gene expression. Am J Physiol Lung Cell Mol Physiol 277:L498–L510.

Fang R. 1999. Induction of ferritin synthesis in human lung epithelial cells (A549) treated with iron-containing particulates and iron mobilization from these particulates [PhD dissertation]. Utah State University, Logan, UT.

Fang R, Aust AE. 1997. Induction of ferritin synthesis in human lung epithelial cells treated with crocidolite asbestos. Arch Biochem Biophys 340:369–375.

Fanucci MV, Plopper CG. 1997. Pulmonary developmental responses to toxicants. In: Comprehensive Toxicology Vol 8, Toxicology of the Respiratory System. (RA Roth ed.). pp 203–220. Pergamon, Elsevier Sci Ltd, New York.

Fernandez A, Wendt JO, Cenni R, Young RS, Witten ML. 2002. Resuspension of coal and coal/municipal sewage sludge combustion generated fine particles for inhalation health effects studies. Sci Total Environ 287:265–274.

Gamble J, Lewis RJ. 1996. Health and respirable particulate (PM_{10}) air pollution: A causal or statistical association? Environ Health Perspect 104:838–850.

Gauderman, WJ, Gilliland GF, Vora H, Avol E, Stram D, McConnell R, Thomas D, Lurmann F, Margolis HG, Rappaport EB, Berhane K, Peters JM. 2002. Association between air pollution and lung function growth in southern California children: Results from a second cohort. Am J Respir Crit Care Med 166(1):76–84.

Gauderman WJ, McConnell R, Gilliland F, London SJ, Thomas D, Avol EL, Vora H, Berhane K, Rappaport EB, Lurmann F, Marigolis HG, Peters J. 2000. Association between air pollution and lung function growth in southern California children. Am J Respir Crit Care Med 162:1383–1390.

Ghio AJ, Stonehuerner J, Pritchard RJ, Piantadosi CA, Quigley DR, Dreher KL, Costa DL. 1996. Humic-like substances in air pollution particulates correlate with concentrations of transition metals and oxidant generation. Inhal Toxicol 8:479–494.

Ghio AJ, Stonehuerner J, Dailey LA, Carter JD. 1999. Metals associated with both the water-soluble and insoluble fractions of an ambient air pollution particle catalyze an oxidative stress. Inhal Toxicol 11:37–49.

Habig WH, Pabst MJ, Jakoby WB. 1974. Glutathoine-S-Transferase: The first step in mercapturic acid formation. J Biol Chem 249:7130–7139.

Halliwell B, Gutteridge JMC. 1999. Free Radicals in Biology and Medicine, 3rd edition. Oxford University Press, Oxford, UK.

Hardy JA, Aust AE. 1995. The effect of iron binding on the ability of crocidolite asbestos to catalyze DNA single-strand breaks. Carcinogenesis 16(2):319–325.

Harrison PM, Arosio P. 1996. Ferritins: Molecular properties, iron storage function and cellular regulation. Biochim Biophys Acta 1275:161–203.

Harrod KS, Mounday AD, Stripp BR, Whitsett JA. 1998. Clara cell secretory protein decreases lung inflammation after acute virus infection. Am J Physiol Lung Cell Mol Physiol 275:L924–L930.

Hayes JD, Pulfor DJ. 1995. The glutathione S-transferase supergene family: Regulation of GST and the contribution of the isoenzymes to cancer chemoprotection and drug resistance. Crit Rev Biochem Mol Bio 30:445–600.

Horak F, Studnicka M, Gartner C, Spengler JD, Tauber E, Urbanek R, Veiter A, Frischer T. 2002. Particulate matter and lung function growth in children: A 3-yr follow-up study in Austrian schoolchildren. Eur Respir J 19(5):838–845.

Hughes L, Cass G, Gone J, Ames M, Olmez I. 1998. Physical and chemical characterization of atmospheric ultrafine particles in the Los Angeles area. Environ Sci Tech 32:1153–1161.

Jakab GJ. 1992. Relationship between carbon black particulate-bound formaldehyde, pulmonary antibacterial defenses and alveolar macrophage phagocytosis. Inhal Toxicol 4:325–342.

Jakab GJ. 1993. The toxicological interactions resulting from inhalation of carbon black and acrolein on pulmonary antibacterial and antiviral defenses. Toxicol Appl Pharmacol 121:167–175.

Jakab GJ, Hemenway DR. 1994. Concomitant exposure to carbon black particulates enhances ozone-induced lung inflammation and suppression of alveolar macrophage phagocytosis. J Toxicol Environ Health 41:221–231.

Jimenez LA, Thompson J, Brown DA, Rahman I, Antonicelli F, Duffin R, Drost EM, Hay RT, Donaldson K, MacNee W. 2000. Activation of NF-κB by PM_{10} occurs via an iron-mediated mechanism in the absence of IκB degradation. Toxicol Appl Pharmacol 166:101–110.

Kadiiska MB, Mason RP, Dreher KL, Costa DL, Ghio AF. 1997. In vivo evidence of free radical formation in the rat lung after exposure to an emission source air pollution particle. Chem Res Toxicol 10:1104–1108.

Karg E, Roth C, Heyder J. 1998. Do inhaled ultrafine particles cause acute health effects in rats? II: Exposure system. J Aerosol Sci 29:S315–S316.

Kelly FJ. 1999. Glutathione: In defense of the lung. Food Chem Toxicol 37:963–966.

Kennedy T, Ghio AJ, Reed W, Samet J, Zagorski J, Quay J, Carter J, Dailey L, Hoidal JR, Devlin RB. 1998. Copper-dependant inflammation and nuclear factor-κB activation by particulate air pollution. Am J Respir Cell Mol Biol 19:366–378.

Klausner RD, Rouault TA, Harford JB. 1993. Regulating the fate of mRNA: The control of cellular iron metabolism. Cell 72:19–28.

Kodavanti UP, Hauser R, Christiani DC, Meng ZH, McGee J, Ledbetter A, Richards J, Costa DL. 1998. Pulmonary responses to oil fly ash particles in the rat differ by virtue of their specific soluble metals. Toxicol Sci 43:204–212.

Köylü UO, Faeth GM. 1994a. Optical properties of overfire soot in buoyant turbulent diffusion flames at long residence times. Trans ASME J Heat Transfer 116:152–159.

Köylü UO, Faeth GM. 1994b. Optical properties of soot in buoyant laminar diffusion flames. Trans ASME J Heat Transfer 116:971–979.

Köylü UO, McEnally CS, Rosner DE, Pfefferle LD. 1997. Simultaneous measurements of soot volume fraction and particle size/microstructure in flames using a thermophoretic sampling technique. Comb Flame 110:494–507.

Laemmli UK. 1970. Cleavage of structural proteins during the assembly of the head of bacteriophage T4. Nature 277:680–685.

Lay JC, Bennett WD, Ghio AJ, Bromberg PA, Costa DL, Kim CS, Koren HS and Delvin RB. 1999. Cellular and biochemical response of the human lung after intrapulmonary instillation of ferric oxide particles. Am J Respir Cell Mol Biol 20:631–642.

Li XY, Gilmour PS, Donaldson K, MacNee W. 1996. Free radical activity and pro-inflammatory effects of particulate air pollution (PM_{10}) in vivo and in vitro. Thorax 51:1216–1222.

Lindenschmidt RC, Witschi HP. 1990. Toxicological interaction in the pathogenesis of lung injury. In: Toxic Interactions. (RS Goldstein, WR Hewitt, JB Hook, eds.). pp 409–442. Academic Press, New York, NY.

Lund LG, Aust AE. 1990. Iron mobilization from asbestos by chelators and ascorbic acid. Arch Biochem Biophys 278:60–64.

Lund LG, Aust AE. 1992. Iron mobilization from corcidolite asbestos greatly enhances corcidolite-dependent formation of DNA single-strand-breaks in ϕX174 RFI DNA. Carcinogenesis 13:637–642.

Oberdörster G. 2001. Pulmonary effects of inhaled ultrafine particles. Int Arch Occup Environ Health 74:1–8.

Pinkerton KE, Mercer RR, Plopper CG, Crapo JD. 1992. Distribution of injury and microdosimetry of ozone in the ventilatory unit of the rat. J Appl Physiol 73:817–824.

Pinkerton KE, Green FHY, Saiki C, Vallyathan V, Plopper CG, Gopal V, Hung D, Bahne EB, Lin SS, Menache MG, Schenker MB. 2000. Distribution of particulate matter and tissue remodeling in the human lung. Environ Health Perspect 108(Suppl 11):1063–1069.

Plopper CG, Chu FP, Haselton CJ, Peake J, Wu J, Pinkerton KE. 1994. Dose-dependent tolerance to ozone. I. Tracheobroncial epithelial reorganization in rats after 20 months' exposure. Amer J Pathol 144:404–421.

Pope CA III, Dockery DW, Schwartz J. 1995. Review of epidemiological evidence of health effects of particulate air pollution. Inhal Toxicol 7:1–18.

Rahman I. 2000. Regulation of nuclear factor-κB, activator protein-1, and glutathione levels by tumor necrosis factor-κ and dexamethasone in alveolar epithelial cells. Bio Pharmacol 60:1041–1049.

Rahman I, MacNee W. 1999. Lung glutathione and oxidative stress: Implications in cigarette smoke-induced airway disease. Am J Physiol Lung Cell Mol Physiol 277:L1067–L1088.

Rahman I, MacNee W. 2000. Oxidative stress and regulation of glutathione in lung inflammation. Eur Respir J 16:534–554.

Rajini P, Gelzleichter TR, Last JA, Witschi HP. 1993. Alveolar and airway cell kinetics in the lungs of rats exposed to

nitrogen dioxide, ozone and a combination of the two gases. Toxicol Appl Pharmacol 121:186–192.

Reinelt D, Linteris GT. 1996. Twenty-Sixth Symposium (International) on Combustion. The Combustion Institute, Pittsburgh PA.

Rice TM, Clarke RW, Godleski JJ, Al-Mutairi E, Jiang N-F, Hauser R, Paulauskis JD. 2001. Differential ability of transition metals to induce pulmonary inflammation. Toxicol Appl Pharmacol 177:46–53.

Schauer JJ, Kleenam MJ, Cass GR, Simoneit BRT. 1999. Measurement of emission from air pollution sources. 2. C1 through C30 organic compounds from medium duty diesel trucks. Environ Sci Technol 33:1578–1587.

Schlesinger RB. 1995. Interaction of gaseous and particulate pollutants in the respiratory tract: Mechanisms and modulators. Toxicology 105:315–325.

Schwartz J. 1995. Air pollution and hospital admissions for respiratory disease. Epidemiology 7:21–28.

Schwartz J, Morris R. 1995. Air pollution and hospital admissions for cardiovascular disease in Detroit, Michigan. Am J Epidemiol 142:23–35.

Smirnov IM, Bailey K, Flowers CH, Garrigues NW, Wesselius LJ. 1999. Effects of TNF-alpha and IL-1beta on iron metabolism by A549 cells and influence on cytotoxicity. Am J Physiol 277:L257–263.

Smith KR, Aust AE. 1997. Mobilization of iron from urban particulates leads to generation of reactive oxygen species in vitro and induction of ferritin synthesis in human lung epithelial cells. Chem Res Toxicol 10:828–834.

Smith KR, Veranth JM, Lighty JS, Aust AE. 1998. Mobilization of iron from coal fly ash was dependent upon the particle size and the source of coal. Chem Res Toxicol 11:1494–1500.

Smith KR, Veranth JM, Hu AA, Lighty JS, Aust AE. 2000. Interleukin-8 levels in human lung epithelial cells are increased in response to coal fly ash and vary with bioavailability of iron, as a function of particle size and source of coal. Chem Res Toxicol 13:118–125.

Soukup JM, Ghio AJ, Becker S. 2000. Soluble components of Utah Valley particulate pollution alter alveolar macrophage function in vivo and in vitro. Inhal Toxicol 12:401–414.

Stokinger HE. 1984. A review of world literature finds iron oxides noncarcinogens. Am Ind Hyg Assoc J 45:127–133.

Sun JD, Wolff RK, Miao SM, and Barr EB. 1989. Influence of adsorption to carbon black particles on the retention and metabolic activation of benzo[*a*]pyrene in rat lungs following inhalation exposure or intratracheal instillation. Inhal Toxicol 1:1–19.

Theil EC. 1994. Iron regulatory elements (IREs): A family of mRNA non-coding sequences. Biochem J 304:1–11.

Tietz F. 1969. Enzymatic method for quantitative determination of nanogram amounts of total and oxidized glutathione: Application to mammalian blood and other tissues. Anal Biochem 27:502–522.

Towbin H, Staehelin T, Gordon J. 1979. Electrophoretic transfer of proteins from polyacrylamide gels to nitrocellulose sheets: Procedure and some applications. Proc Natl Acad Sci USA 76:4350–4354.

Veranth JM, Smith KR, Huggins F, Hu AA, Lighty JS, Aust AE. 2000. Mossbauer spectroscopy indicates that iron in an aluminosilicate glass phase is the source of the bioavailable iron from coal fly ash. Chem Res Toxicol 13:161–164.

Vincent R, Kumarathasan P, Goegan P, Bjarnason SG, Guénette J. Bérubé D, Adamson IY, Desjardins S, Buenett RT, Miller FJ, Battistini B. 2001. Inhalation Toxicology of Urban Ambient Particulate Matter: Acute Cardiovascular Effects in Rats. Research Report 104. Health Effects Institute, Boston, MA.

Vogl G, Elstner EF. 1989. Diesel soot particles catalyze the production of oxy-radicals. Toxicol Lett 47:17–23.

Watkinson WP, Campen MJ, Costa DL. 1998. Cardiac arrhythmia induction after exposure to residual oil fly ash particles in a rodent model of pulmonary hypertension. Toxicol Sci 41:209–216.

Witschi HP, Morse CC. 1983. Enhancement of lung tumor formation in mice by dietary butylated hydroxytoluene: Dose-time relationships and cell kinetics. J Nat Canc Inst 71:859–866.

Zhang J, Megaridis CM. 1996. Soot suppression by ferrocene in laminar ethylene/air nonpremixed flames. Comb Flame 105:528–540.

ABOUT THE AUTHORS

Kent E. Pinkerton, Ph.D., is the director of the Center for Health and the Environment, and a professor in the Department of Anatomy, Physiology, and Cell Biology, School of Veterinary Medicine, University of California, Davis. He completed his undergraduate education at

Brigham Young University and received M.S. and Ph.D. degrees in pathology from Duke University in 1978 and 1982, respectively. His primary research interests are in respiratory cell biology, environmental air pollutants, and the health effects of inhaled nanomaterials.

Yamei Zhou, Ph.D., is a graduate student in the Graduate Group in Comparative Pathology, Center for Health and the Environment, University of California, Davis. Dr. Zhou completed her B.S. degree in Medicine in 1985 and her M.S. degree in Environmental Toxicology in 1996 at Nanjing Medical University, China. Dr. Zhou's doctoral dissertation for the Comparative Pathology department at the University of California, Davis was *Pulmonary Oxidative Stress and NF-kappa B Activation in Response to Inhaled Iron and Soot Particles in Rats*. Her research interests are environmental air pollution and the role of oxidative stress and NF-κB signaling.

Caiyun Zhong, Ph.D., is a graduate student in the Graduate Group in Comparative Pathology, Center for Health and the Environment, University of California, Davis. Dr. Zhong completed his B.S. degree in Medicine at Nanjing Railway Medical College (now Southeast University School of Medicine) in China in 1984 and his M.S. degree in Nutritional Toxicology from Nanjing Medical University in China in 1987. Dr. Zhong's doctoral dissertation for the Comparative Biology department at the University of California, Davis was *Regulation of MAPK/AP-1 and NF-kappa B Signal Pathways in Tobacco Smoke-Induced Pulmonary Cell Proliferation and Apoptosis*. His research interests continue in the area of signal pathways to regulate cell proliferation and apoptosis due to inhaled air pollutants.

Kevin R. Smith, Ph.D., is a project scientist at the Center for Health and the Environment, University of California, Davis. Dr. Smith completed his undergraduate education at Weber State University and received his Ph.D. degree in biochemistry from Utah State University in 2000. Dr. Smith's research interests involve the use of in vivo models of human inflammatory disease to investigate potential pharmacologic agents that may be useful in resolution of pulmonary inflammation, airway remodeling, and disease and histological assessment of airway pathology in rodents.

Stephen V. Teague, B.S., is a staff research associate at the Center for Health and the Environment, University of California, Davis. Mr. Teague completed his undergraduate education at the University of New Mexico. He has extensive experience in the generation and characterization of solid particles, vapors, and gases and in field monitoring of environmental air pollutants. His research interests are the design and construction of novel particle generation and aerosolization systems.

Ian M. Kennedy, Ph.D., is a professor in the Department of Mechanical and Aeronautical Engineering, College of Engineering, University of California, Davis. Dr. Kennedy received his undergraduate education and completed his Ph.D. degree in mechanical engineering at Sydney University, Australia in 1980. His primary research interests are combustion technology and the characterization of combustion-generated particles. He is also involved in the synthesis of sensors in the environmental application of nanomaterials.

Margaret G. Ménache, Ph.D., is a biostatistician in the Masters in Public Health Program, Family and Community Medicine, School of Medicine, University of New Mexico Health Sciences Center, Albuquerque. Dr. Menache completed her undergraduate education at Georgetown University in 1975, her M.S. degree in biostatistics at the University of North Carolina, Chapel Hill in 1991, and her Ph.D. degree in the School of the Environment at Duke University in 1997. Her primary research interests are biostatistical analysis and comparative modeling of the deposition of gases and particles in the respiratory tract of mammalian species.

OTHER PUBLICATIONS RESULTING FROM THIS RESEARCH

Pinkerton K, Zhou Y, Teague S, Peake J, Walther R, Kennedy I, Leppert V, Aust A. 2004. Reduced lung cell proliferation following short-term exposure to ultrafine soot and iron particles in neonatal rats: Key to impaired lung growth? Inhal Toxicol 16(Suppl 1):73–81.

Zhou Y, Zhong C, Kennedy IM, Leppert VJ, Pinkerton KE. 2003. Oxidative stress and NF-κB activation in the lungs of rats: A synergistic interaction between soot and iron particles. Toxicol Appl Pharmacol 190:157–169.

Zhou Y, Zhong C, Kennedy IM, Pinkerton KE. 2003. Pulmonary responses of acute exposure to ultrafine iron particles in healthy adult rats. Environ Toxicol 18:227–235.

Yang G, Teague S, Pinkerton K, Kennedy IM. 2001. Synthesis of an ultrafine iron and soot aerosol for the evaluation of particle toxicity. Aerosol Sci Technol 35:759–766.

ABBREVIATIONS AND OTHER TERMS

ANOVA	analysis of variance
BAL	bronchoalveolar lavage
BALF	bronchoalveolar lavage fluid
BrdU	5-bromo-2-deoxyuridine
CFA	coal fly ash
CNC	condensation nuclei counter
CYP	cytochrome P
EC	elemental carbon
EELS	electron energy loss spectroscopy
EMSA	electrophoretic mobility shift assay
FRAP	ferric reducing antioxidant power
GRR	glutathione redox ratio
GSH	glutathione
GSSG	glutathione disulfide
GST	glutathione-S-transferase
IL	interleukin [-6, -8, -1β]
LDH	lactate dehydrogenase
MDA	malondialdehyde
NADPH	nicotinamide adenine dinucleotide phosphate (reduced form)
NF-κB	nuclear factor-kappa B
NO	nitric oxide
NO_x	nitrogen oxides
OC	organic carbon
PAH	polycyclic aromatic hydrocarbon
PBS	phosphate buffered saline
PM	particulate matter
$PM_{1.0}$	PM wih an aerodynamic diameter ≤ 1.0 μm
$PM_{2.5}$	PM wih an aerodynamic diameter ≤ 2.5 μm
PM_{10}	PM wih an aerodynamic diameter ≤ 10 μm
ROFA	residual oil fly ash
ROS	reactive oxygen species
SRM	standard reference material (U.S. National Institute of Standards and Technology)
TNF-α	tumor necrosis factor-α
U.S. EPA	U.S. Environmental Protection Agency

Research Report 135, *Mechanisms of Particulate Matter Toxicity in Neonatal and Young Adult Rat Lungs*, K. Pinkerton et al.

INTRODUCTION

Ambient particulate matter (PM*) is a complex mixture of solid and liquid particles, ranging from approximately 0.005 to 100 µm in aerodynamic diameter, that are suspended in air. Not only does PM vary in size, but its chemical composition and other physical and biologic properties vary spatially and temporally. This variability in PM characteristics derives from differences in the sources of pollution; these particles may be natural in origin — the result of geographic conditions, weather, or seasonal patterns — or they may be generated by human activities such as driving vehicles and operating manufacturing or power plants. In addition, reactive substances in the atmosphere combine to generate what are known as secondary particles, such as sulfates, which may form a significant fraction of total PM at a site.

Although the characteristics of PM differ from place to place, epidemiologic studies in diverse locations have shown associations between increases in levels of PM and short-term increases in morbidity and mortality; long-term exposure to PM has also been associated with increased mortality from cardiopulmonary causes as well as from cancer (reviewed in U.S. Environmental Protection Agency [U.S. EPA] 2004). On the basis of these findings, and the results of toxicologic studies, many governmental agencies have set regulatory standards or guidelines for concentrations of ambient PM. Particles ≤ 10 µm in aerodynamic diameter (PM_{10}) are of most concern because they are considered respirable by humans. To protect the general population and groups considered most vulnerable to adverse effects from PM in the United States, the U.S. EPA monitors PM_{10} levels and has promulgated National Ambient Air Quality Standards for particles ≤ 2.5 µm in aerodynamic diameter ($PM_{2.5}$ or fine particles). As discussed in the Scientific Background section of this Critique, some scientists believe that ultrafine particles (≤ 100 nm in diameter) may be particularly toxic.

Much work has focused on understanding the effects of particles derived from combustion sources: these particles are in the fine and ultrafine range and generally are composed of an elemental carbon (EC) core that binds metals (such as iron, vanadium, nickel, copper, and platinum), organic carbon (OC) compounds, and sulfates. Critical questions in PM research involve understanding the mechanisms by which particles may cause effects and the key physical and chemical characteristics of particles that are associated with toxicity. To address these questions, in 1996 HEI issued RFA 96-1, *Mechanisms of Particle Toxicity: Fate and Bioreactivity of Particle-Associated Compounds*. Studies were sought that would investigate the bioavailability of constituents of fine and ultrafine particles (derived from mobile sources or from other well-defined combustion processes) and any interactions between particles and cells or cellular compartments occurring after inhalation. In response, Dr. Kent Pinkerton and colleagues from the University of California–Davis submitted an application to evaluate the effects of short-term exposure on the airways of rats using laboratory-generated ultrafine metal particles, either alone or in combination with soot (produced by incomplete combustion of coal, oil, and other fuels and composed primarily of EC and OC). The rationale for the study was that combinations of metal and soot should provide an understanding of the interaction between components of combustion source-derived particles found in ambient air. The HEI Research Committee recommended the study for funding.†

SCIENTIFIC BACKGROUND

TOXICITY OF ULTRAFINE PARTICLES

Before this study began, little was known about the health effects of exposure to ultrafine particles, particularly about the effects resulting from inhalation. Ultrafine particles, emitted in high numbers by combustion engines, are the dominant contributors of particle numbers in $PM_{2.5}$. For

* A list of abbreviations and other terms appears at the end of the Investigators' Report.

† Dr. Pinkerton's two-year study, "Mechanisms of Particle Toxicity in the Respiratory System," began in November 1997. Total expenditures were $214,212. The draft Investigators' Report from Dr. Pinkerton and colleagues was received for review in January 2003. Revised reports were received in January 2004, November 2004, and June 2005. The edited report was accepted for publication in September 2008. During the review process, the HEI Health Review Committee and the investigators had the opportunity to exchange comments and to clarify issues in both the Investigators' Report and the Review Committee's Critique.

example, a mass concentration of 10 µg particles/m^3 would contain only one fine particle of diameter 2.5 µm, but more than 2 million ultrafine particles of diameter 0.02 µm (Oberdörster 1995). Smaller particles have a greater total surface area than larger particles of the same mass. Thus, they may present a larger surface area for interacting with airway tissue or for transporting toxic material associated with the particle surface into the airways.

Some scientists have hypothesized that ultrafine particles may be especially toxic (reviewed in Utell and Frampton 2000, Frampton 2001, and Oberdörster 2001), with the potential to move out of the lungs and deposit in other tissues (Peters et al. 2006, Kreyling et al. 2006). Epidemiologic studies, however, have not resolved the issue of the comparative toxicity of ultrafine particles. Some studies have described associations between increases in adverse respiratory effects and exposure to ultrafine particles in children with asthma (Pekkanen et al. 1997; Peters et al. 1997). However, these studies found no greater effect for ultrafine particles than for fine particles. In addition, Wichmann and colleagues (2000) reported that mortality was associated with ultrafine particle concentrations in the city of Erfurt, Germany. However, the association reported between ultrafine particles and mortality was not greater than associations reported for other components of the PM mix. Peters and colleagues (2005), evaluating data on the induction of nonfatal myocardial infarction, did not find statistically significant associations with ultrafine particle concentrations concurrent with the myocardial infarction or up to 5 days before it.

Toxicologic studies on the airways of rodents have compared the effects of exposure to high concentrations of various sizes of particles that have the same chemical composition. These studies have suggested that, based on mass, ultrafine particles are more effective than fine particles in inducing airway inflammatory responses. Initially these studies evaluated the effects of particles instilled intratracheally (e.g., Oberdörster 1995), but more recent studies have used inhalation, the more physiologically relevant route of exposure, to evaluate the effects of metals (Hahn et al. 2005) and carbon black particles (Gilmour et al. 2004). The inhalation studies have found a pattern similar to that of the intratracheal instillation studies, but showed that composition also played a role.

OXIDATIVE STRESS AS A MECHANISM TO EXPLAIN THE TOXICITY OF METAL-CONTAINING PARTICLES

Many metals are found in urban air PM. Iron is the most abundant of the "transition metals," which include vanadium, copper, and platinum (Hughes et al. 1998). Before the current study started, however, little was known about how exposure to components of PM, such as metals, might exert health effects. Earlier studies had indicated that the instillation of the organic fraction of diesel exhaust into the trachea of mice resulted in the production of oxygen radicals, and that the production of superoxide and hydroxyl radicals could be reduced by removing the organic fraction from diesel particles (Sagai et al. 1993; Kumagai et al. 1995).

Superoxide and oxygen-based free radicals, together with hydrogen peroxide, are referred to as reactive oxygen species (ROS) (Halliwell and Gutteridge 1999). Under normal conditions, ROS are cleared from cells by the action of enzymes such as superoxide dismutase and glutathione (GSH) peroxidase or by other, non-enzymatic, ROS scavengers. Other studies showed that metals can cause an imbalance in the production of oxidants, initiating a state known as *oxidative stress* that may cause cell activation or cell damage (reviewed in Samet and Ghio 2007). Intracellular signal transduction pathways may be activated, including the activation of transcription factors such as nuclear factor-kappa B (NF-κB). These activation pathways result in the synthesis of inflammatory cytokines and chemokines that recruit inflammatory cells; production of these mediators by airway cells contributes to lung inflammation and injury.

A voluminous literature exists on oxidative stress as a plausible mechanism to explain the induction of PM-mediated inflammatory responses. Studies in rodents have provided documentation of the cardiovascular and inflammatory effects of exposure to particles rich in transition metals — especially iron, nickel, and vanadium — emitted and collected from oil-fired and coal-fired electrical power plants (residual oil fly ash and coal fly ash, respectively). Exposure to high levels of these particles in residual oil fly ash has been found to induce lung inflammation (Kadiiska et al. 1997), cardiac arrhythmias (Watkinson et al. 1998), and inflammatory cytokines in human bronchial epithelial cells (Carter et al. 1997). Coal fly ash has been shown to be a source of bioavailable iron (Smith et al. 1998) and to induce inflammatory cytokines in human lung epithelial cells (Smith et al. 2000). Aust and coworkers (2002) demonstrated a plausible connection between the release of iron from coal fly ash particles within lung epithelial cells, oxidative stress caused by ROS production, and lung inflammation. They demonstrated that the smaller coal fly ash particles ($PM \leq 1.0$ µm in aerodynamic diameter [$PM_{1.0}$]) were more active in inducing inflammatory responses than were larger particles. $PM_{1.0}$ contained more iron than did the larger particles.

Adverse health effects for residents exposed to PM_{10} in the Utah Valley included decreased lung function and

increased incidence of respiratory symptoms (Pope 1996). Results of toxicologic studies in humans, rats, and in vitro cell lines have suggested a key role for transition metal components of the Utah Valley particles in explaining the reported epidemiologic associations (Ghio and Devlin 2001; Dye et al. 2001; Pagan et al. 2003). Furthermore, exposures to large amounts of metal-containing fumes, such as those generated during processes such as welding, have been associated with inflammatory responses in rodents (Antonini et al. 1998) and changes in the expression of genes associated with oxidative stress and inflammatory responses in humans (Wang et al. 2005).

SOOT

Soot particles, produced as a result of incomplete combustion of coal, diesel oil, and other fuels, are composed primarily of EC and several OC compounds. Soot also contains oxygen, nitrogen, hydrogen, metals, and polyaromatic hydrocarbons.

In early studies in mice, inhalation of ultrafine carbon black particles — a form of EC — at high concentrations (10 mg/m^3) produced no observable effects on the respiratory system, suggesting that the particles are inert, but simultaneous exposure to carbon black and ozone resulted in lung inflammatory responses that were greater than responses to ozone alone (Jakab 1992, 1993; Jakab and Hemenway 1994). More recent studies of controlled inhalation exposures to ultrafine EC particles have shown limited cardiovascular responses in humans (Frampton et al. 2006) and mice (Andre et al. 2006).

Before the current study started, previous studies had indicated that the intratracheal instillation of the organic fraction of diesel exhaust into mice resulted in the production of oxygen radicals, and that the production of superoxide and hydroxyl radicals could be reduced by removing the organic fraction from diesel particles (Sagai et al. 1993, Kumagai et al. 1995). Several subsequent toxicologic and epidemiologic studies have reported associations between the organic fractions of ambient PM and adverse respiratory and cardiovascular health outcomes (reviewed in Mauderly and Chow 2008).

Dr. Pinkerton speculated that soot might act as a carrier for other pollutants, such as transition metals, in ambient air, and hence might transport these pollutants into the respiratory tract. The pollutants could change the deposition and clearance of the respiratory tract, which could alter biologic functions. The studies described in the current report were among the first to measure the oxidative and inflammatory response in airway cells to inhalation of ultrafine iron particles. They also evaluated whether the activity of ultrafine iron particles was modified when the iron was combined with soot particles.

SUMMARY OF STUDY

OBJECTIVES AND SPECIFIC AIMS

The major objective of this study was to determine if the type and magnitude of biologic effects in the lung, in response to inhaled ultrafine particles, depended on particle composition. Originally, Pinkerton and colleagues proposed to evaluate the effects of two metals — iron and cerium — alone or combined with soot. Because of time and budgetary pressures, the investigators focused on whether exposure to iron particles alone or combinations of iron and soot particles could induce oxidative stress and inflammatory responses in the lungs and airways. To accomplish these objectives, the investigators pursued four specific aims:

1. Design, construct, and characterize a flame combustion system to generate ultrafine particles of iron, of soot, and of combinations of iron and soot. This combustion system would interface with a small-animal exposure unit for inhalation studies.
2. Determine the characteristics of the iron and soot particle matrix formed during the fuel combustion process.
3. Determine the effects in the airways of healthy young adult and neonatal rats shortly after exposure to ultrafine particles of iron, soot, or combinations of iron and soot.
4. Identify endpoints that best correlate with acute respiratory toxicity caused by the particles of iron, soot, or combinations of iron and soot.

STUDY DESIGN AND METHODS

Particle Generation and Inhalation Systems

Particle Generation The investigators developed a diffusion flame apparatus to produce aerosols of iron particles, soot particles, or combinations of iron and soot particles. Iron pentacarbonyl vapor was used as the source of iron particles. The investigators generated aerosols of ultrafine iron particles by mixing iron pentacarbonyl and ethylene — the primary fuel used in the combustion system to generate soot — before the mixture reached the flame burner nozzle (Figure 1 in the Investigators' Report). By increasing the iron pentacarbonyl in the mixture, flame combustion completely oxidized the ethylene, leaving only aerosols of iron particles.

A mixture of ethylene and acetylene (a stronger soot producer than ethylene) was used to generate soot. A mixture of ethylene and acetylene in the presence of iron pentacarbonyl

was used to produce the combinations of iron and soot particles. The flame combustion system was designed to operate at a constant soot production rate, while the iron loading could be varied from 0 to 100 μg/m^3.

Inhalation System Aerosols of particles were diluted with filtered air in a primary dilution chamber. The diluted aerosol flowed into a secondary dilution chamber where additional filtered air further mixed, cooled, and diluted the particles to the desired concentrations. From the secondary dilution chamber, the particles flowed to each individual animal exposure inhalation unit, which was fitted with a sealed lid to deliver particles by unidirectional flow. The inhalation system used to expose rats to the particles generated by flame combustion is illustrated in Figures 2 and 3 of the Investigators' Report.

Physical and Chemical Characterization of Particles Generated

Particle size distribution was measured with a differential mobility analyzer.

The number of particles was measured with a condensation nuclei counter. This provided a rapid measure of particle number and number fluctuations at the interface of the primary and secondary dilution chambers and allowed the investigators to adjust airflow conditions in the system during animal exposures. The chemical composition of the particles was determined by electron energy loss spectroscopy (EELS) and X-ray diffraction. EELS also provided information about the stoichiometry of the particles.

The shape and size of particles collected on carbon grids were revealed by transmission electron microscopy.

The total mass concentrations of soot particles and combinations of iron and soot particles were determined by weighing particle aerosols collected on preweighed filters. The amount of iron in the particles was measured by X-ray fluorescence.

EC and OC were analyzed in the combinations of iron and soot particles collected on filters.

Animal Exposures

Young adult male rats (10–12 weeks) were placed in the inhalation units and exposed to particles for six hours per day on three consecutive days in five exposure scenarios: two concentrations of iron particles alone (57 and 90 μg/m^3); soot particles alone (250 μg/m^3/day); combinations of iron and soot particles (250 μg/m^3/day with an iron concentration of 45 μg/m^3); and a filtered air control.

Male and female neonatal rats were exposed to particles for six hours per day for three consecutive days at age 10–12 days and again at age 23–25 days in three exposure scenarios: to the combination of 30 μg/m^3 iron particles and soot particles in a total particle concentration of 250 μg/m^3/day; the combination of 100 μg/m^3 iron particles and soot particles in a total particle concentration of 250 μg/m^3/day; and a filtered air control. Rats were weaned at 21 days of age; so 10–12-day-old rats were exposed with their dams in the inhalation unit, while the 23–25-day-old neonates were exposed alone.

These postnatal exposure periods represent different windows of development in the postnatal lung: days 10–12 are a period of rapid cell proliferation and lung growth, and days 23–25 are a period of decreased cell proliferation but continued lung growth and alveolar expansion.

Half of the animals in each experiment were used for analyses of bronchoalveolar lavage fluid (BALF) and the other half for analyses of lung tissue.

Analyses of BALF and Lung Tissue

Pinkerton and coworkers obtained BALF 2 hours and lung tissue 24 hours after the end of the third day's exposure, respectively. They examined the following endpoints in BALF: cell viability and number; the proportions of macrophages, lymphocytes, and neutrophils (cell differentials); and measures of cell damage, such as total protein and lactate dehydrogenase (LDH) activity. They also measured levels of markers of oxidative stress: glutathione-S-transferase (GST) activity; ferric reducing antioxidant power (FRAP — a measure of lung cells' total antioxidant power, a decrease indicating that the cells' antioxidant capacity was depleted); GSH (reduced) (a protective intracellular antioxidant); oxidized GSH (glutathione disulfide [GSSG]); glutathione redox ratio (GRR); nitric oxide (NO — which can be oxidized to NO_2 and NO_3 under conditions of oxidative stress); and malondialdehyde (MDA — one of the end products arising from damage to cell membranes by peroxidation of membrane polyunsaturated fatty acids).

The investigators also analyzed homogenates of lung tissue for: (1) DNA-binding activity of the transcription factor NF-κB; (2) several markers of oxidative stress that they also assayed in BALF (GSH, GSSG, GRR, GST; NO, MDA, and FRAP); (3) markers of inflammation (the proinflammatory cytokines interleukin-1β [IL-1β] and tumor necrosis factor-α [TNF-α]); (4) ferritin (an iron-binding protein); and (5) enzymes from the cytochrome P-450 family (CYP1A1, CYP2B1, and CYP2E1), which are involved in the detoxification of multiple pollutants.

Cell Proliferation and Lung Injury

The investigators evaluated cell proliferation, an indicator of tissue injury and repair, in the airways by measuring the incorporation of 5-bromo-2-deoxyuridine (BrdU) into airway cells. BrdU is an analogue of thymidine, a component of DNA, and is incorporated into DNA by cells undergoing DNA synthesis. To assess BrdU incorporation in young adult rats, the investigators subcutaneously implanted miniosmotic pumps containing BrdU one day before exposures to particles or air. In neonatal rats exposed on days 10–12 after birth, the investigators injected BrdU two hours before killing the animals on day 13. BrdU labeling, detected immunocytochemically with a monoclonal antibody specific for BrdU, was performed in fixed sections of the respiratory tract and central acinus. The fixed sections were prepared 18–24 hours after the exposures ended. The investigators calculated a labeling index as the percentage of BrdU-labeled cells to total epithelial cells examined.

Pinkerton and colleagues also examined fixed sections of the central acinus for changes that may have occurred during particle exposures. They morphometrically quantified the epithelium's thickness and cellular characteristics. They had previously used this technique to establish that this region is sensitive to ozone-induced injury (1992).

In Vitro and in Vivo Estimation of Iron Mobilization from Combinations of Iron and Soot Particles

As a measure of in vitro bioavailability, the investigators determined the amount of iron mobilized from combinations of iron and soot particles collected on filters by incubating the filters with 1 mM citrate, an iron chelator, for 24 hours. The mixture was centrifuged, and the amount of the iron–citrate complex in the supernatant was visualized by adding ferrozine. As a measure of in vivo bioavailability, the investigators measured ferritin level in lung homogenates using an immunoassay.

Statistical Analyses

Pinkerton and coworkers analyzed the data from three sets of exposure experiments (iron, soot, and combinations of iron and soot) with an analysis of variance (ANOVA) for each set. Before the ANOVAs, they tested the data for homogeneity of variance with the Bartlett test. They analyzed the results of this test over the Tukey ladder of powers and transformed the data as needed. The investigators also used the post hoc Levene test with ANOVA, and changed any Bartlett transformations that were still not normalized by the Levene test until they found an appropriate statistical transformation.

The investigators classified the endpoints as indicative of a cytotoxic, oxidative stress, or proinflammatory response. Within each classification, the one or two endpoints considered most likely to be affected by a toxic insult were treated as primary variables.

RESULTS

CHARACTERISTICS OF PARTICLES AND GASES GENERATED

The iron particles generated were predominantly ultrafine and were combined with oxygen to produce ferric oxide (Fe_2O_3). Soot particles and combinations of iron and soot particles were found in two distribution ranges. Soot particles were found at approximately 20 nm in diameter, but they formed chains or clusters larger than 100 nm (that is, in the fine particle range). Most of combinations of iron and soot particles had a mean diameter in the ultrafine range (70–80 nm), but some were also found in the fine particle range (in excess of 100 nm). In combinations of iron and soot particles, most of the iron particles appeared separate from soot particles but in close proximity to them. On average, the combinations of iron and soot particles contained 60% EC and 40% OC, but the OC species were not characterized further. It is not clear whether the soot particles generated in the absence of iron pentacarbonyl had a similar ratio of EC and OC.

The investigators detected carbon monoxide at 5.8 ppm in the primary dilution chamber, but concentrations were greatly reduced (nondetectable to 0.8 ppm) in the secondary dilution chamber, which led to the animal exposure units. Concentrations of nitrogen oxides were 4.7 ppm in the primary dilution chamber. These also were reduced in the secondary dilution chamber (nondetectable to 0.4 ppm). The investigators found no evidence of polycyclic aromatic hydrocarbons in the primary dilution chamber. Pinkerton and colleagues suggest that it was unlikely that iron-containing gases were present in the aerosols, because flame temperatures were high enough to completely decompose iron pentacarbonyl to iron and carbon monoxide.

IN VITRO MOBILIZATION OF IRON

The amount of iron mobilized by citrate from combinations of iron and soot particles was 37.7 ± 0.9 nmol iron/mg particle. The combinations of iron and soot particles used in these experiments contained 10% iron by mass, equivalent to an iron content of 1791 nmol/mg particle. Thus, the iron mobilized by citrate in 24 hours was $37.7/1791 \times 100\% = 2.1\%$.

BIOLOGIC RESPONSES IN YOUNG ADULT RATS AFTER EXPOSURE TO PARTICLES

Iron Particles Alone

After exposure to either 57 or 90 μg/m^3 iron particles there were no changes in GSH, GSSG, or TNF-α levels, NF-κB DNA binding activity, LDH activity, total cell number, cell viability, or cell differentials in BALF or lung tissue. Rats exposed to 90 μg/m^3 iron particles showed a statistically significant increase in total protein in BALF compared with rats exposed to filtered air or 57 μg/m^3 iron particles. Some markers of oxidative stress changed after exposure to the particles with the higher iron concentration: FRAP levels decreased and GST levels increased in both BALF and lung tissue. In addition, IL-1β and ferritin levels were higher in lung tissue of rats exposed to 90 μg/m^3 iron particles compared with controls and animals exposed to 57 μg/m^3 iron particles. Trend tests indicated that in lung tissue, increasing iron concentration was associated with decreased FRAP and increased GST and IL-1β. Morphometric changes or changes in cell replication were not reported.

Soot Particles Alone

Rats exposed to 250 μg/m^3 soot particles showed no changes in any measured parameter of inflammation or oxidative stress. In addition, the anatomical appearance of terminal bronchioles and the lung parenchyma immediately beyond these bronchioles showed no changes from controls.

Combinations of Iron and Soot Particles

Several measures of oxidative stress, inflammation, and tissue injury in either BALF or lung tissue — including levels of TNF-α and total protein, LDH activity, total cell number, cell viability, cell differentials, NO, MDA, GSH, and GRR — were not affected by exposure to combinations of iron and soot particles, but some responses were detected. The level of GSSG increased, FRAP decreased, and GST activity increased. Ferritin levels also increased. In addition, IL-1β levels increased compared with controls, as did the activities of NF-κB and all the cytochrome P-450 isoforms.

No changes from control levels were detected in uptake of BrdU by epithelial or interstitial cells or in histopathologic analysis at several anatomical sites.

BIOLOGIC RESPONSES IN NEONATAL RATS AFTER EXPOSURE TO COMBINATIONS OF IRON AND SOOT PARTICLES

Neonatal rats exposed to combinations of iron and soot particles containing either 30 or 100 μg/m^3 iron in a total mass concentration of 250 μg/m^3 showed several changes in either BALF or lung tissue compared with control animals. For BALF at both iron concentrations, increases were detected in GST activity and in levels of GSSG and GRR; FRAP decreased. After exposure to a combination of iron and soot particles containing 100 μg/m^3 iron, BALF showed reduced cell viability and increased LDH activity; lung tissue showed increased IL-1β (but not TNF-α) and ferritin levels.

Compared with control animals, BrdU cell labeling was reduced within the epithelium of the proximal alveolar region (a site of alveolar growth and proliferation during the postnatal period) of 13-day-old rats exposed to combinations of iron and soot particles (at both 30 and 100 μg/m^3 iron). In contrast, there were no changes within the terminal bronchioles or randomly selected alveolar regions compared with controls.

HEI EVALUATION OF THE STUDY

Pinkerton and colleagues conducted a study to determine the effects of exposure to ultrafine particles of different composition, alone or in combination, on the respiratory system of neonatal and young adult rats. They hypothesized that the binding of iron to soot may affect the deposition of the metal and change its biologic activity. They used a diffusion flame system to produce ultrafine particles of iron, soot, and combinations of iron and soot. The choice of these components was appropriate because both iron and soot are present in ambient particles.

A key finding of the study was that the biologic response to inhalation of ultrafine particles depended on particle composition, specifically on the iron content of the particles. Thus, in adult rats exposure to the higher concentration of iron particles (90 μg/m^3) had effects that were not observed after exposure to the lower concentration of iron (57 μg/m^3): namely, changes in some measures of oxidative stress and increases in levels of ferritin and the proinflammatory cytokine IL-1β. Similar conclusions may be drawn from the results showing more effects — increased levels of ferritin and IL-1β, decreased cell viability, and increased LDH activity — in neonatal animals exposed to a higher proportion of iron-containing particles than in animals exposed to particles with a lower proportion of iron.

The investigators also found that a low concentration of iron particles (45 μg/m^3) in the presence of soot, which by itself induced no changes compared with controls, had more biologic effects than a similar concentration of iron particles alone (57 μg/m^3). The pattern of endpoints changed by exposure to the combination of iron and soot particles was similar to the pattern of endpoints affected by the higher concentration of iron particles alone (90 μg/m^3). This suggests that the effects of soot and iron were synergistic. If reproduced in other studies, it has implications for the toxicity of particles in a mixture, suggesting that the interaction between different particles may affect their toxicities. The mechanism by which this may occur can only be a matter of speculation. It is possible that in the current study the presence of soot affected the deposition of iron in the lungs, as the investigators originally hypothesized, but no data were collected to evaluate this hypothesis.

A novel finding of the study was that the level of intracellular ferritin was generally higher in animals for which the exposures to combinations of iron and soot particles affected oxidative stress and inflammatory responses. (However, this was not found in neonatal animals exposed to the combination of iron and soot particles containing the lower proportion of iron.) These data provide evidence that iron — of an unknown soluble form — was released from the inhaled particles within lung epithelial cells. This finding is consistent with the investigators' demonstration that iron is released from combinations of iron and soot particles in an in vitro assay designed to measure iron bioavailability. The percentage of bioavailable iron in the particle combinations of iron and soot in this assay was in the same range as that found in several samples of coal fly ash (Aust et al. 2002). Taken together with the other biologic responses reported in this study, these findings support the conclusions of other investigators that implicate soluble — that is, bioavailable — iron released within lung cells as inducing biologic effects that include oxidative stress and inflammation (summarized by Aust et al. 2002).

In addition, the finding that exposure of neonatal rats to combinations of iron and soot particles decreased the proliferation and expansion of cells in the proximal alveolar airway suggests that exposure to air pollutants during a period of rapid lung development and alveolarization can affect lung growth. This supports results of studies such as the Children's Health Study in Southern California, which has been studying the effects of children's chronic exposures to air pollution in communities with different levels and patterns of air pollutants (Gauderman et al. 2002, 2004).

Pinkerton and coworkers made good attempts to characterize the particles they generated as well as potential contaminants. Their findings, that gaseous contaminants formed during their combustion process (including carbon monoxide, nitrogen oxides, and polycyclic aromatic hydrocarbons) were at low to undetectable levels in the exposure chambers, provide assurance that the effects of the particles were probably not confounded by the gases. However, the presence of iron pentacarbonyl (used to generate the iron particles) cannot be ruled out even though the flame temperatures were high enough to decompose it.

Some questions remain about the particle generation and delivery system. The lack of consistency in the concentrations of iron in the different experiments — which complicates comparison of effects among groups of exposed animals — suggests that the combustion process used to generate iron particles was not entirely reproducible across experiments. Moreover, because the analysis of the iron content was done after completion of the exposure, it was not possible to adjust the dilution conditions during the exposures.

One limitation of the study was that the investigators assessed only one postexposure time point for BALF assays (2 hours) and one for lung tissue assays (24 hours). They thought these time points were optimal for detecting postexposure biologic changes. Nonetheless, as the investigators acknowledge, each endpoint may have had its own unique kinetics of response after exposure to each type of aerosol. Thus, assessing responses at a single time point may have missed the optimal time point for some biologic responses. It is notable that the responses measured in the study occurred in the absence of overt histologic lung injury. Because the investigators designed their study to assess acute changes in lung responses, it is possible, but not proven, that such injury might have been detected at longer time periods after exposure.

The investigators suggest that the combinations of iron and soot particles that they generated bore a generic similarity to diesel exhaust particles, because both have a similar size distribution and contain similar percentages of OC. The combinations of iron and soot particles generated in this study contained 40% OC (within the range of the percentage found in diesel particles [U.S. EPA 2002]), but the investigators did not identify the OC components formed. However, the investigators recognize that the particles they generated and diesel particles differ in several characteristics. Diesel particles are more complex chemically and physically in that they contain a carbon core to which hundreds of compounds, including organic and inorganic compounds, adhere. By contrast, the particles that Pinkerton and colleagues generated comprised, at least in part, distinct iron and soot particles and also contained a much larger percentage of iron (12% to 40%) than diesel particles (< 0.5% [U.S. EPA 2002]).

Extrapolating the study findings in rats to possible responses in humans is difficult; although rats and humans have common oxidative stress pathways, the species are likely to have both qualitatively and quantitatively different responses to stressors. In addition, the particle concentrations of combinations of iron and soot to which the rats were exposed are much higher than those that humans would be exposed to in ambient air.

SUMMARY

Using a flame generation system Pinkerton and colleagues generated particles of iron, soot, and combinations of iron and soot and characterized the particles physically and chemically. They exposed young adult and neonatal rats to these particles by inhalation and measured several indicators of oxidative stress and inflammation in the airways and lung tissue.

Iron particles and soot particles were predominantly in the ultrafine range, but soot particles formed chains or clusters that were in the fine particle range. The combinations of iron and soot particles generated contained a high percentage of commingled particles, with a bimodal distribution similar to that of soot particles alone. Combinations of iron and soot particles contained EC and OC, but the organic components were not further characterized.

In both young adult and neonatal rats the biologic response to inhalation of ultrafine particles depended on particle composition, specifically on the iron content of the particles. In adult rats changes in some markers of oxidative stress, an increased release of the proinflammatory cytokine IL-1β, and increased levels of ferritin were detected at a higher, but not a lower, iron concentration. In neonatal rats more effects — increased levels of ferritin and IL-1β, decreased cell viability, and increased LDH activity — were detected after exposure to particles containing a higher proportion of iron than with a lower proportion of iron. Overt evidence of inflammation was not found, however, in either young adult or neonatal rats. It is noteworthy that particle effects were measured in the airways and lung tissue at only one time point after exposure, so it is possible that different results might have been obtained at different time points.

Exposure of neonatal rats to combinations of iron and soot particles impaired cell proliferation in the epithelium of the peripheral airways. This finding suggests that exposure to air pollutants during a period of rapid lung development may affect lung growth.

The finding that cell proliferation in the alveolar region of the lung was impaired after neonatal rats were exposed to combinations of iron and soot particles suggests that exposure to air pollutants during a period of rapid lung development may affect lung growth.

The investigators also found that the presence of soot particles enhanced the effects seen with iron particles alone, suggesting that the effects of soot and iron were synergistic. If reproduced in other studies, it would suggest that the interaction between different particles may affect their toxicities.

Although the investigators suggest that the particles generated in this study share some characteristics with diesel particles — both are predominantly in the ultrafine range and contain a significant percentage of carbon — they recognize that the particles differ in several other key physical and compositional characteristics. Thus, the relevance of the particles generated in this study to the emissions of a particular source, such as diesel, is uncertain.

Extrapolating the study findings to humans is difficult because of likely differences in oxidative stress responses between rats and humans and because the levels of particles were high compared with human ambient air exposures.

ACKNOWLEDGMENTS

The Health Review Committee thanks the ad hoc reviewers for their help in evaluating the scientific merit of the Investigators' Report. The Committee is also grateful to Dr. Maria Costantini for her oversight of the study, to Drs. Bernard Jacobson and Geoffrey Sunshine for their assistance in preparing its Critique, to Mary Brennan and Dr. Carol Moyer for science editing of this Report and its Critique, to Ruth Shaw for its composition, and to Melissa Cotter, Jenny Lamont, Flannery Carey McDermott, and Kasey Oliver for their roles in preparing this Research Report for publication.

REFERENCES

André E, Stoeger T, Takenaka S, Bahnweg M, Ritter B, Karg E, Lentner B, Reinhard C, Schulz H, Wjst M. 2006. Inhalation of ultrafine carbon particles triggers biphasic proinflammatory response in the mouse lung. Eur Respir J 28:275–285.

Antonini JM, Clarke RW, Krishna Murthy GG, Sreekanthan P, Jenkins N, Eagar TW, Brain JD. 1998. Freshly generated stainless steel welding fume induces greater lung inflammation in rats as compared to aged fume. Toxicol Lett 98:77–86.

Aust AE, Ball JC, Hu AA, Lighty JS, Smith KR, Straccia AM, Veranth JM, Young WC. 2002. Particle Characteristics Responsible for Effects on Human Lung Epithelial Cells. Research Report 110. Health Effects Institute, Boston, MA.

Carter JD, Ghio AJ, Samet JM, and Devlin RB. 1997. Cytokine production by human airway epithelial cells after exposure to an air pollution particle is metal-dependent. Toxicol Appl Pharmacol 146:180–188.

Dye JA, Lehmann JR, McGee JK, Winslett DW, Ledbetter AD, Everitt JL, Ghio AJ, Costa DL. 2001. Acute pulmonary toxicity of particulate matter filter extracts in rats: Coherence with epidemiologic studies in Utah Valley residents. Environ Health Perspect 109(Suppl 3):395–403.

Frampton MW. 2001. Systemic and cardiovascular effects of airway injury and inflammation: Ultrafine particle exposure in humans. Environ Health Perspec 109:529–532.

Frampton MW, Stewart JC, Oberdörster G, Morrow PE, Chalupa D, Pietropaoli AP, Frasier LM, Speers DM, Cox C, Huang LS, Utell MJ. 2006. Inhalation of ultrafine particles alters blood leukocyte expression of adhesion molecules in humans. Environ Health Perspect 114:51–58.

Gauderman WJ, Avol E, Gilliland F, Vora H, Thomas D, Berhane K, McConnell R, Kuenzli N, Lurmann F, Rappaport E, Margolis H, Bates D, Peters J. 2004. The effect of air pollution on lung development from 10 to 18 years of age. N Engl J Med 351:1057–1067.

Gauderman WJ, Gilliland GF, Vora H, Avol E, Stram D, McConnell R, Thomas D, Lurmann F, Margolis HG, Rappaport EB, Berhane K, Peters JM. 2002. Association between air pollution and lung function growth in southern California children: Results from a second cohort. Am J Respir Crit Care Med 166:76–84.

Ghio AJ, Devlin RB. 2001. Inflammatory lung injury after bronchial installation of air pollution particles. Am J Respir Crit Care Med 164:704–708.

Gilmour PS, Ziesenis A, Morrison ER, Vickers MA, Drost EM, Ford I, Karg E, Mossa C, Schroeppel A, Ferron GA, Heyder J, Greaves M, MacNee W, Donaldson K. 2004. Pulmonary and systemic effects of short-term inhalation exposure to ultrafine carbon black particles. Toxicol Appl Pharmacol 195:35–44.

Hahn FF, Barr EB, Ménache MG, Segrave JC. 2005. Particle Size and Composition Related to Adverse Health Effects in Aged, Sensitive Rats. Research Report 129. Health Effects Institute, Boston, MA.

Halliwell B, Gutteridge JMC. 1999. Free Radicals in Biology and Medicine, 3rd ed. Oxford University Press. Oxford, U.K.

Hughes L, Cass G, Gone J, Ames M, Olmez I. 1998. Physical and chemical characterization of atmospheric ultrafine particles in the Los Angeles area. Environ Sci Tech 32:1153–1161.

Jakab GJ. 1992. Relationship between carbon black particulate-bound formaldehyde, pulmonary antibacterial defenses and alveolar macrophages. Inhal Toxicol 4:325–342.

Jakab GJ. 1993. The toxicologic interactions resulting from inhalation of carbon black and acrolein on pulmonary antibacterial and antiviral defenses. Toxicol Appl Pharmacol 121:167–175.

Jakab GJ, Hemenway DR. 1994. Concomitant exposure to carbon black particulates enhances ozone-induced lung inflammation and suppression of alveolar macrophage phagocytosis. J Toxicol Environ Health 41:221–231.

Kadiiska MB, Mason RP, Dreher KL, Costa DL, Ghio AF. 1997. In vivo evidence of free radical formation in the rat lung after exposure to an emission source air pollution particle. Chem Res Toxicol 10:1104–1108.

Kreyling G, Semmler–Behnke M, Moller W. 2006. Ultrafine particle-lung interactions: Does size matter? J Aerosol Med 19:74–83.

Kumagai Y, Taira J, Sagai M. 1995. Apparent inhibition of superoxide dismutase activity in vitro by diesel exhaust particles. Free Radic Biol Med. 18:365–71.

Mauderly JL, Chow JC. 2008. Health effects of organic aerosols. Inhal Toxicol 20:257–288.

Oberdörster G. 1995. Lung particle overload: Implications for occupational exposures to particles. Regul Toxicol Pharmacol 21:123–135.

Oberdörster G. 2001. Pulmonary effects of inhaled ultrafine particles. Int Arch Occup Environ Health 74:1–8.

Pagan I, Costa DL, McGee JK, Richards JH, Dye JA. 2003. Metals mimic airway epithelial injury induced by in vitro exposure to Utah Valley ambient particulate matter extracts. J Toxicol Environ Health A. 66:1087–1112.

Pekkanen J, Timonen KL, Ruuskanen J, Reponen A, Mirme A. 1997. Effects of ultrafine and fine particles in urban air on peak expiratory flow among children with asthmatic symptoms. Ennviron Res 74:24–33.

Peters A, Veronesi B, Calderón-Garcidueñas L, Gehr P, Chen LC, Geiser M, Reed W, Rothen-Rutishauser B, Schürch S, Schulz H. 2006. Translocation and potential neurological effects of fine and ultrafine particles a critical update. Part Fibre Toxicol 3:13.

Peters A, von Klot S, Heier M, Trentinaglia I, Cyrys J, Hörmann A, Hauptmann M, Wichmann H-E, Löwel H. 2005. Part I. Air pollution, personal activities, and onset of myocardial infarction in a case-crossover study. In: Particulate Air Pollution and Nonfatal Cardiac Events. Research Report 124. Health Effects Institute, Boston, MA.

Peters A, Wichmann HE, Tuch T, Heinrich J, Heyder J. 1997. Respiratory effects are associated with the number of ultra-fine particles. American Journal of Respiratory and Critical Care Medicine 155:1376–1383.

Pinkerton KE, Mercer RR, Plopper CG, Crapo JD. 1992. Distribution of injury and microdosimetry of ozone in the ventilatory unit of the rat. J Appl Physiol 73:817–824.

Pope CA III. 1996. Particulate pollution and health: A review of the Utah valley experience. J Expo Anal Environ Epidemiol 6:23–34.

Sagai M, Saito H, Ichinose T, Kodama M, Mori Y. 1993. Biological effects of diesel exhaust particles. I. In vitro production of superoxide and in vivo toxicity in mouse. Free Radic Biol Med 14:37–47.

Samet JM, Ghio AJ. 2007. Particle-associated metals and oxidative stress in signaling. In: Particle Toxicology. (Donaldson K and Borm P, eds.) pp 161–181. CRC Press.

Smith KR, Veranth JM, Hu AA, Lighty JS, Aust AE. 2000. Interleukin-8 levels in human lung epithelial cells are increased in response to coal fly ash and vary with bioavailability of iron, as a function of particle size and source of coal. Chem Res Toxicol 13:118–125.

Smith KR, Veranth JM, Lighty JS, Aust AE. 1998. Mobilization of iron from coal fly ash was dependent upon the particle size and the source of the coal. Chem Res Toxicol 11:1494–1500.

U.S. Environmental Protection Agency. 2002. Health Assessment Document For Diesel Engine Exhaust. EPA/600/8-90/057F. National Center for Environmental Assessment, Office of Research and Development, U.S. Environmental Protection Agency, Washington, D.C.

U.S. Environmental Protection Agency. 2004. Air Quality Criteria for Particulate Matter. EPA/600/P-99/002aF. National Center for Environmental Assessment, Office of Research and Development, U.S. Environmental Protection Agency, Research Triangle Park, NC.

Utell MJ. Frampton MW. 2000. Acute health effects of ambient air pollution: The ultrafine particle hypothesis. J Aerosol Med 13:355–59.

Wang Z, Neuburg D, Li C, Kim JY Chen JC, Christiani DC. 2005. Global gene expression profiling in whole-blood samples from individuals exposed to metal fumes. Environ Health Perspect 113:233–241.

Watkinson WP, Campen MJ, Costa DL. 1998. Cardiac arrhythmia induction after exposure to residual oil fly ash particles in a rodent model of pulmonary hypertension. Toxicol Sci 41:209–216.

Wichmann H-E, Spix C, Tuch T, Wölke G, Peters A, Heinrich J, Kreiling WG, Heyder J. 2000. Part I. Role of particle number and particle mass. In: Daily Mortality and Fine and Ultrafine Particles in Erfurt, Germany. Research Report 98. Health Effects Institute, Cambridge, MA.

RELATED HEI PUBLICATIONS: PARTICULATE MATTER AND DIESEL EXHAUST

Number	Title	Principal Investigator	Date*
Research Reports			
134	Black-Pigmented Material in Airway Macrophages from Healthy Children: Association with Lung Function and Modeled PM_{10}	J. Grigg	2008
131	Characterization of Particulate and Gas Exposures of Sensitive Subpopulations Living in Baltimore and Boston	P. Koutrakis	2005
129	Particle Size and Composition Related to Adverse Health Effects in Aged, Sensitive Rats	F.F. Hahn	2005
128	Neurogenic Responses in Rat Lungs After Nose-Only Exposure to Diesel Exhaust	M.L. Witten	2005
127	Personal, Indoor, and Outdoor Exposures to $PM_{2.5}$ and Its Components for Groups of Cardiovascular Patients in Amsterdam and Helsinki	B. Brunekreef	2005
126	Effects of Exposure to Ultrafine Carbon Particles in Healthy Subjects and Subjects with Asthma	M.W. Frampton	2004
124	Particulate Air Pollution and Nonfatal Cardiac Events		2005
	Part I. Air Pollution, Personal Activities, and Onset of Myocardial Infarction in a Case–Crossover Study	A. Peters	
	Part II. Association of Air Pollution with Confirmed Arrhythmias Recorded by Implanted Defibrillators	D. Dockery	
120	Effects of Concentrated Ambient Particles on Normal and Hypersecretory Airways in Rats	J.R. Harkema	2004
118	Controlled Exposures of Healthy and Asthmatic Volunteers to Concentrated Ambient Particles in Metropolitan Los Angeles	H. Gong Jr.	2003
112	Health Effects of Acute Exposure to Air Pollution	S.T. Holgate	2003
	Part I. Healthy and Asthmatic Subjects Exposed to Diesel Exhaust		
	Part II. Healthy Subjects Exposed to Concentrated Ambient Particles		
110	Particle Characteristics Responsible for Effects on Human Lung Epithelial Cells	A.E. Aust	2002
104	Inhalation Toxicology of Urban Ambient Particulate Matter: Acute Cardiovascular Effects in Rats	R. Vincent	2001
99	A Case–Crossover Analysis of Fine Particulate Matter Air Pollution and Out-of-Hospital Sudden Cardiac Arrest	H. Checkoway	2000

Continued

** Reports published since 1995.*
Copies of these reports can be obtained from the Health Effects Institute and many are available at www.healtheffects.org.

RELATED HEI PUBLICATIONS: PARTICULATE MATTER AND DIESEL EXHAUST

Number	Title	Principal Investigator	Date*
98	Daily Mortality and Fine and Ultrafine Particles in Erfurt, Germany *Part I.* Role of Particle Number and Particle Mass	H-E. Wichmann	2000
97	Identifying Subgroups of the General Population That May Be Susceptible to Short-Term Increases in Particulate Air Pollution: A Time-Series Study in Montreal, Quebec	M.S. Goldberg	2000
96	Acute Pulmonary Effects of Ultrafine Particles in Rats and Mice	G. Oberdörster	2000
95	Association of Particulate Matter Components with Daily Mortality and Morbidity in Urban Populations	M. Lippmann	2000
91	Mechanisms of Morbidity and Mortality from Exposure to Ambient Air Particles	J.J. Godleski	2000
Special Reports			
	Revised Analyses of Time-Series Studies of Air Pollution and Health		2003
	Research Directions to Improve Estimates of Human Exposure and Risk from Diesel Exhaust		2002
	Reanalysis of the Harvard Six Cities Study and the American Cancer Society Study of Particulate Air Pollution and Mortality: A Special Report of the Institute's Particle Epidemiology Reanalysis Project		2000
	Diesel Emissions and Lung Cancer: Epidemiology and Quantitative Risk Assessment		1999
	Particulate Air Pollution and Daily Mortality: The Phase I Report of the Particle Epidemiology Evaluation Project		
	Phase I.A. Replication and Validation of Selected Studies		1995
	Phase I.B. Analyses of the Effects of Weather and Multiple Air Pollutants		1997
	Diesel Exhaust: A Critical Analysis of Emissions, Exposure and Health Effects		1995
HEI Communications			
8	The Health Effects of Fine Particles: Key Questions and the 2003 Review (Report of the Joint Meeting of the EC and HEI)		1999
HEI Research Program Summaries			
	Research on Particulate Matter		1999
HEI Perspectives			
	Understanding the Health Effects of Components of the Particulate Matter Mix: Progress and Next Steps		2002
	Airborne Particles and Health: HEI Epidemiologic Evidence		2001

** Reports published since 1995.*
Copies of these reports can be obtained from the Health Effects Institute and many are available at www.healtheffects.org.

HEI BOARD, COMMITTEES, and STAFF

Board of Directors

Richard F. Celeste, Chair *President, Colorado College*

Enriqueta Bond *Past President, Burroughs Wellcome Fund*

Purnell W. Choppin *President Emeritus, Howard Hughes Medical Institute*

Jared L. Cohon *President, Carnegie Mellon University*

Stephen Corman *President, Corman Enterprises*

Gowher Rizvi *Vice Provost, University of Virginia*

Linda Rosenstock *Dean, School of Public Health, University of California–Los Angeles*

Archibald Cox, Founding Chair *1980–2001*

Donald Kennedy, Vice Chair Emeritus *Editor-in-Chief Emeritus,* Science*; President Emeritus and Bing Professor of Biological Sciences, Stanford University*

Health Research Committee

Mark J. Utell, Chair *Professor of Medicine and Environmental Medicine, University of Rochester Medical Center*

Melvyn C. Branch *Joseph Negler Professor of Engineering, Emeritus, Mechanical Engineering Department, University of Colorado*

Kenneth L. Demerjian *Ray Falconer Endowed Chair and Director, Atmospheric Sciences Research Center and Department of Earth and Atmospheric Science, University at Albany, State University of New York*

Joe G.N. Garcia *Lowell T. Coggeshall Professor of Medicine and Chair, Department of Medicine, University of Chicago*

Uwe Heinrich *Executive Director, Fraunhofer Institute of Toxicology and Experimental Medicine, Hanover, Germany*

Grace LeMasters *Professor of Epidemiology and Environmental Health, University of Cincinnati College of Medicine*

Sylvia Richardson *Professor of Biostatistics, Department of Epidemiology and Public Health, Imperial College School of Medicine, London, United Kingdom*

Howard E. Rockette *Professor and Chair, Department of Biostatistics, Graduate School of Public Health, University of Pittsburgh*

James A. Swenberg *Kenan Distinguished Professor of Environmental Sciences, Department of Environmental Sciences and Engineering, University of North Carolina–Chapel Hill*

Ira B. Tager *Professor of Epidemiology, School of Public Health, University of California–Berkeley*

HEI BOARD, COMMITTEES, and STAFF

Health Review Committee

Homer A. Boushey, Chair *Professor of Medicine, Department of Medicine, University of California–San Francisco*

Ben Armstrong *Reader in Epidemiological Statistics, Department of Public Health and Policy, London School of Hygiene and Tropical Medicine, United Kingdom*

Michael Brauer *Professor, School of Environmental Health, University of British Columbia, Canada*

Bert Brunekreef *Professor of Environmental Epidemiology, Institute of Risk Assessment Sciences, University of Utrecht, the Netherlands*

Alan Buckpitt *Professor of Toxicology, Department of Molecular Biosciences, School of Veterinary Medicine, University of California–Davis*

John R. Hoidal *A.D. Renzetti Jr. Presidential Professor and Chair, Department of Medicine, University of Utah Health Sciences Center*

Stephanie London *Senior Investigator, Epidemiology Branch, National Institute of Environmental Health Sciences*

Nancy Reid *University Professor, Department of Statistics, University of Toronto, Canada*

William N. Rom *Sol and Judith Bergstein Professor of Medicine and Environmental Medicine and Director of Pulmonary and Critical Care Medicine, New York University Medical Center*

Armistead Russell *Georgia Power Distinguished Professor of Environmental Engineering, School of Civil and Environmental Engineering, Georgia Institute of Technology*

Officers and Staff

Daniel S. Greenbaum *President*
Robert M. O'Keefe *Vice President*
Rashid Shaikh *Director of Science*
Barbara Gale *Director of Publications*
Jacqueline C. Rutledge *Director of Finance and Administration*
Helen I. Dooley *Corporate Secretary*

Kate Adams *Staff Scientist*
Marian Berkowitz *Research Associate*
Aaron J. Cohen *Principal Scientist*
Maria G. Costantini *Principal Scientist*
Philip J. DeMarco *Compliance Manager*
Terésa Fasulo *Science Administration Manager*
Hope Green *Editorial Assistant (part time)*
L. Virgi Hepner *Senior Science Editor*
Debra A. Kaden *Principal Scientist*
Francine Marmenout *Senior Executive Assistant*
Flannery Carey McDermott *Editorial Assistant*
Teresina McGuire *Accounting Assistant*
Sumi Mehta *Senior Scientist*
Nicholas Moustakas *Policy Associate*
Kelly Pitts *Research Assistant*
Hilary Selby Polk *Science Editor*
Robert A. Shavers *Operations Manager*
Geoffrey H. Sunshine *Senior Scientist*
Annemoon M.M. van Erp *Senior Scientist*

HEALTH
EFFECTS
INSTITUTE

101 Federal Street, Suite 500
Boston, MA 02110, USA
+1-617-488-2300
www.healtheffects.org

RESEARCH
REPORT

Number 135
October 2008